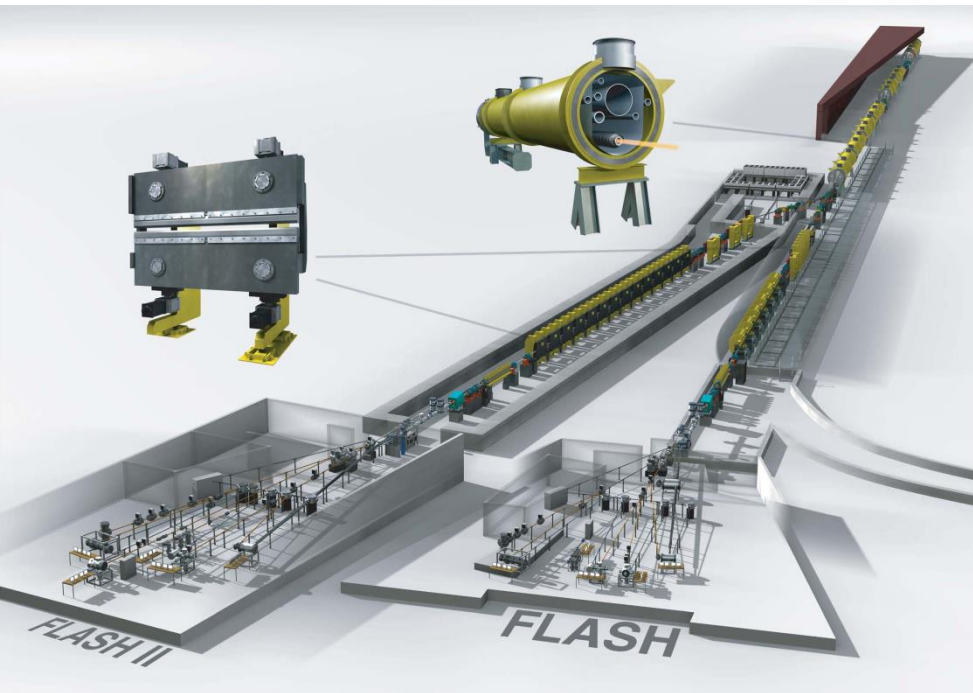


Characterization of Light (Photon Diagnostics @ FLASH).



Sven Toleikis

DESY Ukraine Winter School 2023

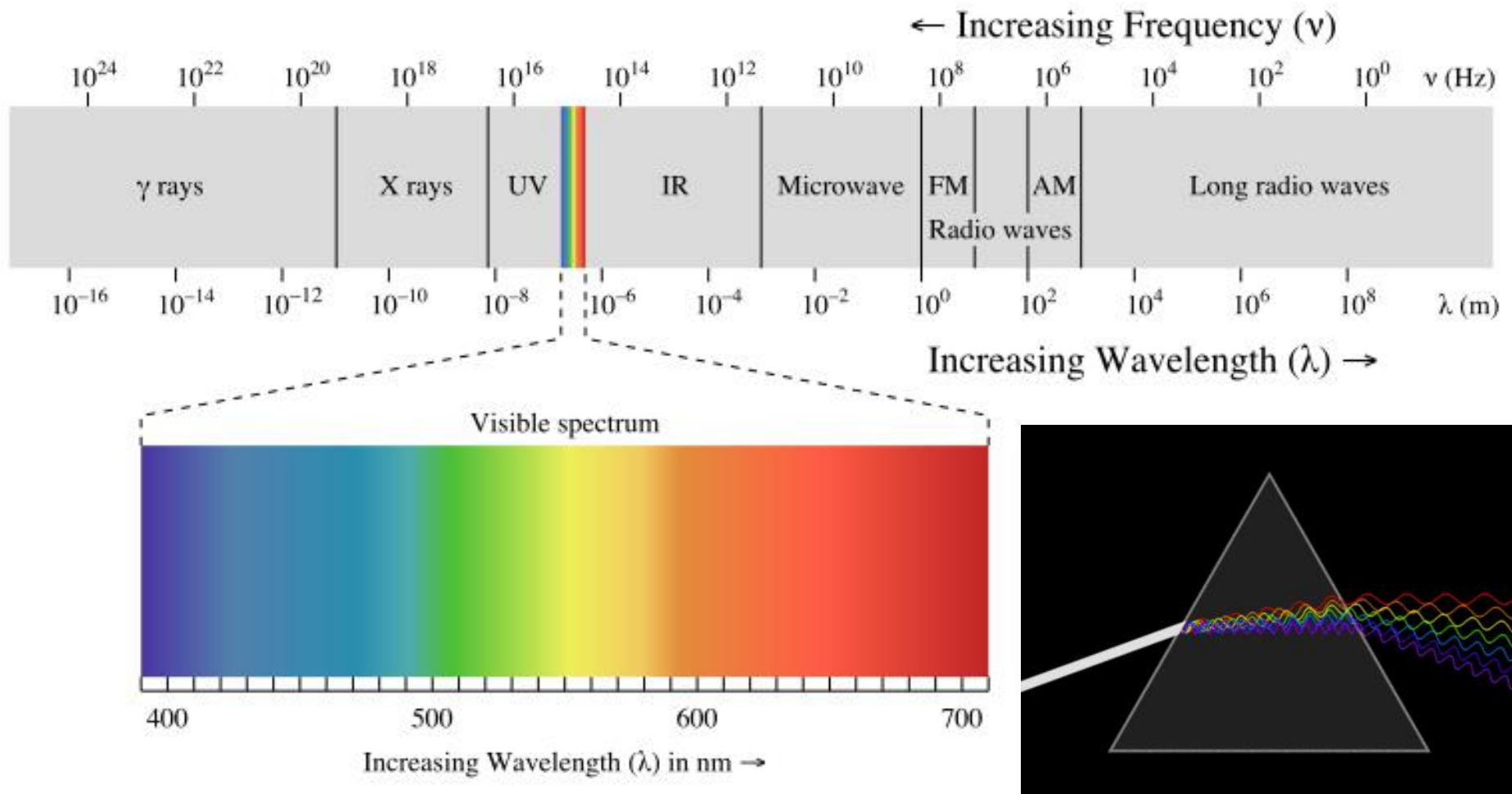
16 Februar 2023

Outline

- Introduction – what is light?
- Light generation
 - XUV FEL light at FLASH
 - THz light at FLASH
- Light transportation
 - Beamlines: beam transport (mirrors), beam manipulation, etc.
- Light characterization
 - Intensity (# of photons) / Beam position
 - Wavelength
 - Pulse duration / Jitter (to another light source)
 - Polarization
 - Coherence / Wavefront
- Light utilization
 - Example experiments

Light – Intro I

- Light -> more general: electro-magnetic radiation



Light – Intro II

- Frequency <-> Wavelength <-> Energy

CLASS	FREQUENCY	WAVELENGTH	ENERGY
Y	300 EHz	1 pm	1.24 MeV
HX	30 EHz	10 pm	124 keV
	3 EHz	100 pm	12.4 keV
SX	300 PHz	1 nm	1.24 keV
EUV	30 PHz	10 nm	124 eV
NUV	3 PHz	100 nm	12.4 eV
NIR	300 THz	1 μm	1.24 eV
MIR	30 THz	10 μm	124 meV
FIR	3 THz	100 μm	12.4 meV
EHF	300 GHz	1 mm	1.24 meV
SHF	30 GHz	1 cm	124 μeV
UHF	3 GHz	1 dm	12.4 μeV
VHF	300 MHz	1 m	1.24 μeV
HF	30 MHz	10 m	124 neV
MF	3 MHz	100 m	12.4 neV
LF	300 kHz	1 km	1.24 neV
VLF	30 kHz	10 km	124 peV
VF/ULF	3 kHz	100 km	12.4 peV
SLF	300 Hz	1 Mm	1.24 peV
ELF	30 Hz	10 Mm	124 feV
	3 Hz	100 Mm	12.4 feV

Sources at DESY:

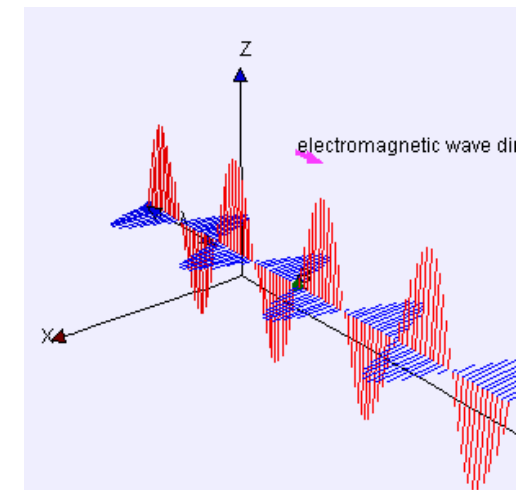
- > PETRAIII:
250 eV (XUV) – 200 keV (hard X-rays)
- > FLASH:
90 nm – 3.5 nm (~14 eV – 350 eV)
- > Optical lasers:
UV to NIR
- > THz@FLASH:
1 μm – 300 μm (300 THz – 1 THz)

Light – Intro III

- electro-magnetic radiation – theory
- electric field **E**, magnetic field **B**, electric potential φ , magnetic potential **A**

Maxwell's equations (vector fields)

$\nabla \cdot \mathbf{E} = \frac{\rho}{\epsilon_0}$	<u>Gauss' law</u>
$\nabla \cdot \mathbf{B} = 0$	<u>Gauss's law formagnetism</u>
$\nabla \times \mathbf{E} = -\frac{\partial \mathbf{B}}{\partial t}$	<u>Faraday's law</u>
$\nabla \times \mathbf{B} = \mu_0 \mathbf{J} + \mu_0 \epsilon_0 \frac{\partial \mathbf{E}}{\partial t}$	<u>Ampère–Maxwell law</u>



linearly polarized plane wave

Maxwell's equations (*Potential formulation*)

$$\nabla^2 \varphi + \frac{\partial}{\partial t} (\nabla \cdot \mathbf{A}) = -\frac{\rho}{\epsilon_0}$$

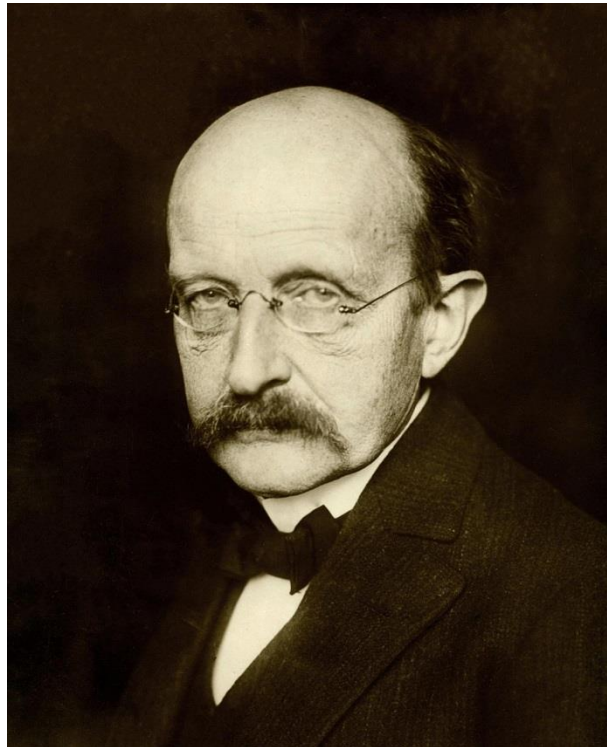
$$\mathbf{E} = -\nabla \varphi - \frac{\partial \mathbf{A}}{\partial t}$$

$$\left(\nabla^2 \mathbf{A} - \frac{1}{c^2} \frac{\partial^2 \mathbf{A}}{\partial t^2} \right) - \nabla \left(\nabla \cdot \mathbf{A} + \frac{1}{c^2} \frac{\partial \varphi}{\partial t} \right) = -\mu_0 \mathbf{J}$$

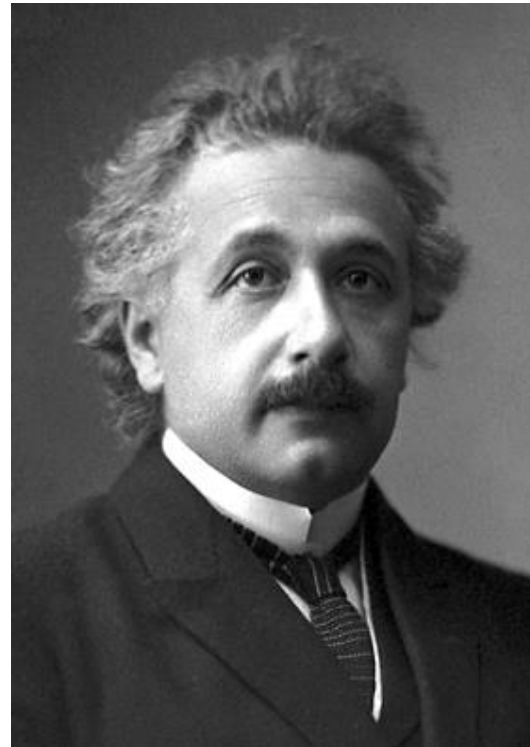
$$\mathbf{B} = \nabla \times \mathbf{A}$$

Light – Intro IV

- Electro-Magnetic radiation is quantized: $E = hf = \frac{hc}{\lambda}$
- Universal particle-wave duality (Louis de Broglie)

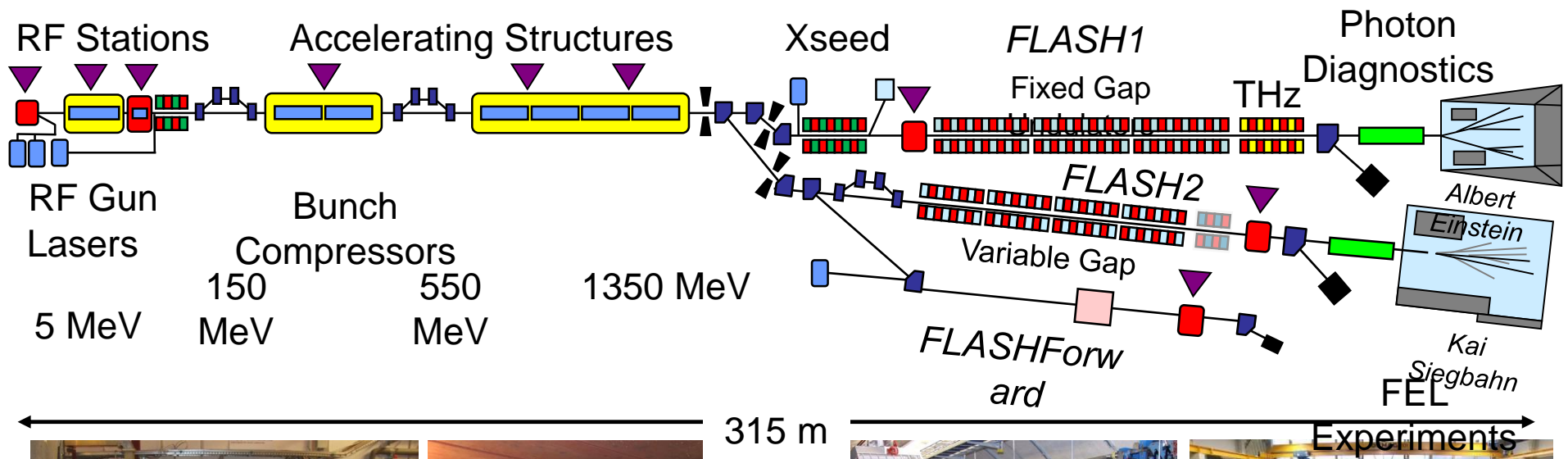


Max Planck (1858-1947)
Nobel Prize in Physics 1918

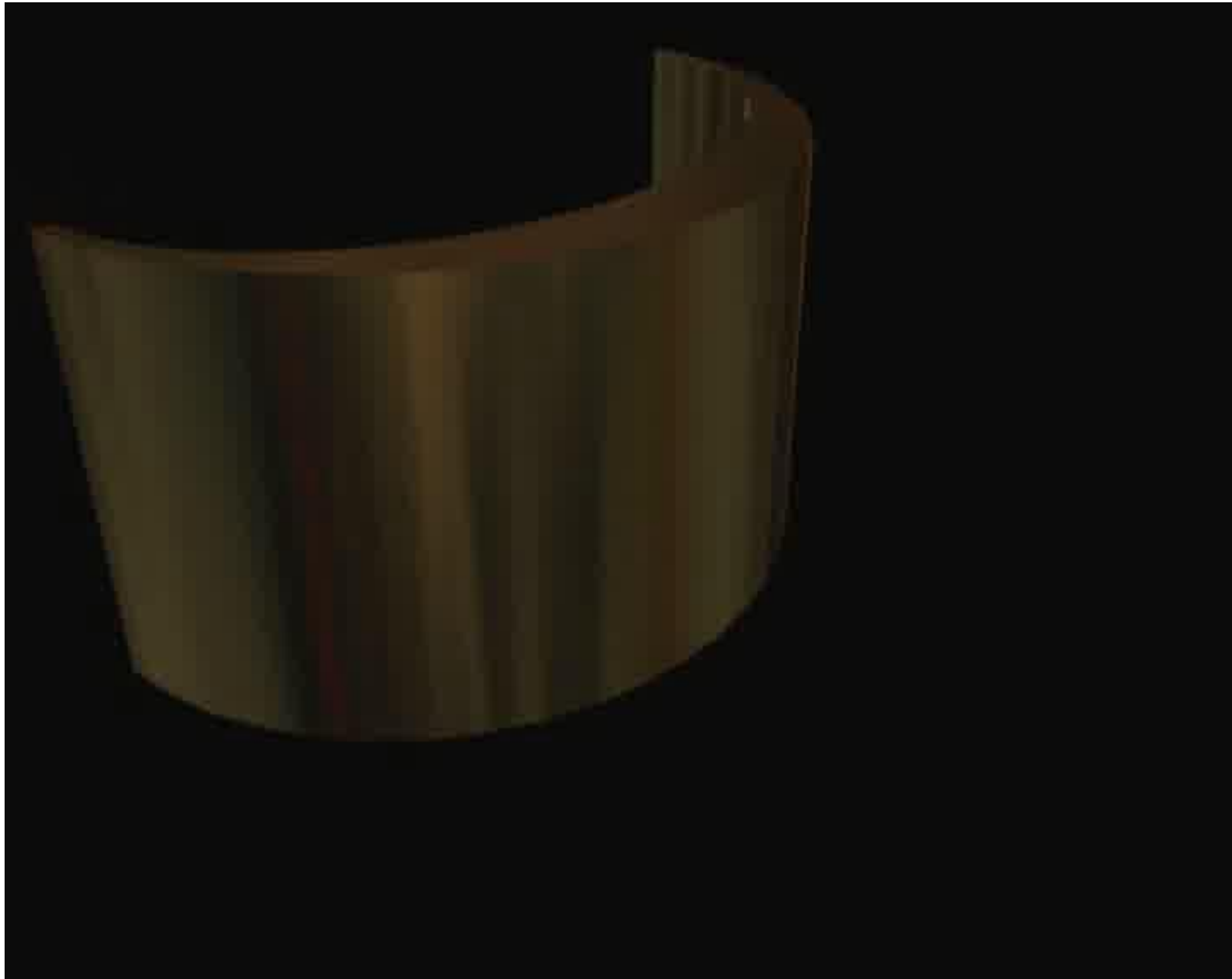


Albert Einstein (1879-1955)
Nobel Prize in Physics 1921

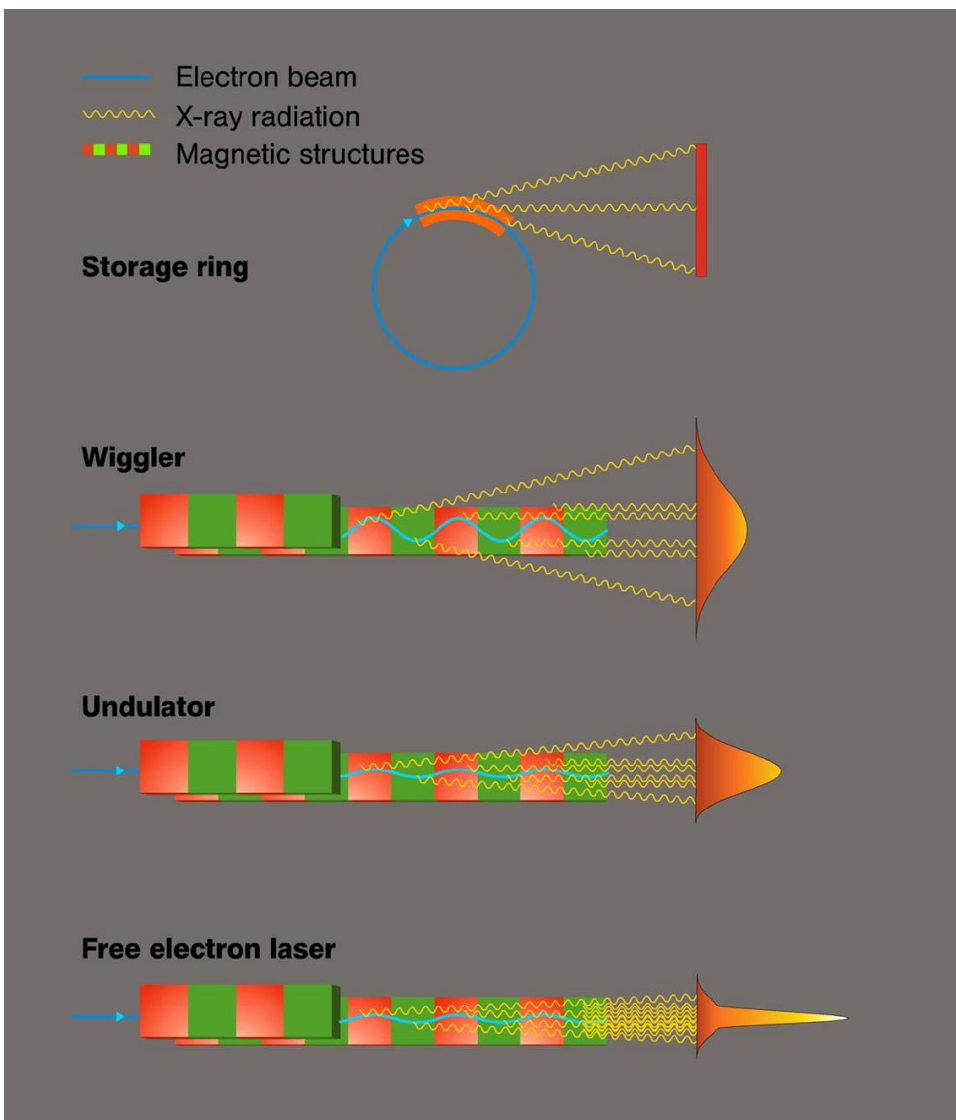
The FLASH facility



SASE movie



Generation of light – accelerator based



N_U or N_W = # of magnetic periods

N_e = # of electrons in a bunch

bending magnet radiation

$\propto N_W \times \text{bending magnet}$

$\propto N_U^2 \times \text{bending magnet}$

$\propto N_U^2 \times N_e \times \text{bending magnet}$

N_e = # of electrons in a bunch; e.g. @ FLASH with typ. 0.5 nC per bunch
-> $N_e = 3.12 \times 10^9 !!!$

Current photon parameters of FLASH

Wavelength range (fundamental):

3.5-60 nm (FL1); 3.5-90 nm (FL2)

Spectral width (FWHM):

0.5– 1.5 %

Pulse energy:

**up to 200 μ J (average),
500 μ J (peak), ~1 mJ (FL2)**

Pulse duration (FWHM):

~5 fs - 200 fs

Peak power (fundamental):

1 - 5 GW

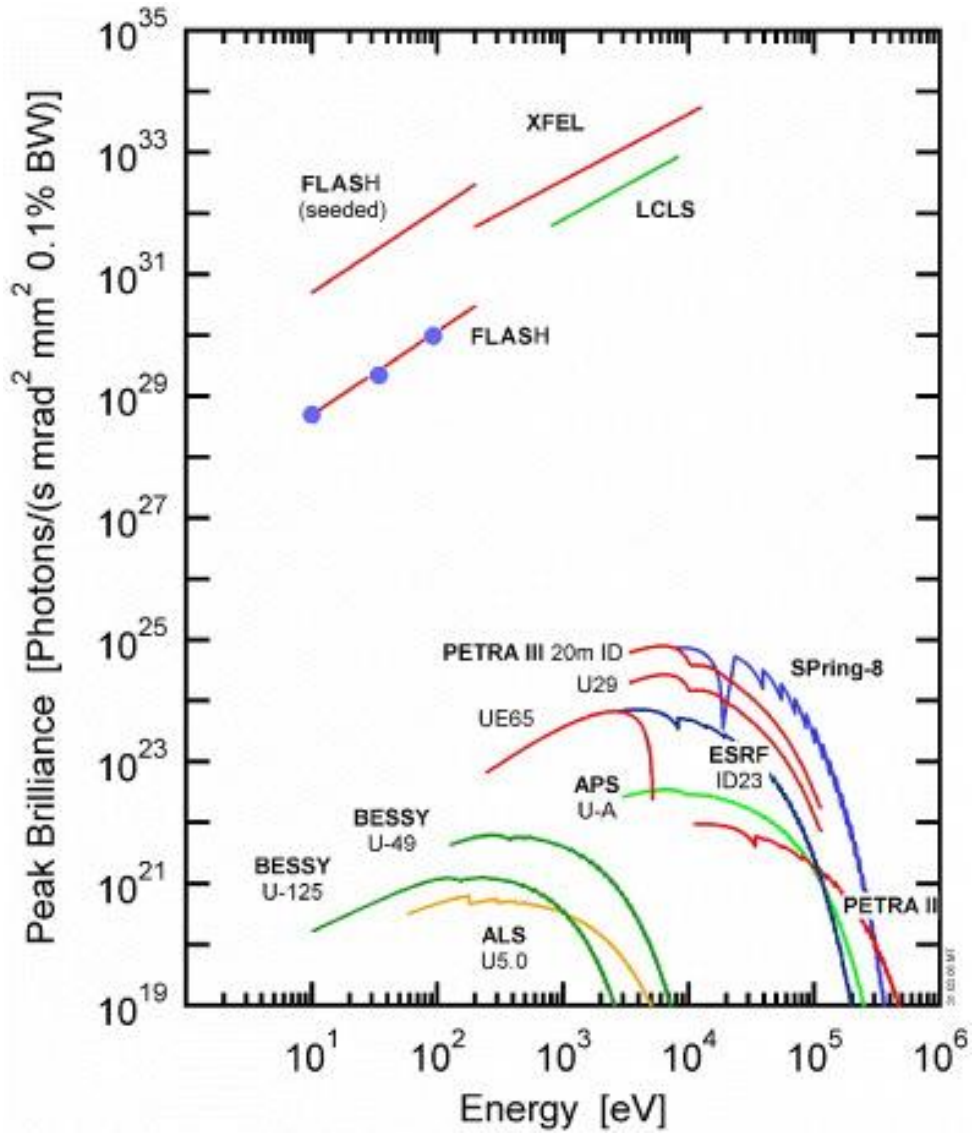
Average power (fundamental):

**up to 5 W
(up to 6000 pulses/s)**

Peak brilliance:

up to ~10³⁰

Photons/(s mrad² mm² 0.1% BW)



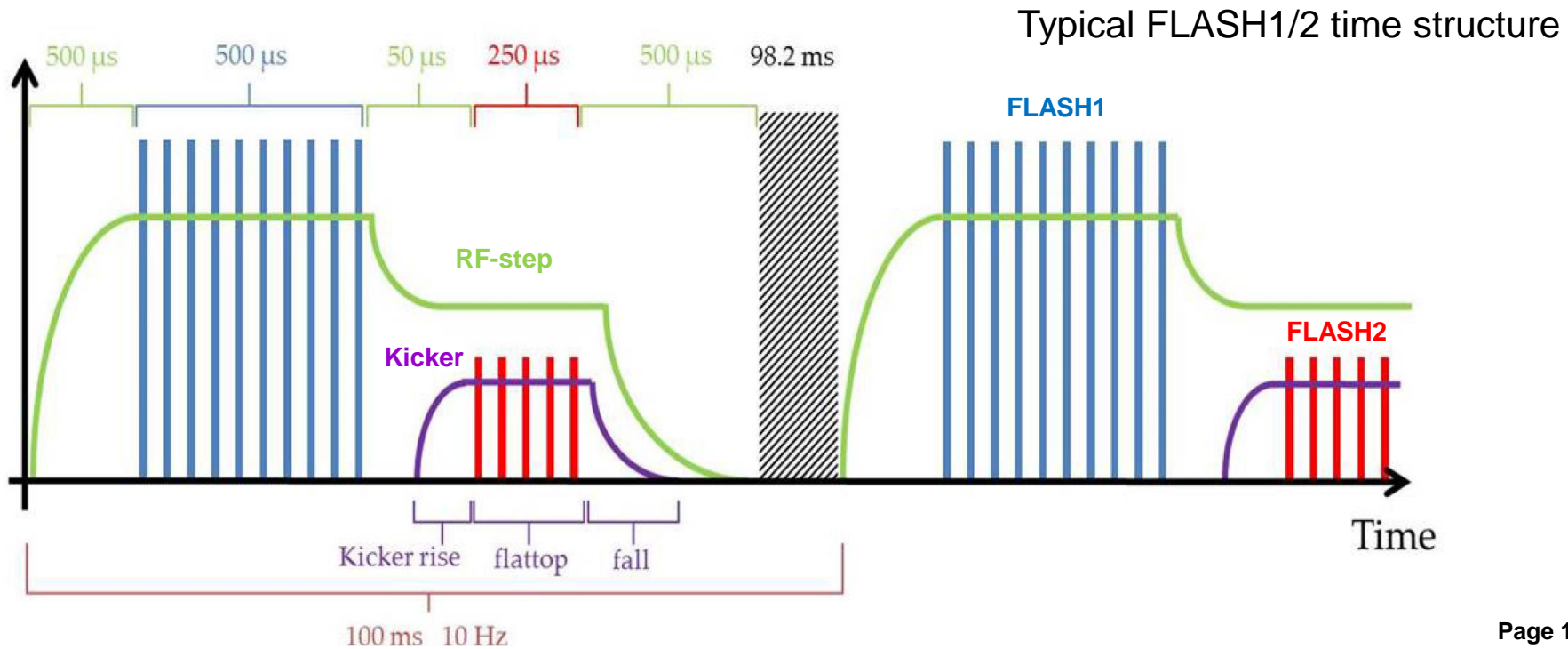
SASE FEL Properties

- > high intensity (GW peak power)
- > coherence (laser-like radiation)
- > femtosecond pulses!
- > narrow bandwidth!
- > full wavelength tunability!
- > down to X-rays!

- > But: shot-to-shot fluctuations (w/o seeding)
 - > very good photon diagnostics are mandatory!

Simultaneous FLASH1 and FLASH2 operation

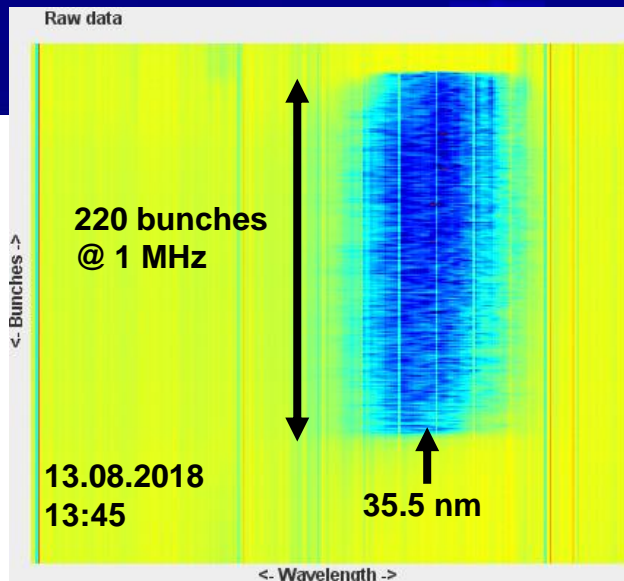
- Superconducting accelerator technology allows long RF-pulses (10 Hz, up to 800 μ s)
→ long electron bunch train, which can be shared between FLASH1 and FLASH2 with 10 Hz
- Fast kicker and Lambertson septum used to extract a part of the bunch train to FLASH2
- Two injector lasers: FLASH1 and FLASH2 bunch pattern and charge selected independently
- Flexible RF-system: amplitude and phase is adjusted independently for FLASH1 and FLASH2



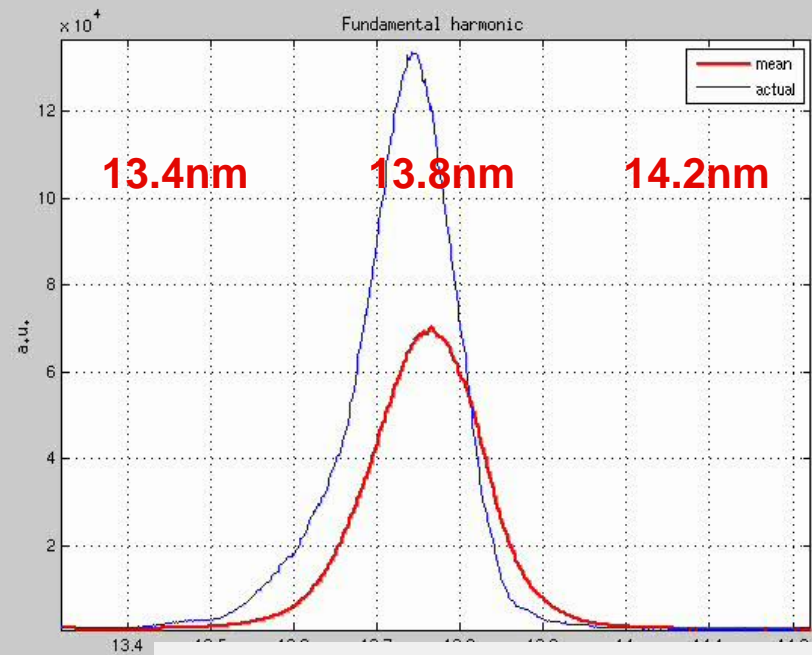
FLASH performance

Spatial Profile

Ce:YAG screen for the spatial profile

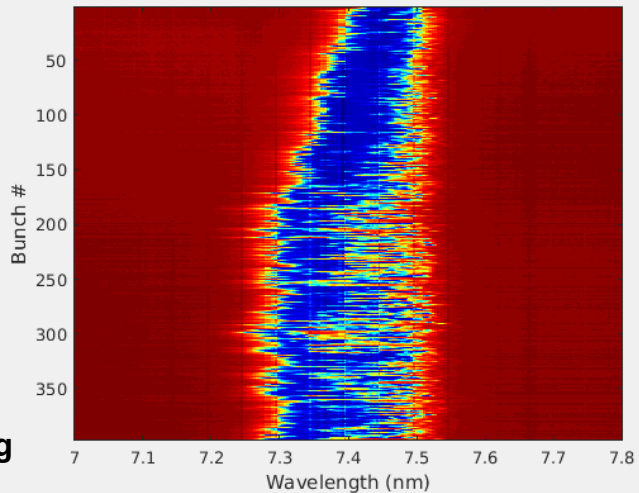


Spectral distribution



VLS spectrometer
with Kalypso line detector
@ 1 MHz

28.05.2018
During tuning



THz @ FLASH1

XUV undulators



Undulator:

- Intensity $\sim N_e^2$ (up to 100 μ J)
- Synchronized to XUV pulse (<5 fs jitter)
- narrowband (~10%)
 - + tunable (0.6 – 300 μ m)
- polarization: linear

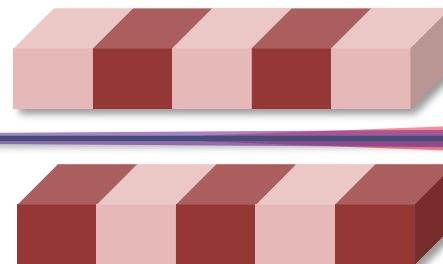
Dump magnet:

- Intensity up to 10 μ J
- broadband (single cycle)
- ~100% @ 1.5 THz
- polarization: Radial

Peak fields:

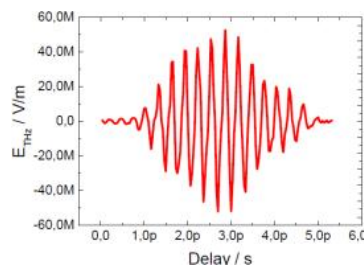
$E \sim GV/m$ & $B \sim 1 T$
DESY.

THz undulator

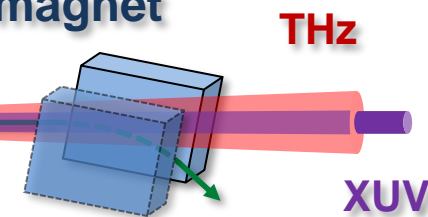


Tunable + narrow band:

1 – 300 μ m (4 meV – 1 eV)

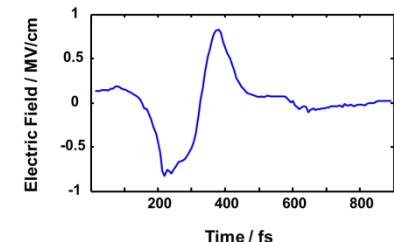


Dump magnet

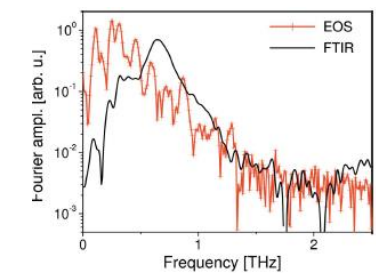
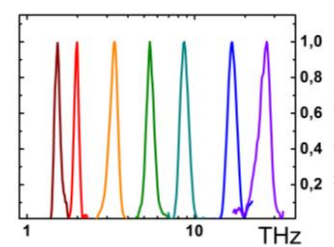
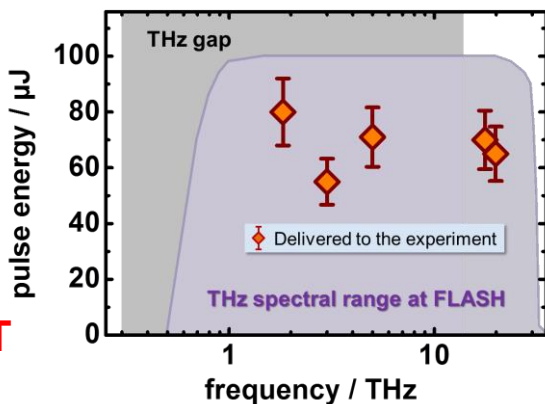


+ Single cycle

(50 – 300 mm) (4 – 24 meV)



THz pulse energy

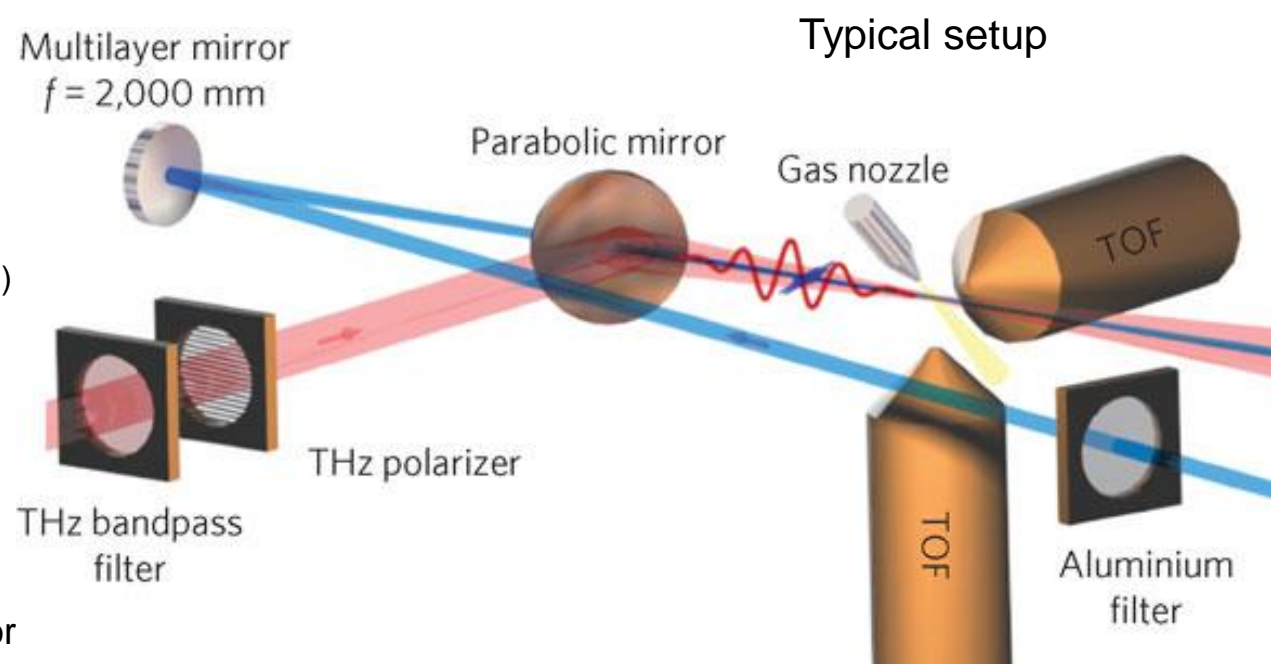


THz

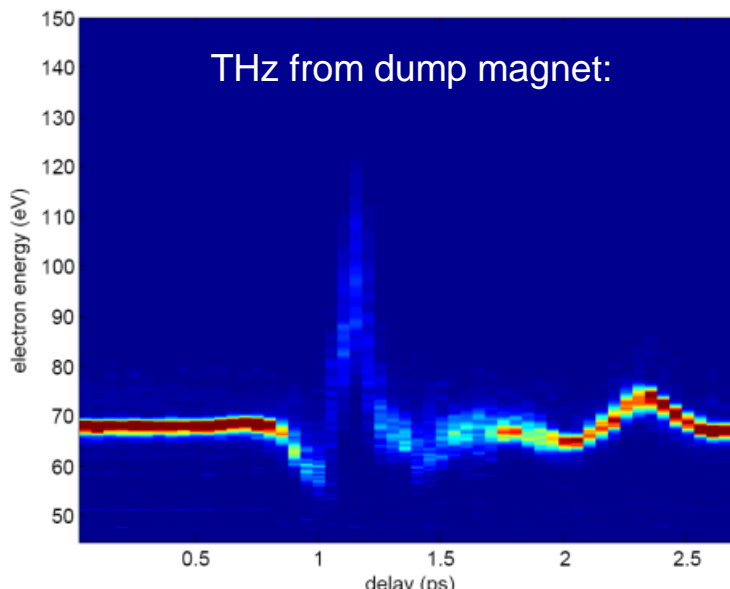
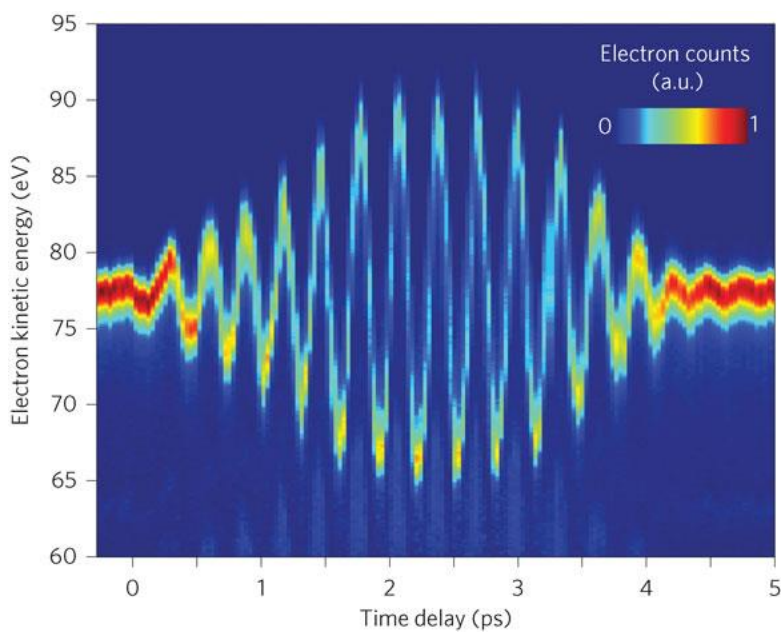
XUV

THz streaking experiment

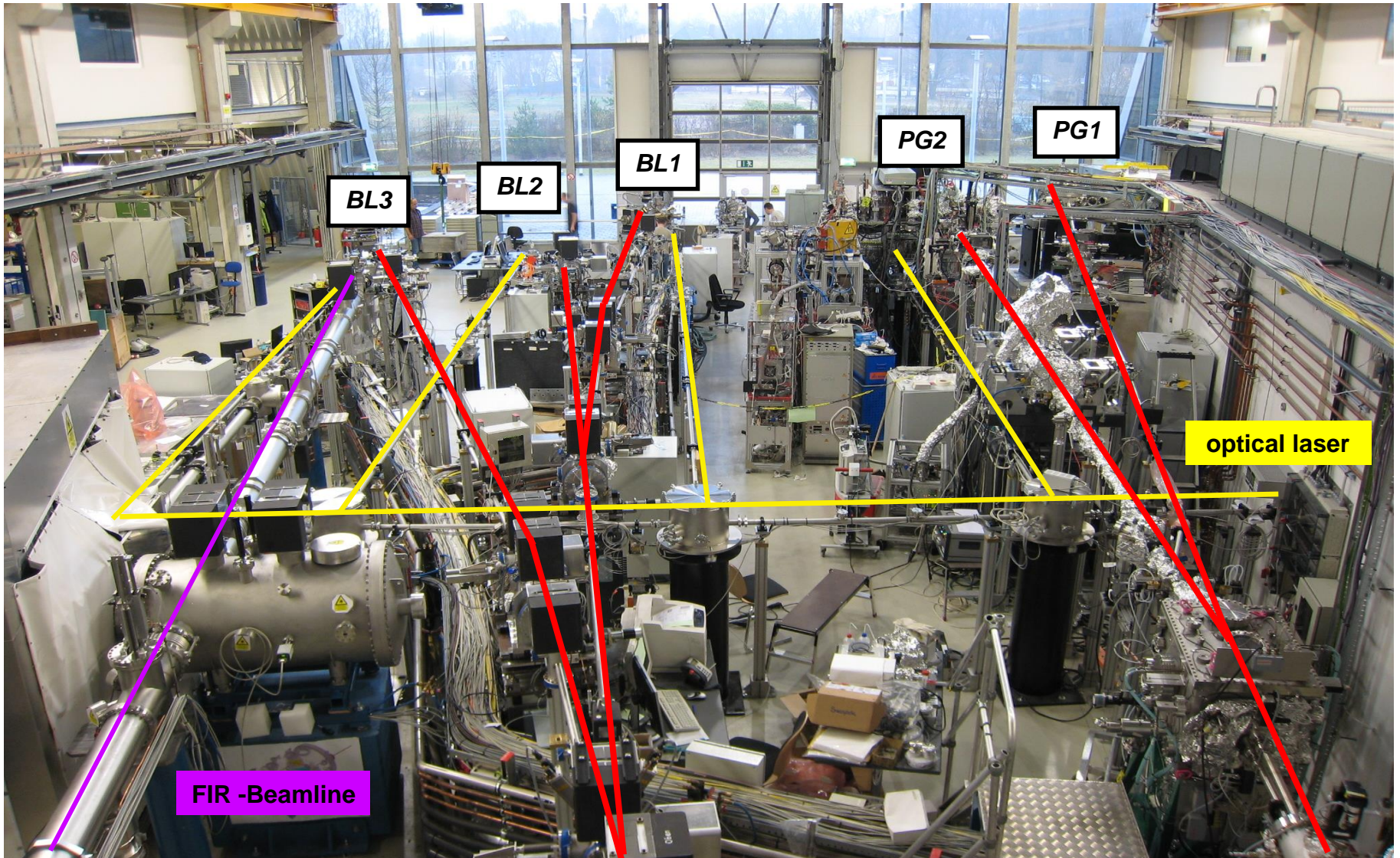
Nature Photonics **3**, 523 (2009)
Phys. Rev. Lett. **108**, 253003 (2012)



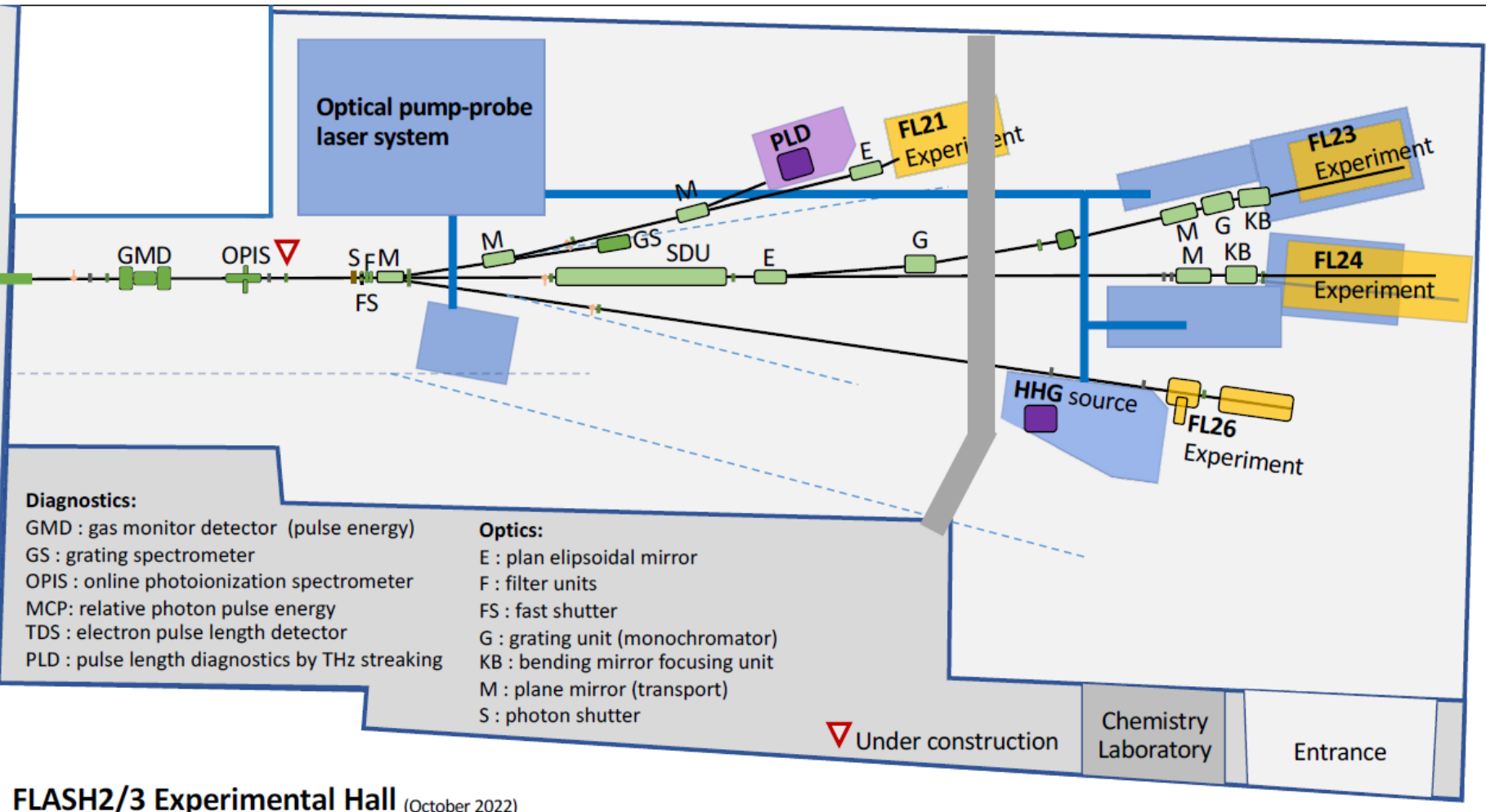
THz from undulator



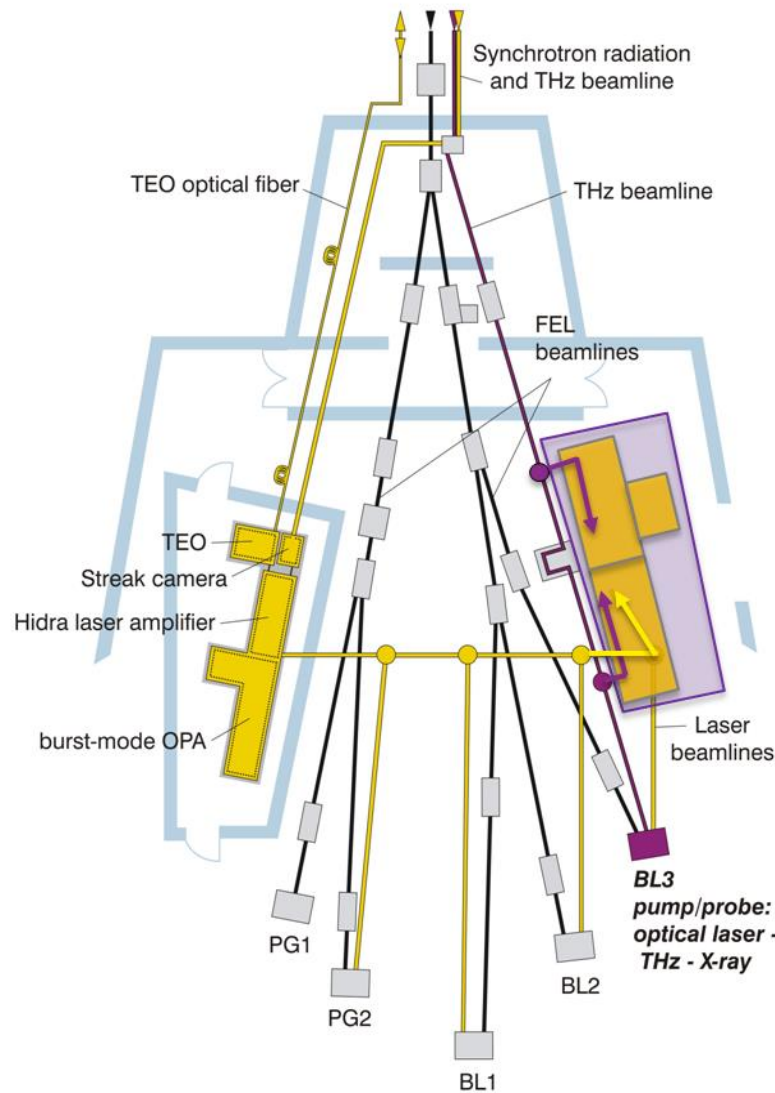
FLASH1 experimental hall – Albert-Einstein hall



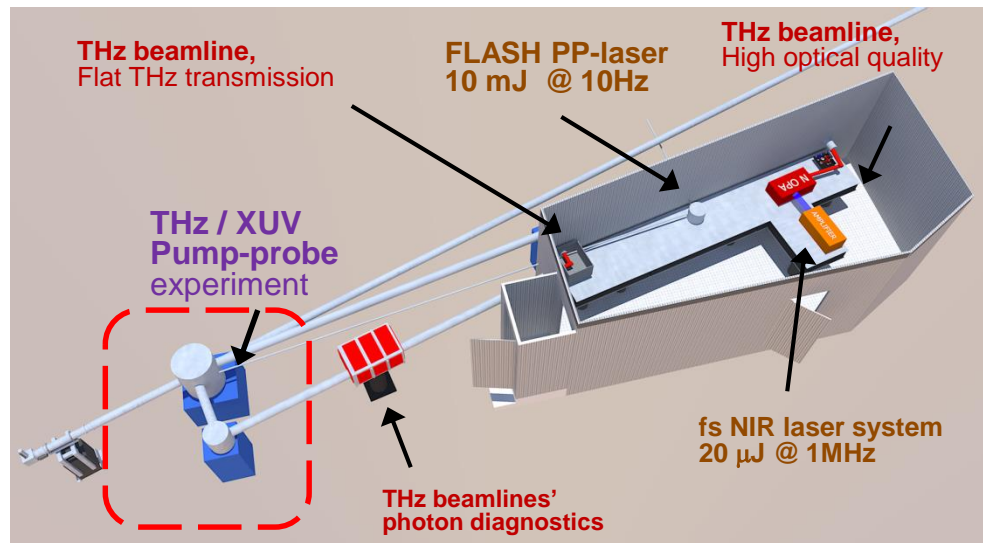
FLASH2 experimental hall – Kai Siegbahn hall



THz beamline at FLASH



THz laboratory and THz/XUV beamline



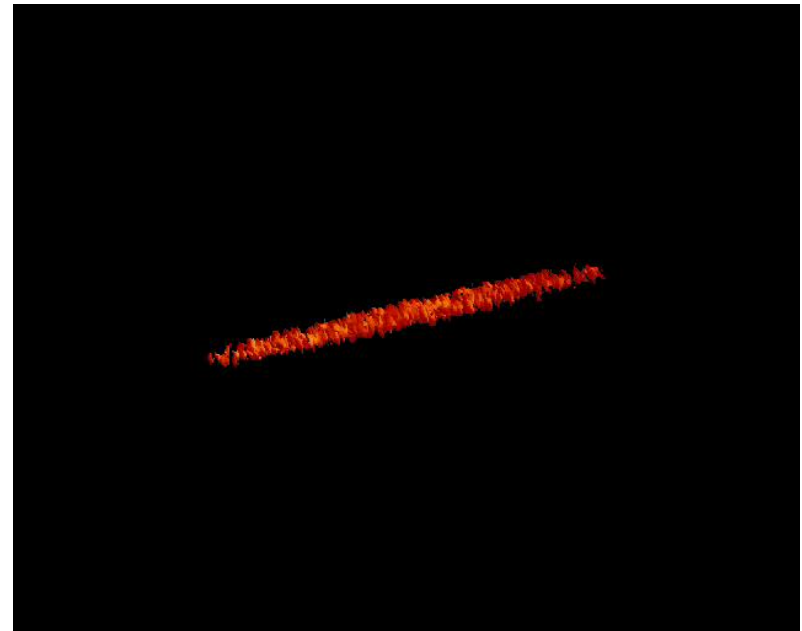
THz hutch laser (synchronized to FLASH):

- Wavelength: 1030 nm, 515 nm
- Rep. rate: 2 MHz
- Pulse energy: 100 μ J
- Avg. power: 20 W

Diagnostic tools for FELs.

What kind of diagnostic tools do user need to make efficient use of FELs?

- intensity
- beam position
- focus size
- spectral distribution
- temporal radiation pulse profile
- coherence
- polarization



Courtesy S. Reiche

**Due to the SASE specific shot-to-shot fluctuation the users need
most of this information for every single pulse
=> online, non-destructive**

Light characterisation at FLASH - Introduction.

The *Atomic Photoionization Process* is a perfect candidate for non-destructive, pulse-resolved photon metrology tools.

- | | |
|------------------------------------|---|
| ➤ intensity | Gas-Monitor Detectors (GMD) |
| ➤ beam position | GMD Split Electrodes |
| ➤ focus size | Wigner-Distribution Measurement |
| ➤ spectral distribution | Photoionization spectra |
| ➤ temporal radiation pulse profile | Non-linear autocorrelation or
(THz or angular) streaking |
| ➤ coherence | Wigner-Distribution Measurement |
| ➤ polarisation | Angular photoemission distribution |

The effort for developing such detector systems is extremely high, in particular due to the tight requirements on robustness and reliability.

Requirements for Intensity and Beam Position Detectors

- cover full dynamic range: ~ 6 - 7 orders of magnitude from spontaneous emission to SASE in saturation
- on-line pulse resolved detectors (non-destructive with respect to the beam)
- low degradation under radiant exposure by FEL beam with a peak power of few GW; high linearity
- ultra-high vacuum compatibility

No commercial detectors available!

Gas-monitor detectors for online intensity and beam position monitoring

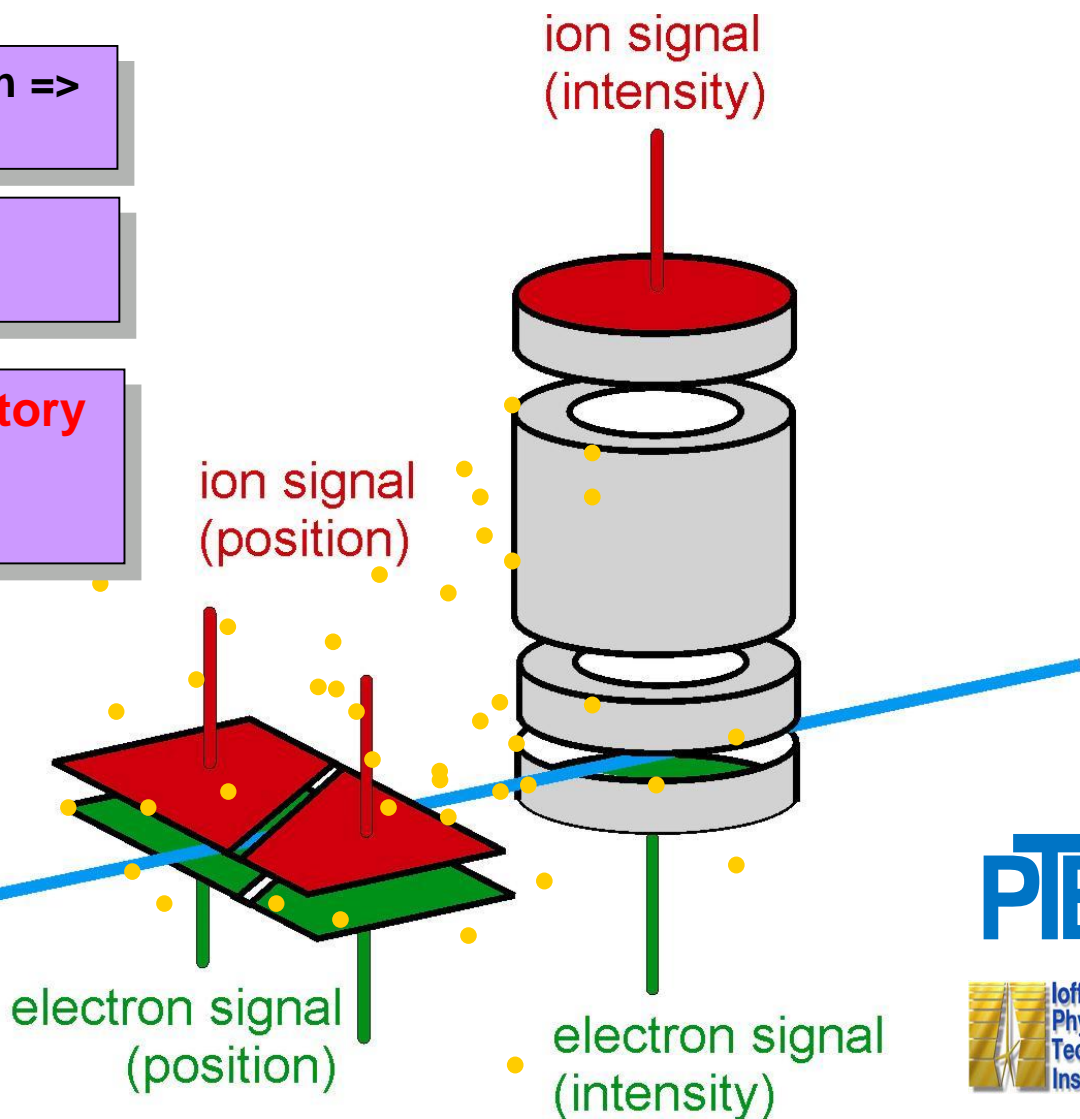
Based on atomic photoionization =>
no degradation, indestructible

Low particle density =>
transparent

Calibrated in the PTB laboratory
Uncertainty for the pulse
energy: less than 10%

Photon beam

$10^{-6} - 10^{-4}$ mbar



Reference number at the German Patent Office: 102 44 303

Equation behind the Gas-Monitor Detector

Number of particles detected (electrons or ions). Average photoionization charge needed to evaluate.

$$N_{\text{particle}} = N_{\text{photon}} \cdot \sigma(\hbar\omega) \cdot z \cdot \eta \cdot n = N_{\text{photon}} \cdot Q.E.(\hbar\omega)$$

Cross Section

Detection Efficiency

Atomic Gas Density (requires temperature and pressure info)

Charge accumulated by the detector

Detector Acceptance Length

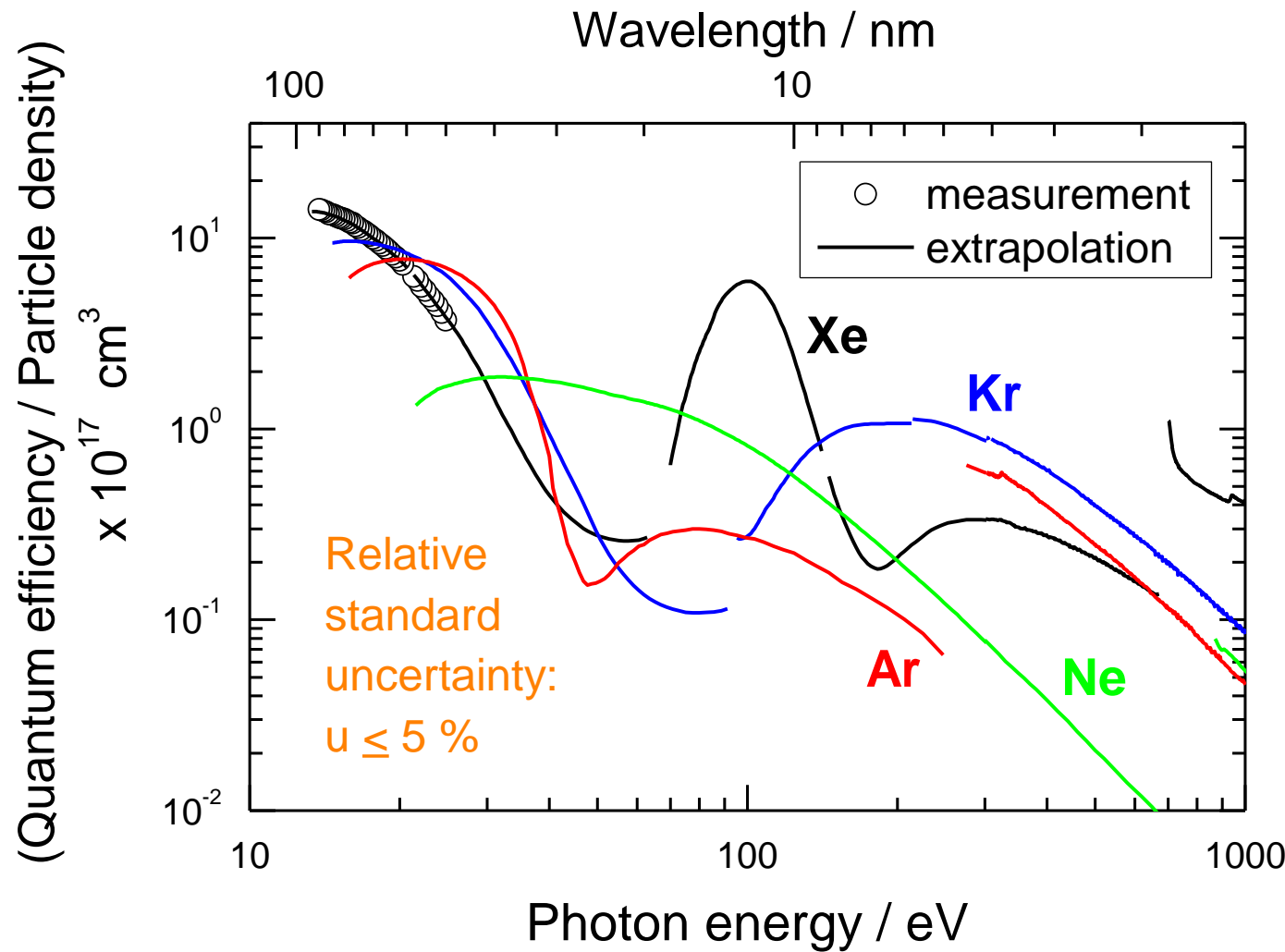
$$N_{\text{particle}} = \frac{Q}{e \cdot \gamma}$$

Elementary charge

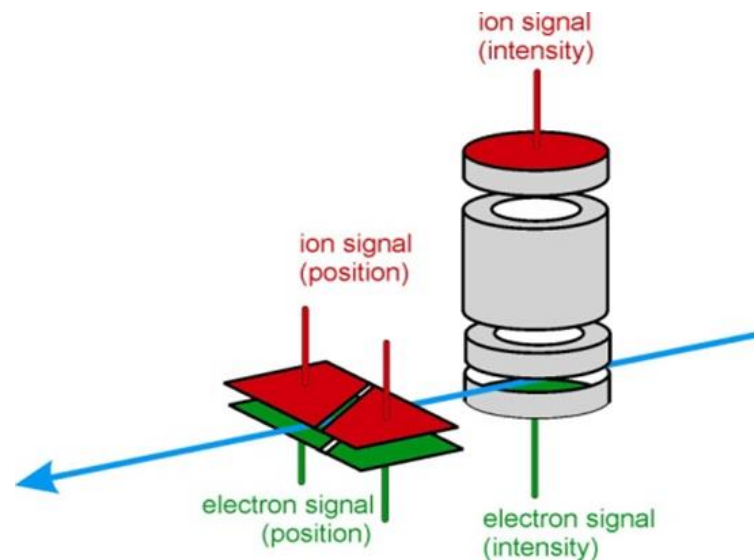
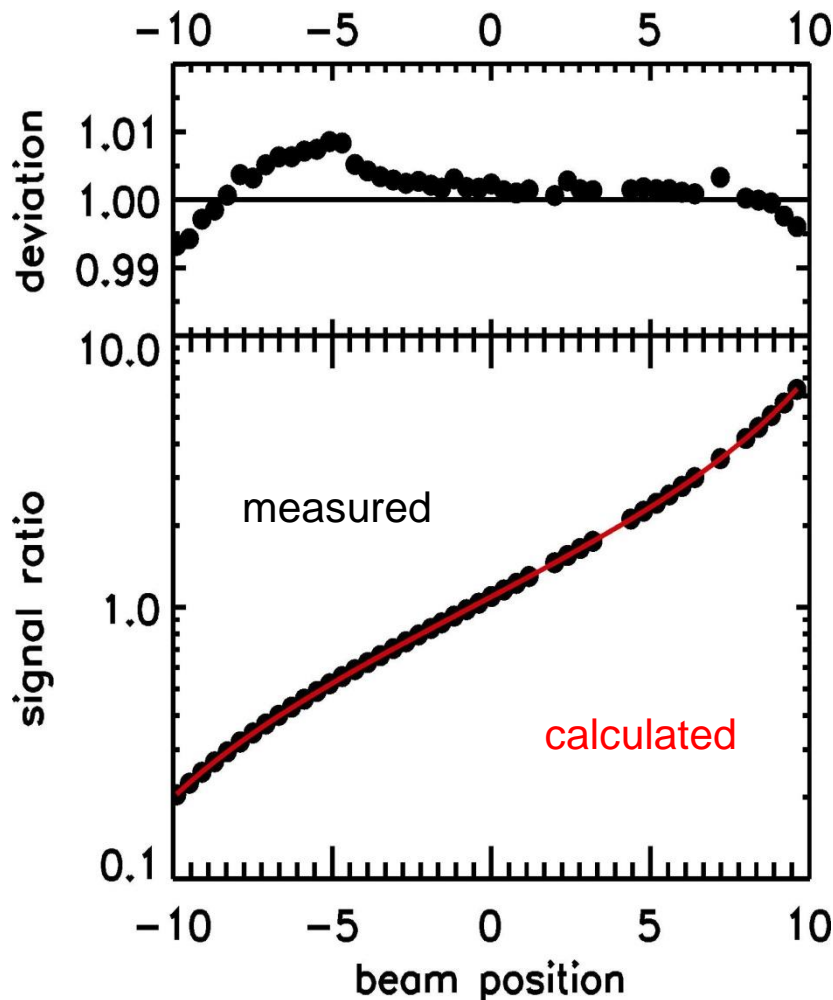
Mean ion charge

Quantum Efficiency of the FLASH GMD

calibrated in the PTB laboratory at BESSY II.



Beam position monitor

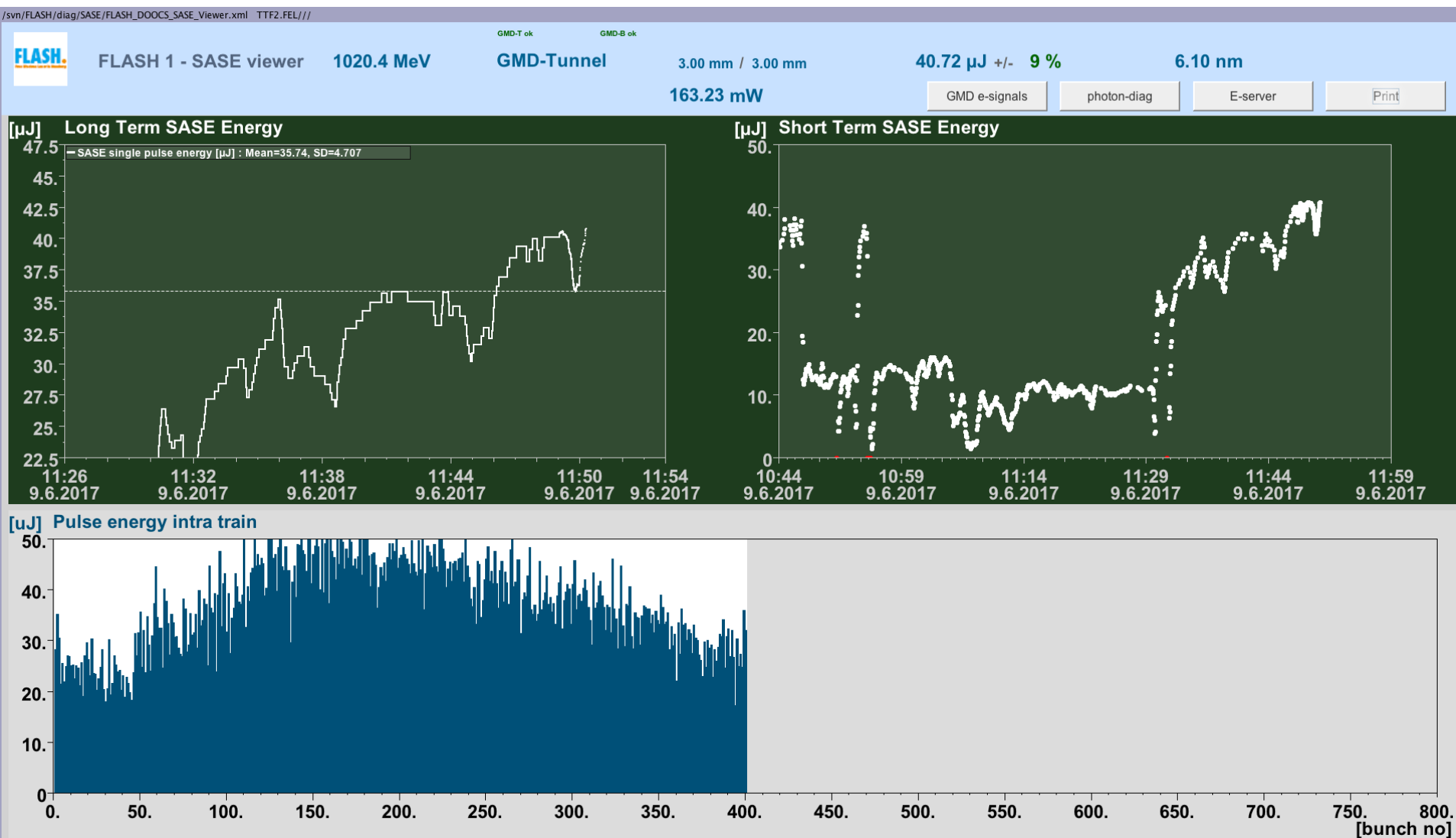


Accuracy for on-line measurements of relative beam positions: $\sim 20 \mu\text{m}$

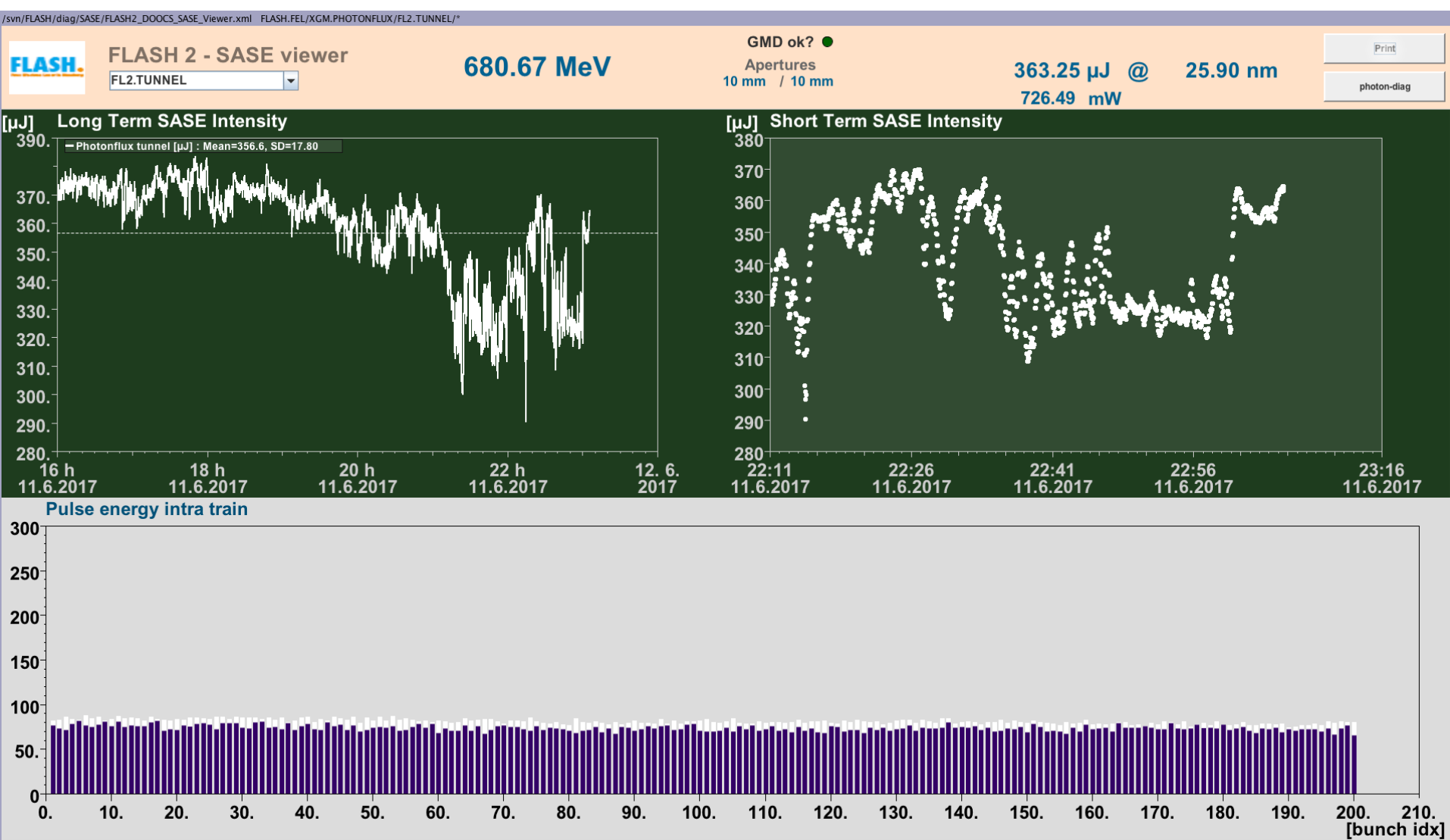
Two gas-monitor detector sets, which are 20 m apart, allow on-line monitoring of the angle: $\sim 1 \mu\text{rad}$

In collaboration with PTB in Berlin and IOFFE institute St. Petersburg

Example performance – FLASH 1



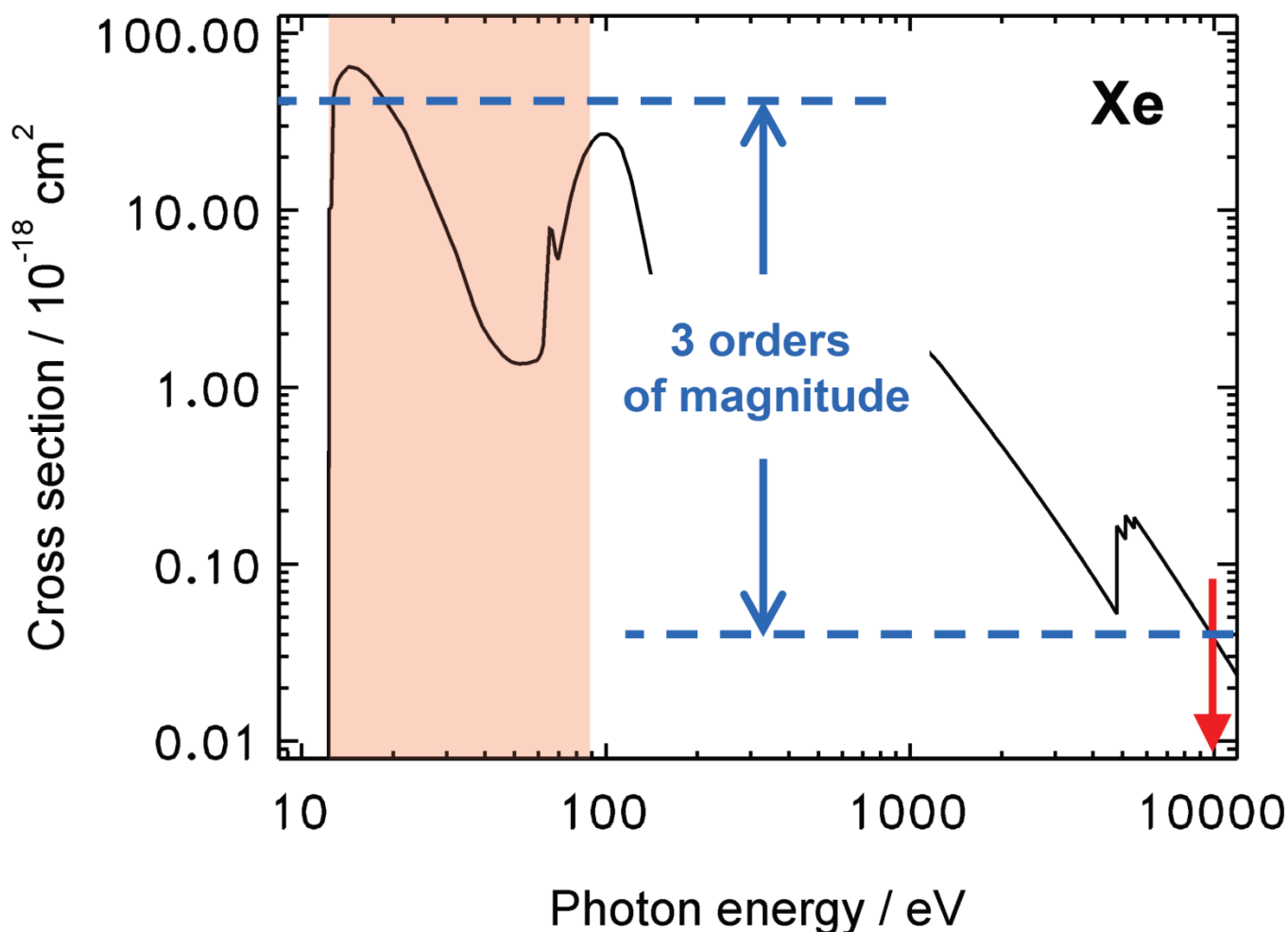
Example performance – FLASH 2



Specification of the intensity measurements for European XFEL

- Photon energy range: up to 12.4 keV (TDR) **(presently >24 keV)**
- Number of pulses per second: 30000
- Time resolution: < 200 ns
- Uncertainty for the pulse energy: <10 %
- Relative uncertainty (pulse to pulse): < 1 % (for more than 10^{10} photon per pulse)
- Operating pressure: 10^{-6} mbar – 10^{-4} mbar

Photoabsorption cross sections of Xenon



B.L. Henke et al., Atomic Data and Nuclear Data Tables **54**, 181-342 (1993).

3rd generation GMDs for European XFEL

- Measured uncertainty due to statistical nature of photoionization:

$$\delta = \frac{\sqrt{N_{\text{ion}}}}{N_{\text{ion}}} = \frac{1}{\sqrt{N_{\text{ion}}}} \quad \Rightarrow \quad \delta = 1 \% \quad \text{if } N_{\text{ion}} = 10^4 \text{ ions generated per pulse}$$

- What the detector size should be?

Photon energy: 12.4 keV

Target gas Xe: $\sigma = 0.021 \text{ Mb}$ ($q \approx 8$)

Pressure: $p = 10^{-4} \text{ mbar}$ ($n_{\text{atom}} = 2.4 \times 10^{12} \text{ cm}^{-3}$)

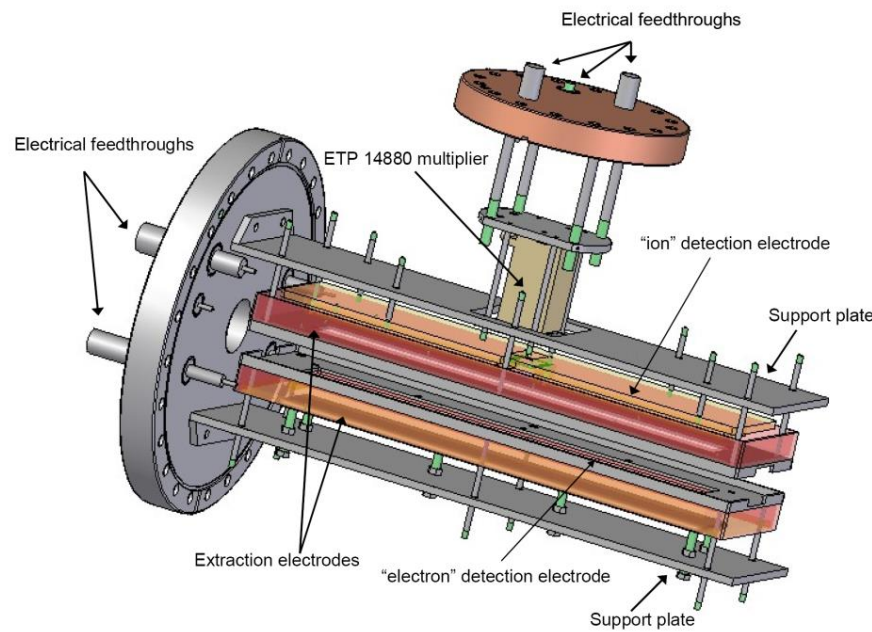
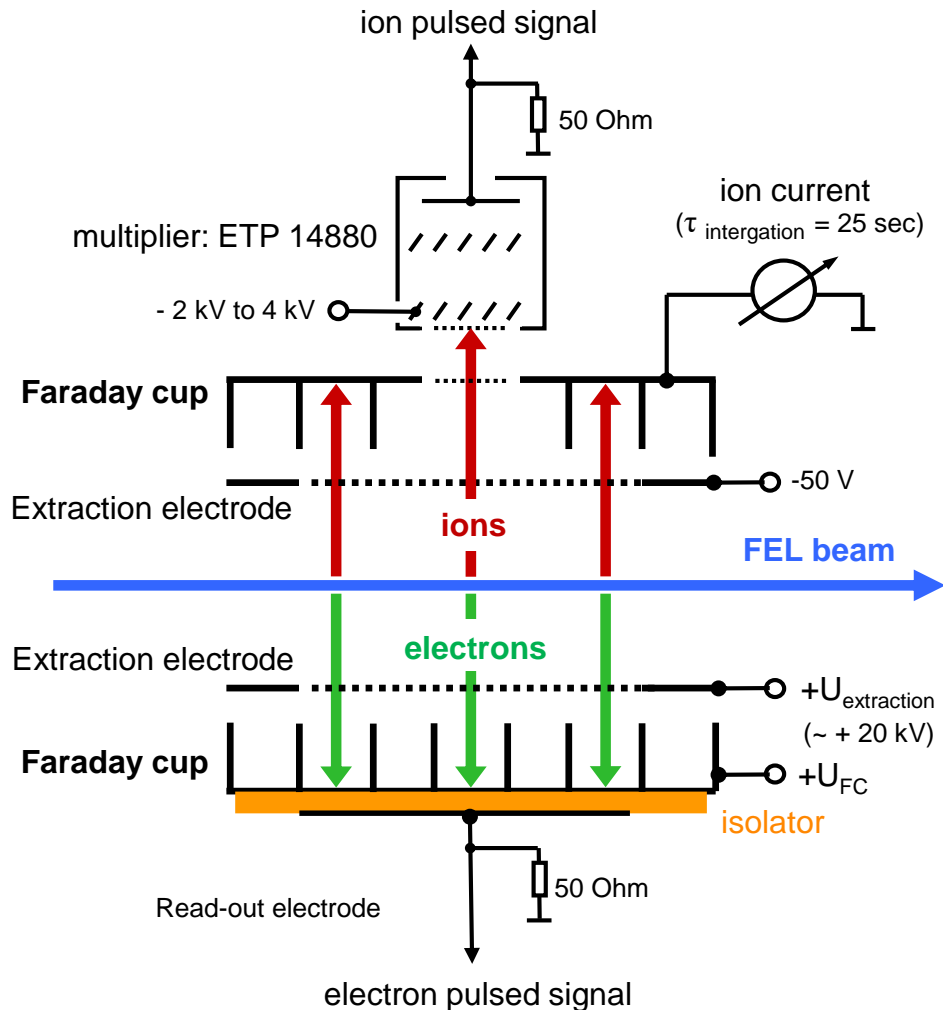
Number of photons per pulse: $N_{\text{photon}} = 10^{10}$

Effective length z :

$$z = \frac{N_{\text{ion}}}{N_{\text{photon}} \cdot \sigma_{\text{ph}}(\hbar\omega) \cdot n_{\text{atom}}}.$$

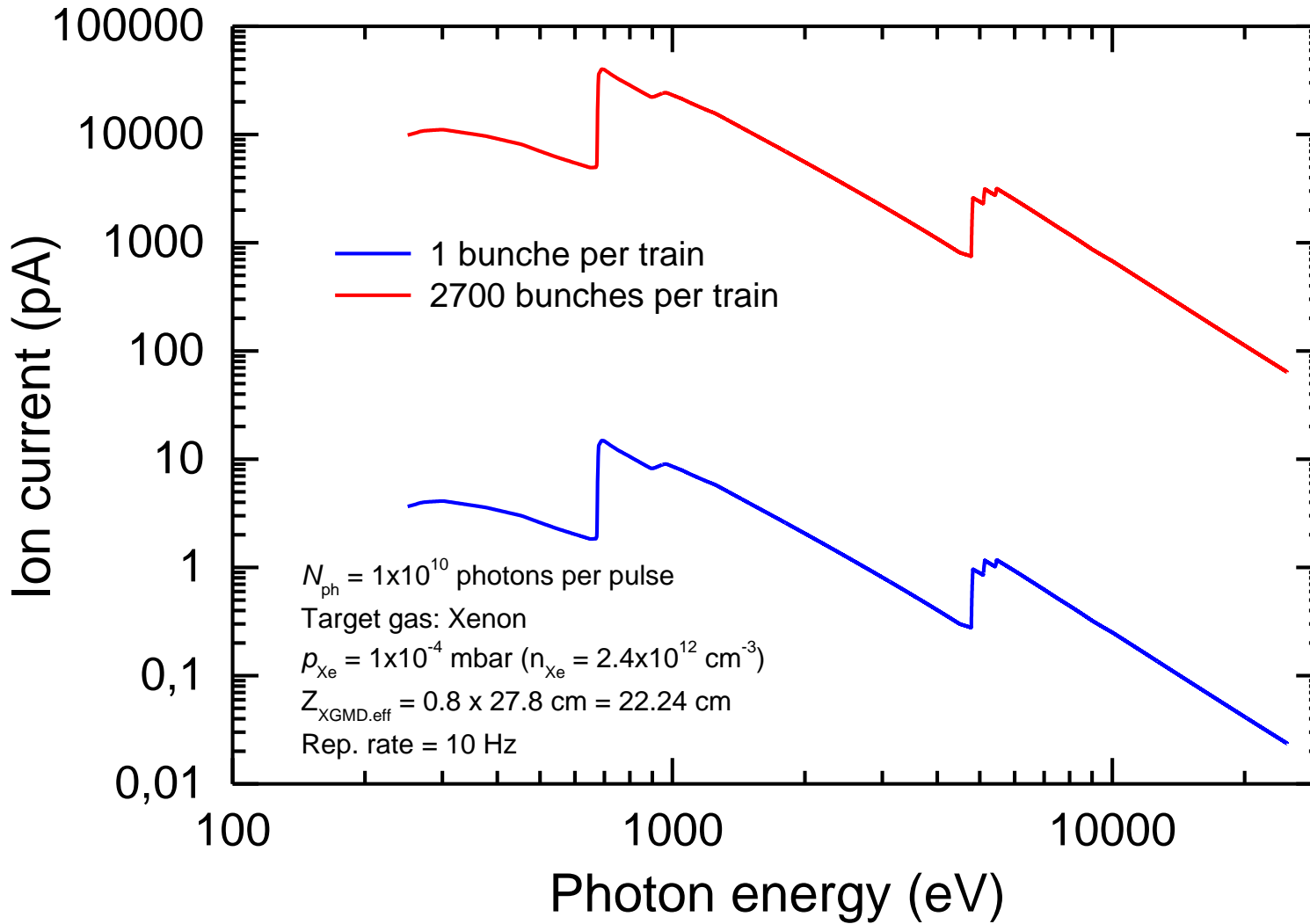
Minimum length : **Z = 20 cm !!!**

3rd generation GMD for European XFEL

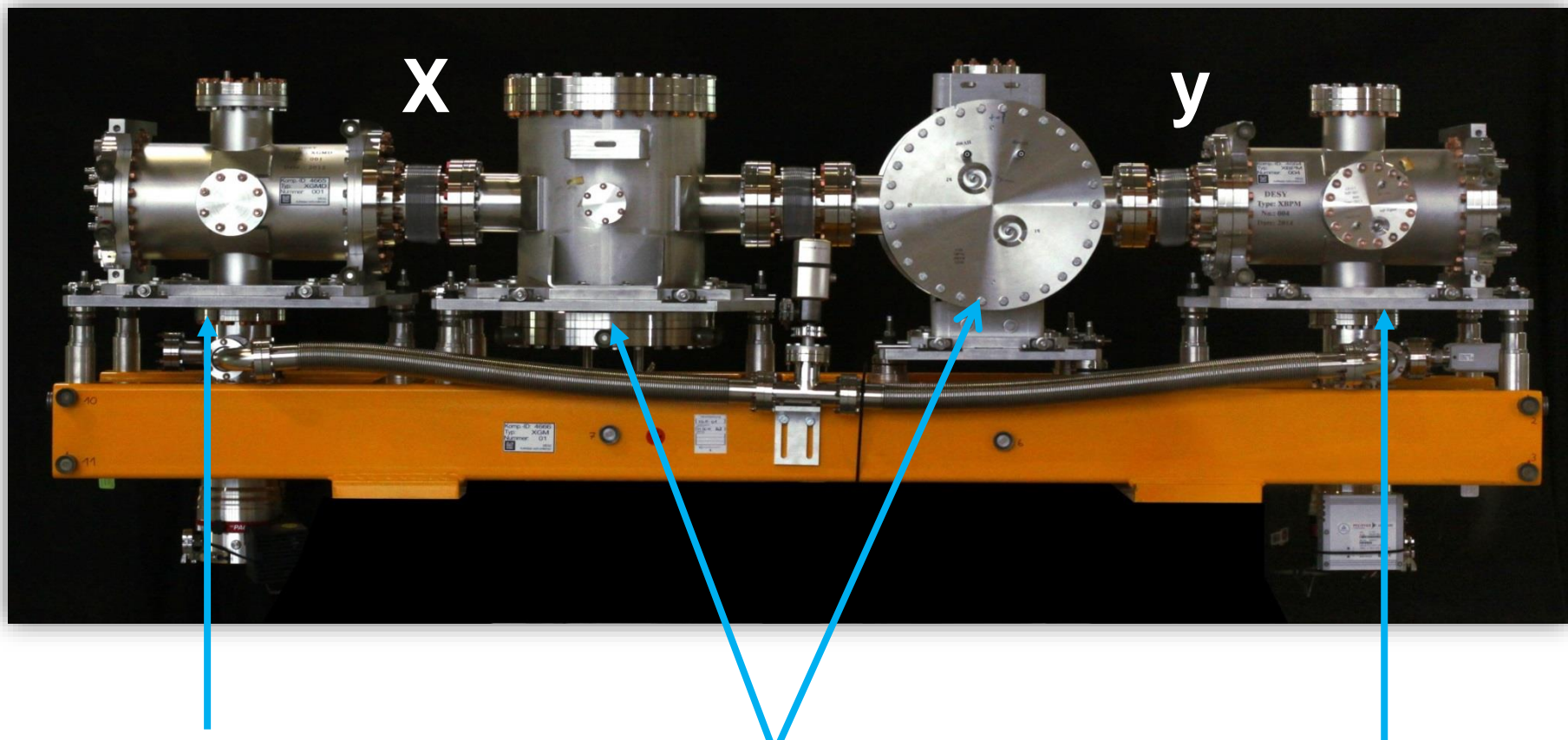


High extraction voltage of up to 20 kV – 30 kV has to be applied to prevent detection of highly energetic photoelectrons by the ion detector.

XGMD signal: average ion current from Faraday



XGM for European XFEL and SwissFEL: Intensity and beam position with an extended dynamic range.



XGMD with split Faraday cup detection electrodes (horizontal beam position)

Two HAMPs with huge area open electron multipliers each equipped with a pair of split anodes (horizontal X and vertical Y beam position)

XGMD with split Faraday cup detection electrodes (vertical beam position)

Example – European XFEL – SASE 1,2,3



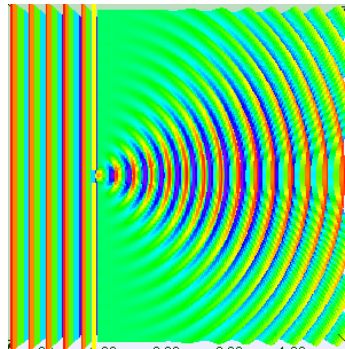
Spectral distribution

Principle of a diffraction grating

- > Light is a wave -> diffraction occurs
- > Huygens–Fresnel principle
-> principle of superposition of waves
- > Grating equation

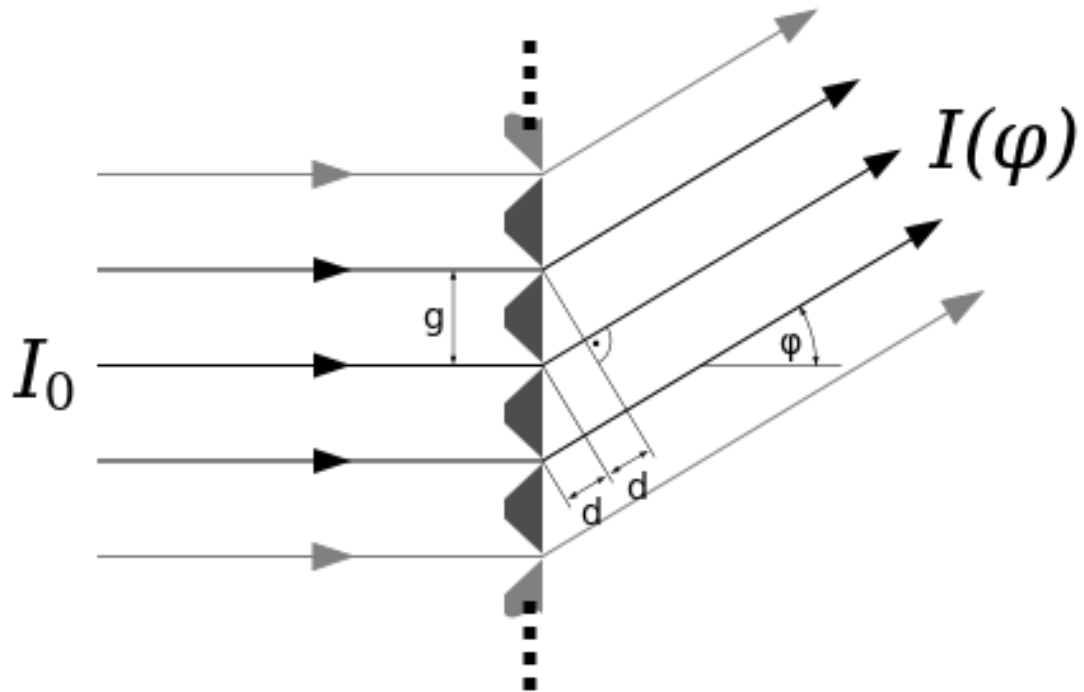
$$d_m = g \cdot \sin \varphi_m = m \cdot \lambda, \quad m \in \mathbb{N}$$

- > Angle of diffracted light
is wavelength dependent!

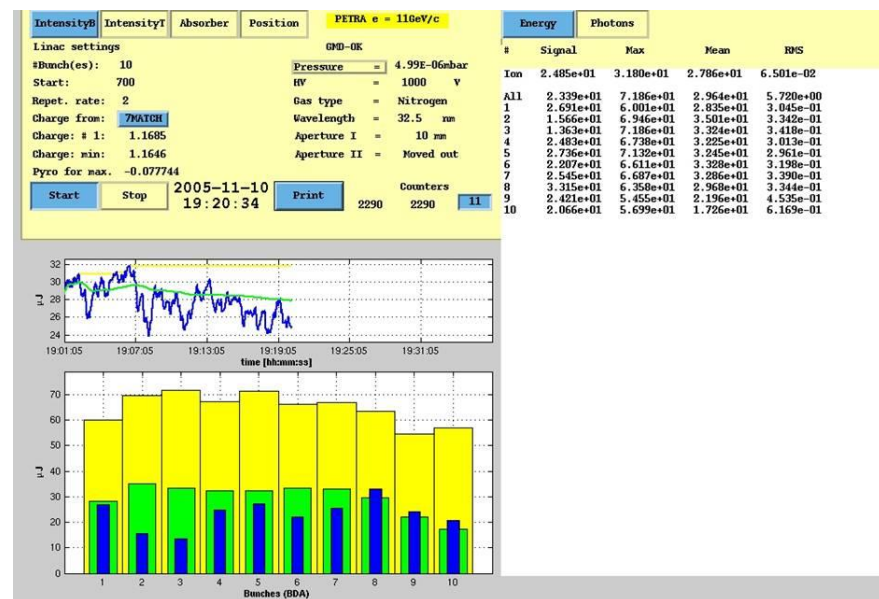
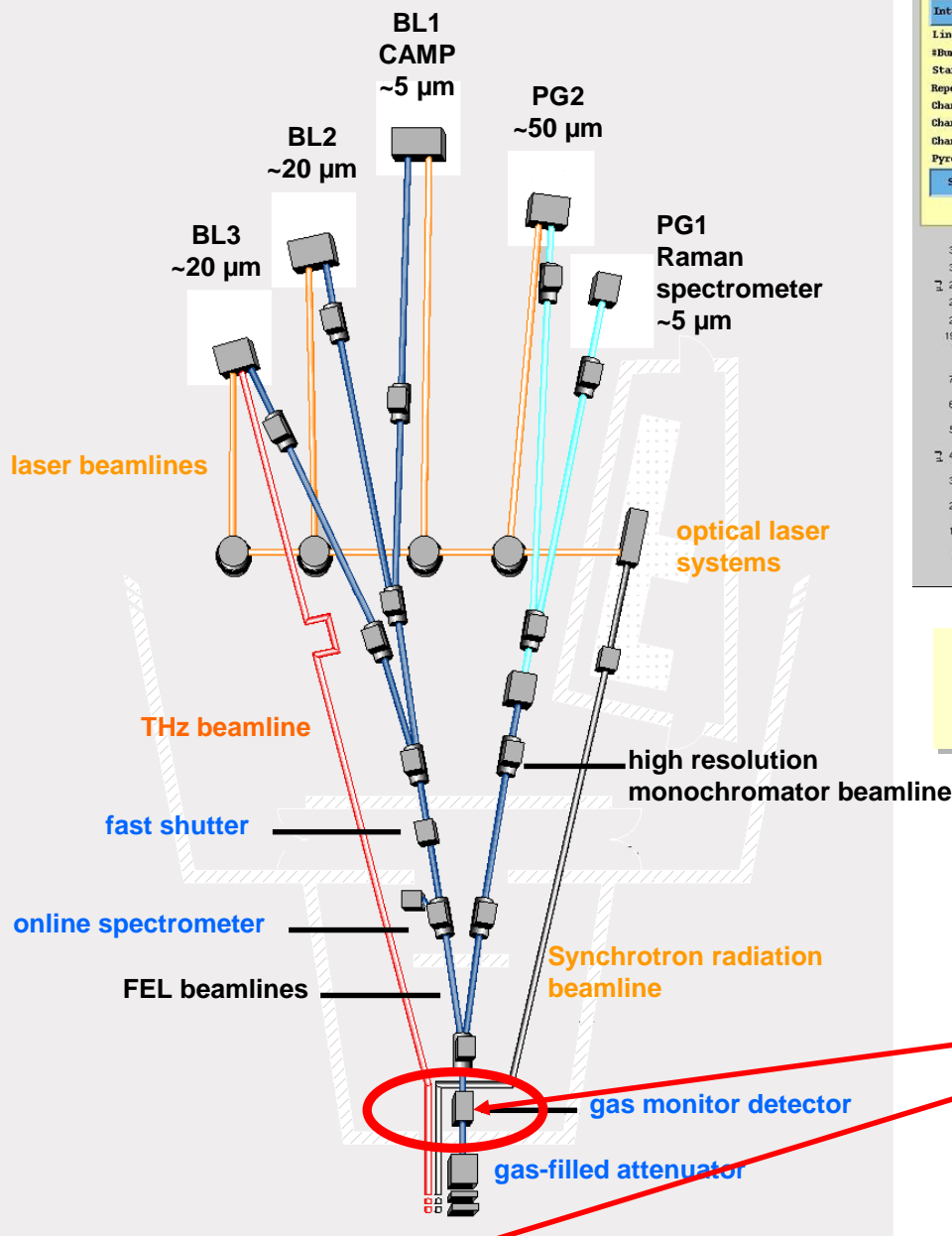


Example: num.
approx.

slit width =
wavelength



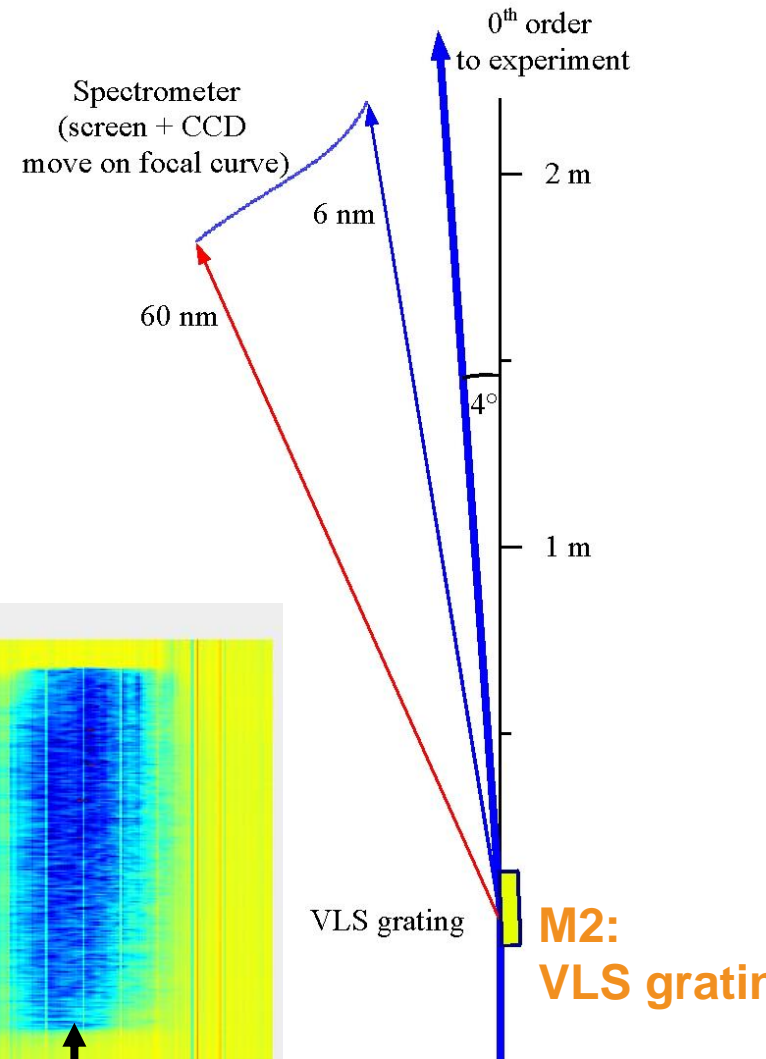
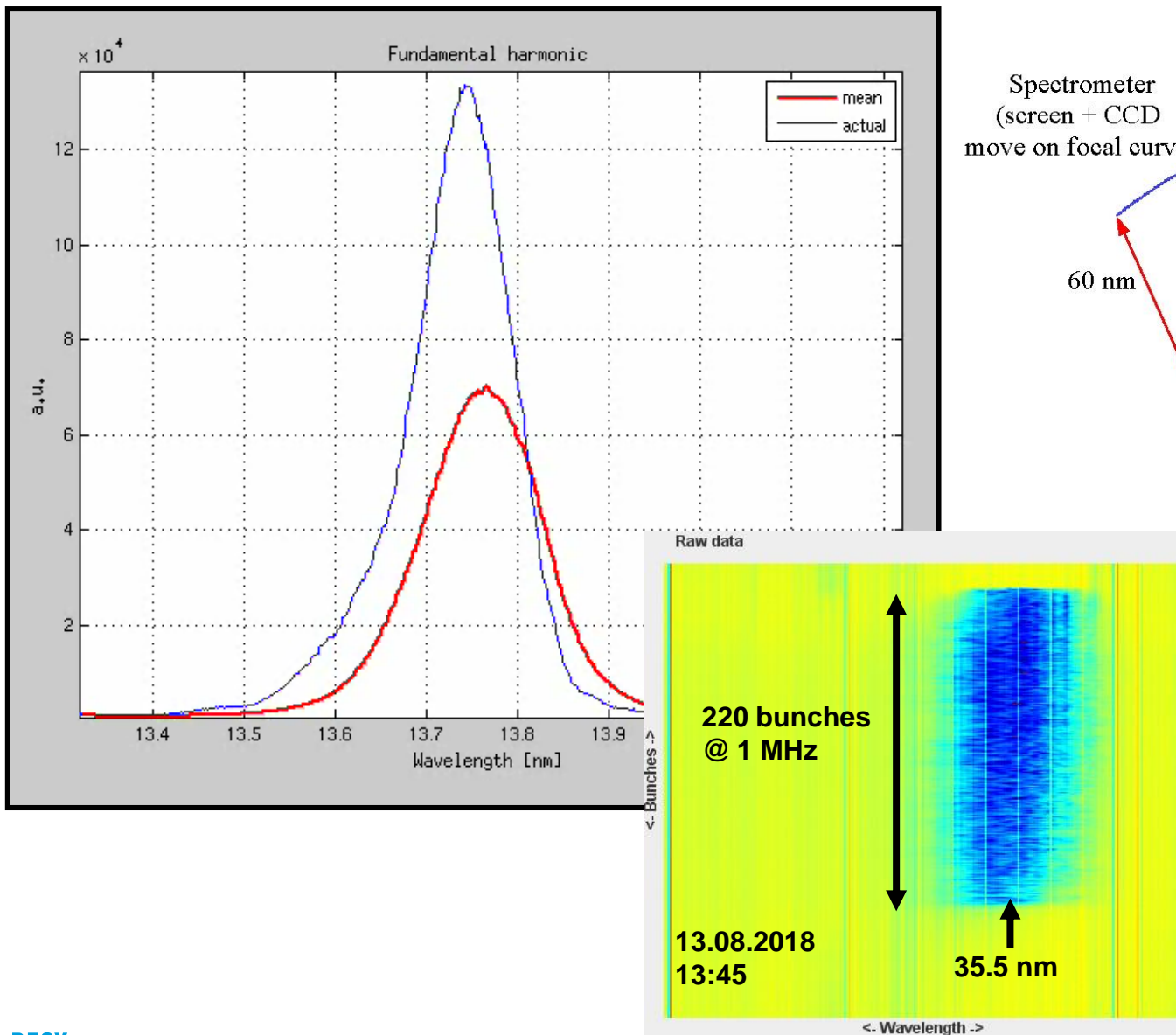
Light transportation – FLASH1 beamlines



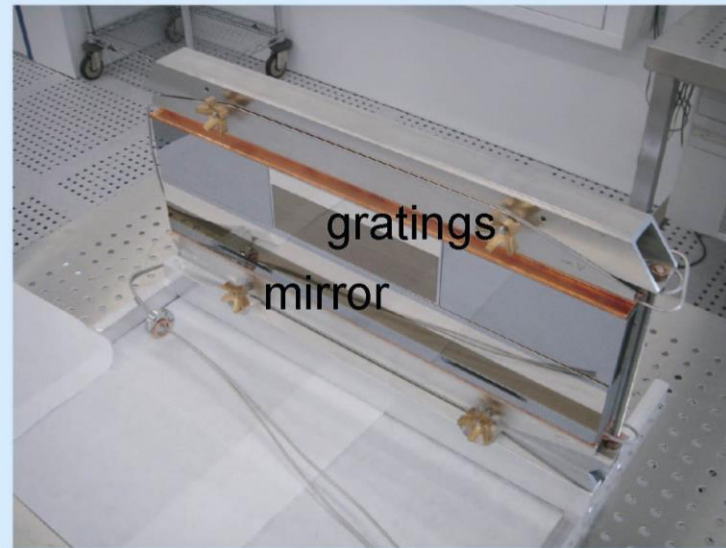
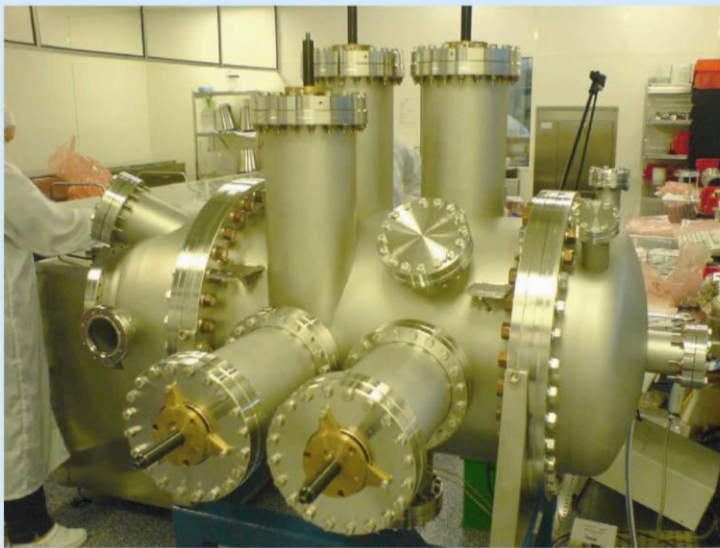
Two gas monitor detector sets: before and behind the gas attenuator



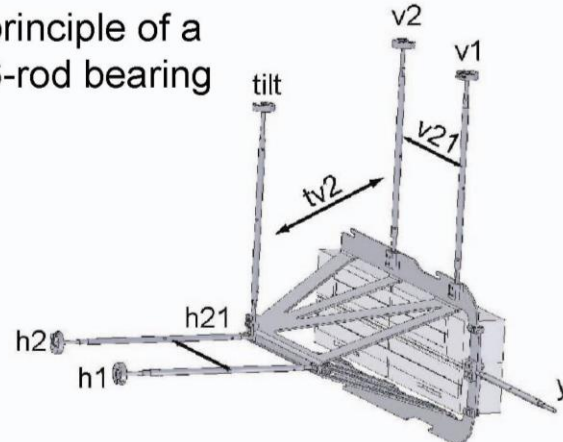
VLS online Spectrometer



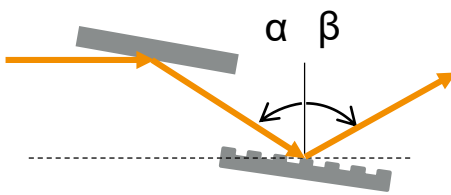
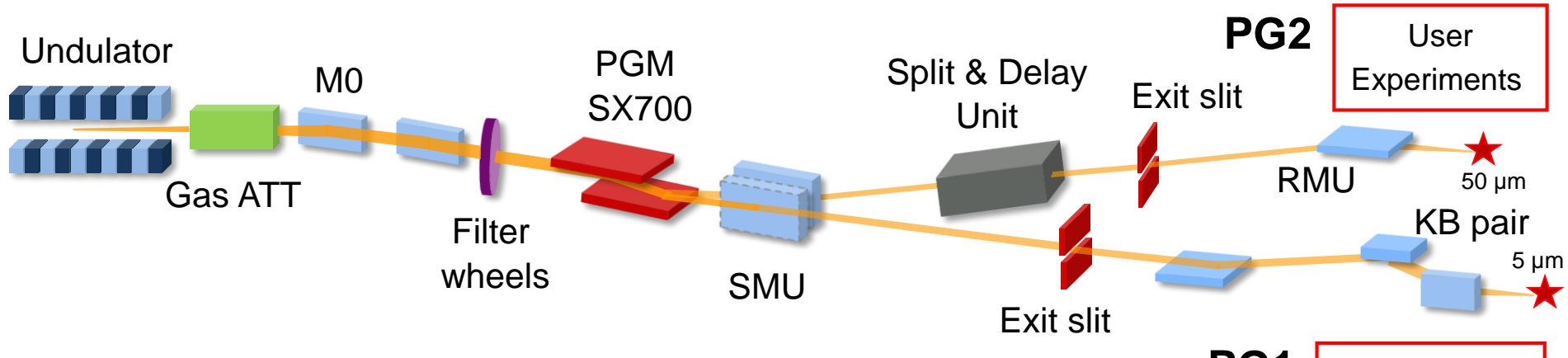
VLS online spectrometer for single pulses



principle of a
6-rod bearing



Plane Grating (PG) Monochromator Beamline



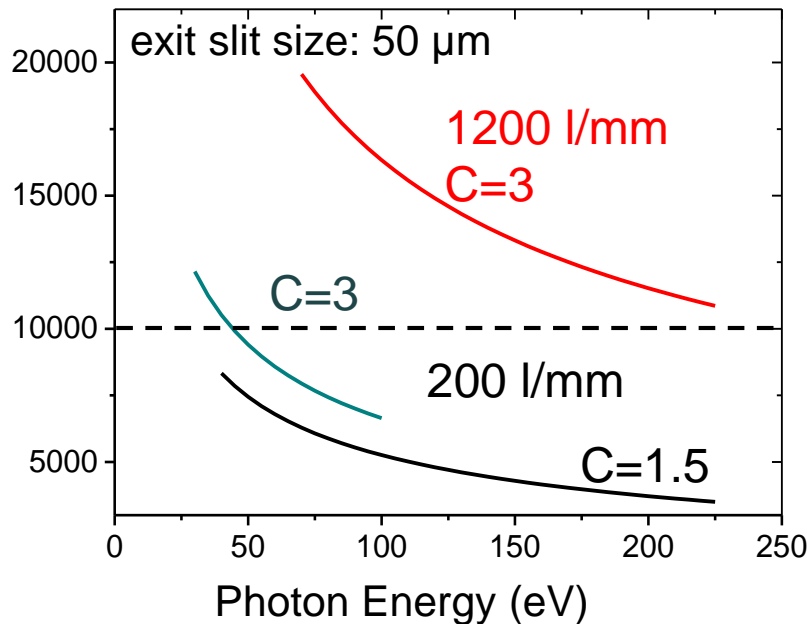
$$c_{ff} = \frac{\cos \beta}{\cos \alpha}$$

- 2 beamline branches PG1 & PG2
- Slitless operation
- High flux mode/high resolution mode
- 0th order operation
- PG2 spectrometer mode available

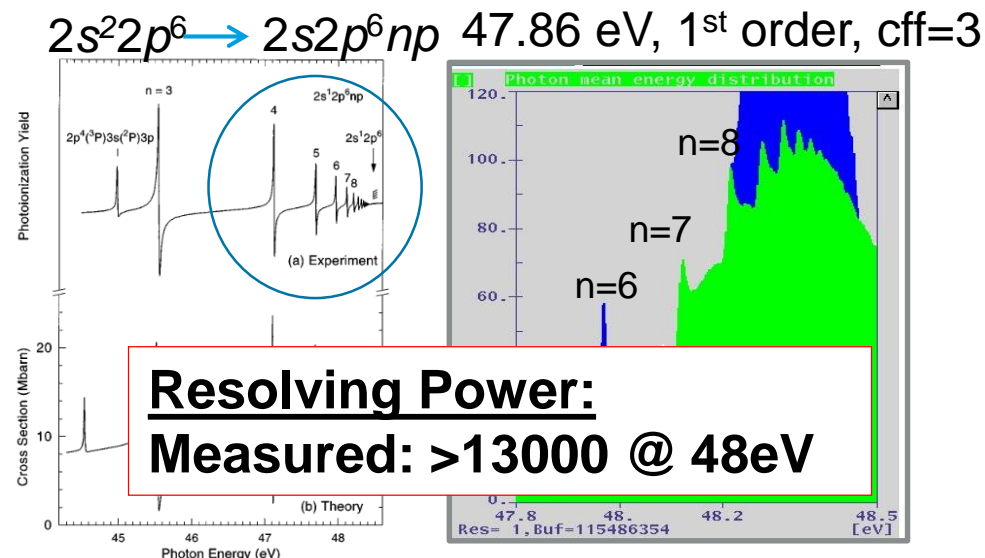
PG Monochromator Beamline - Performance

- Photon energy range: 20...250 eV (fund.) (...600eV 3rd harm.)
- Resolving power : >10⁴
- Photon Flux: 10⁹...10¹² photons/pulse
- Spot size at sample: 40 x 100 μm (h x v)

Resolving Power



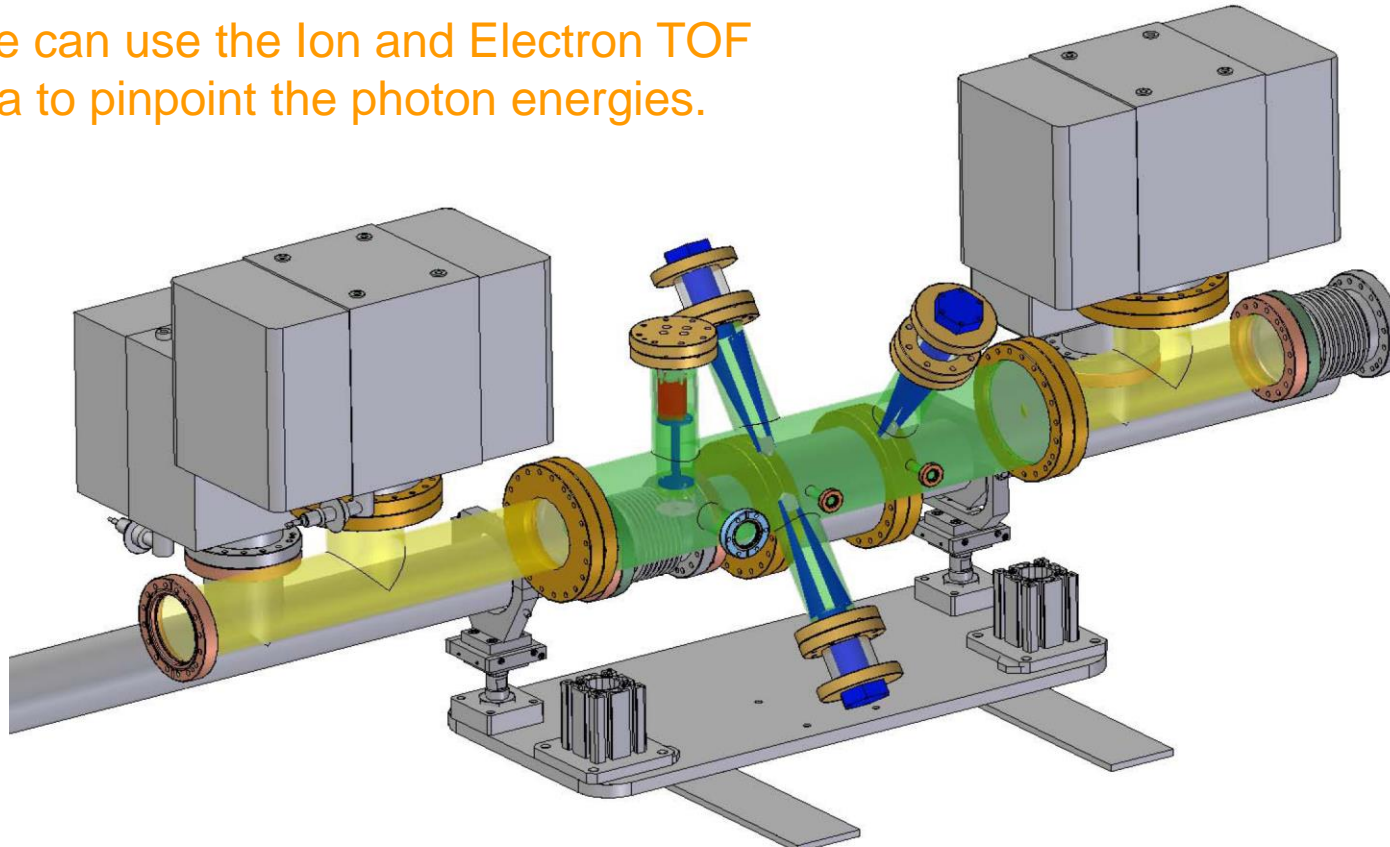
Calibration: using Ne gas absorption lines



PG in spectrometer mode

Online determination of the spectral distribution using ion and electron TOF spectrometer

One can use the Ion and Electron TOF data to pinpoint the photon energies.



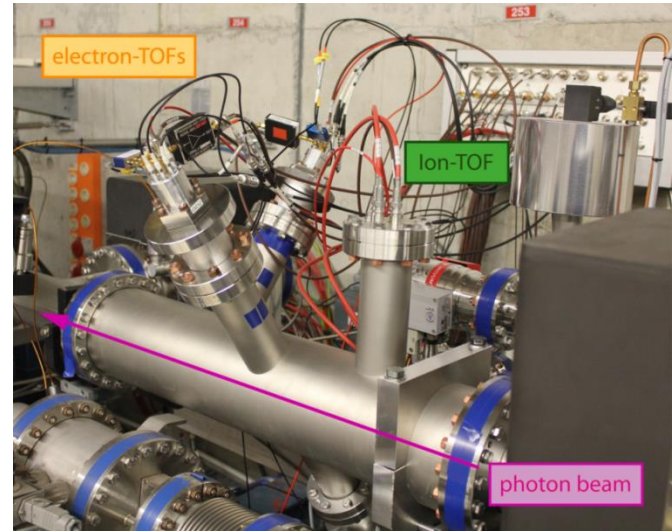
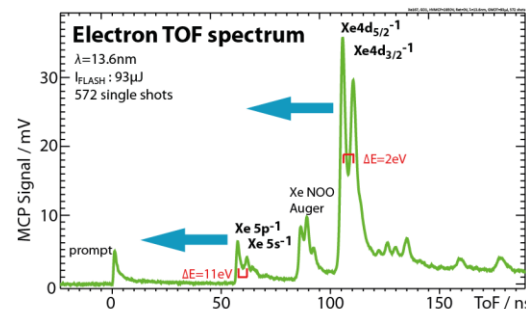
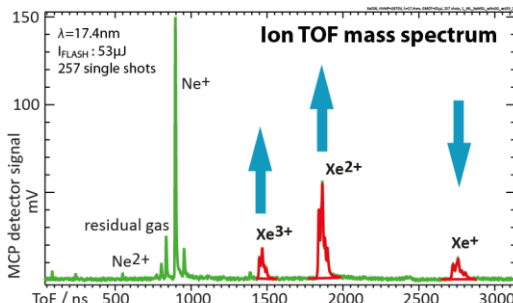
M. Wellhöfer, J. T. Hoeft, M. Martins, W. Wurth, M. Braune, J. Viefhaus, K. Tiedtke, M. Richter,
Photoelectron spectroscopy as a non-invasive method to monitor SASE-FEL spectra. JINST 3, P02003 (2008)

Cross-calibration campaign of OPIS using PG2

OPIS - Online Photoionization Spectrometer:

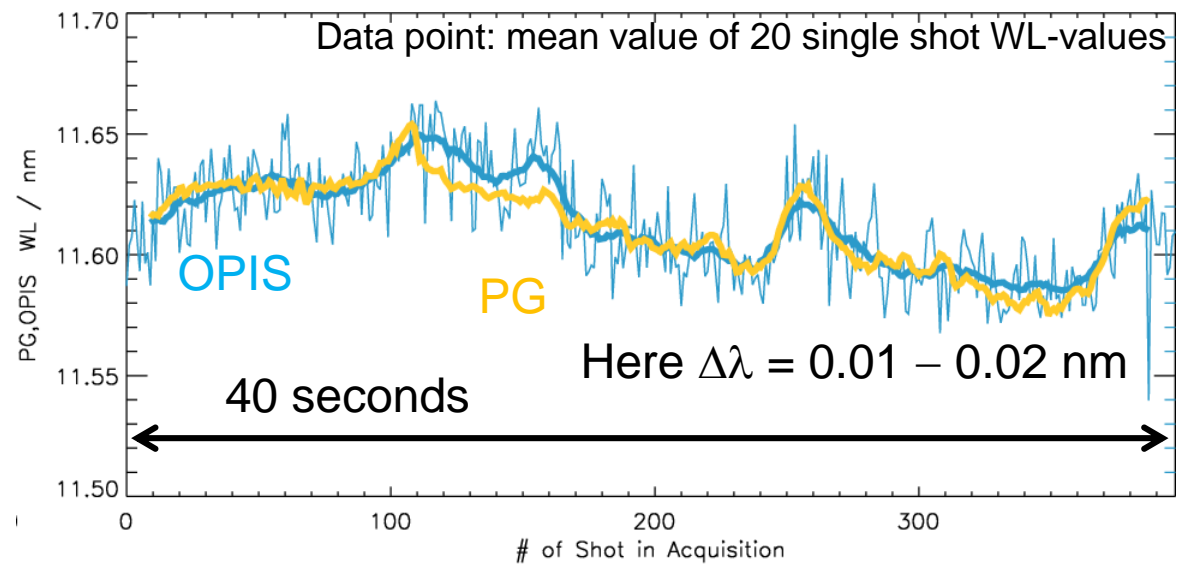
- installed in FLASH1 tunnel
- Online wavelength monitoring

Using Ion and Electron TOF to determine the FEL wavelength



FEL wavelength (moving average)

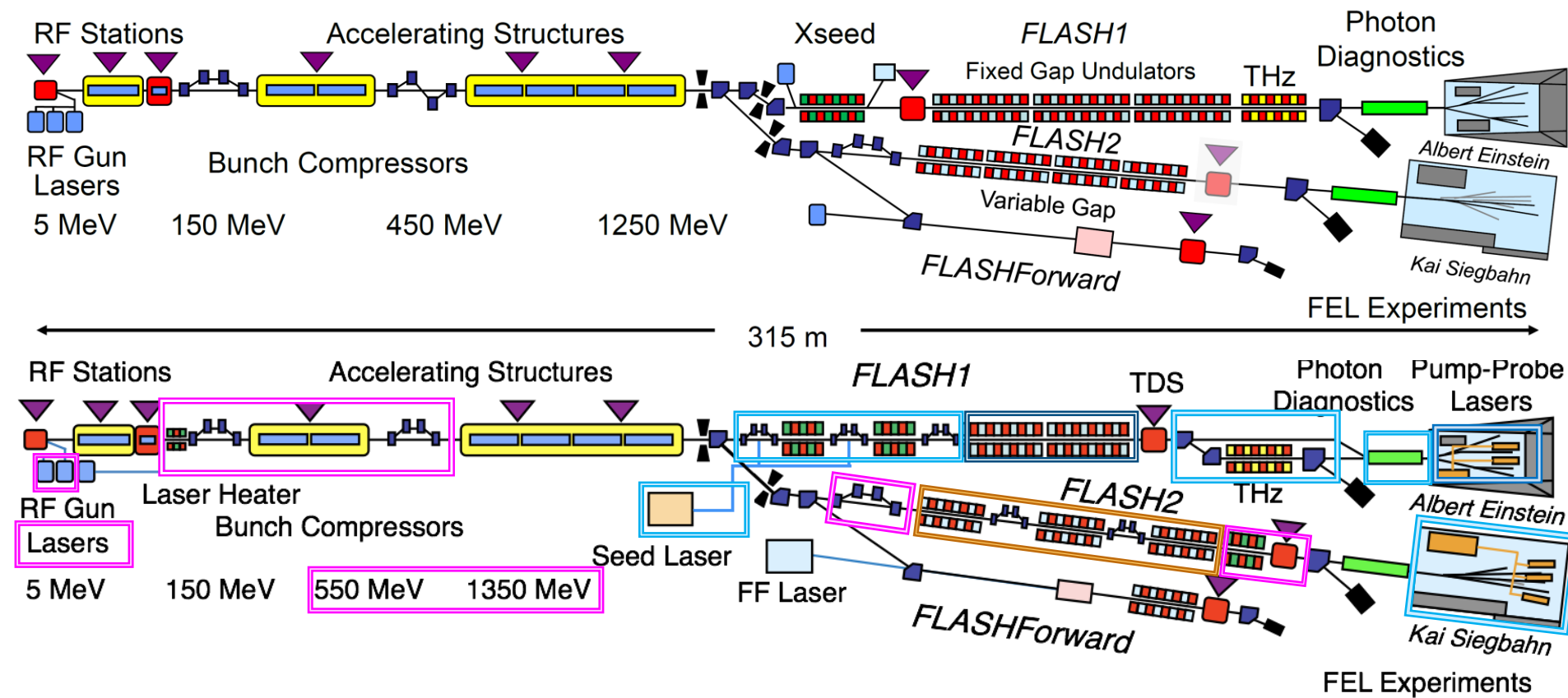
- Cross calibration campaign
- OPIS, PG spectrometer, CS spectrometer & VLS spectrometer
- Range 5-31 nm



FLASH2020+

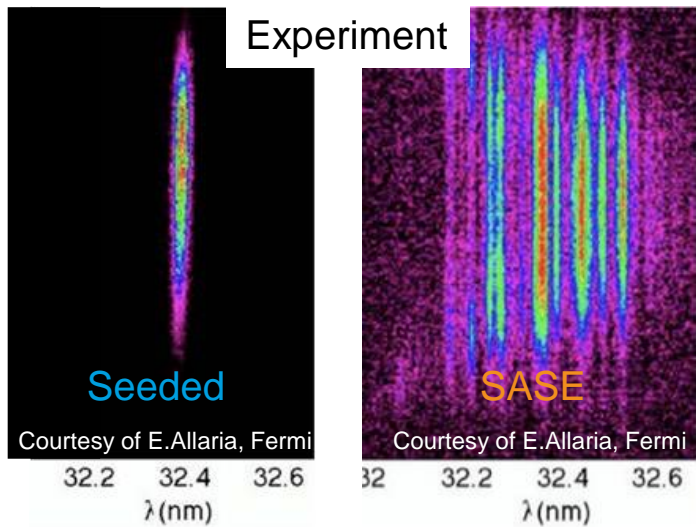
FLASH 'now' vs 2025

FLASH2020+ Upgrades of the facility

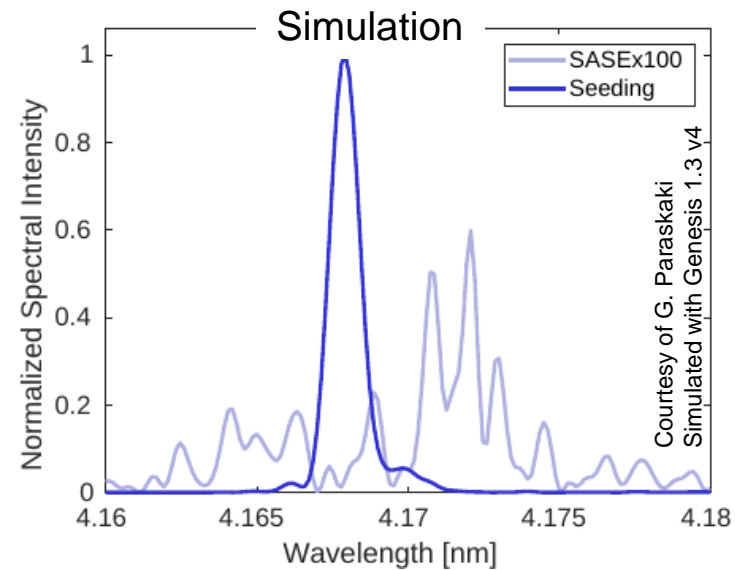
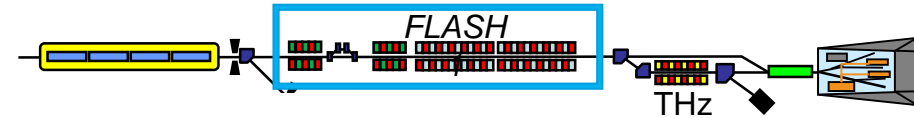


Difference between seeded and SASE pulses

Advantages of seeded FELs



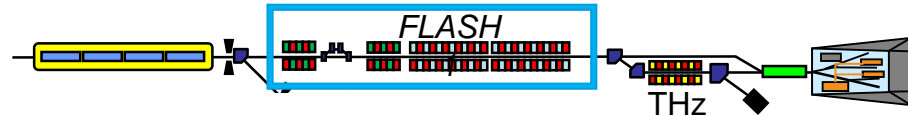
- | Seeded | |
|--------------------------|-------------------------------------|
| • Narrow bandwidth | • Laser controlled pulse properties |
| • Stability | • Synchronisation to seed laser |
| • Longitudinal coherence | |
| • Brilliance | |



- | SASE | |
|-------------------|--|
| • Pulse energy | |
| • Repetition rate | |

FLASH2020+ seeding in FLASH1

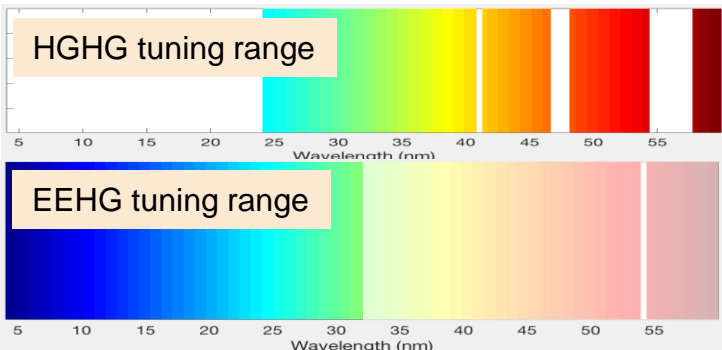
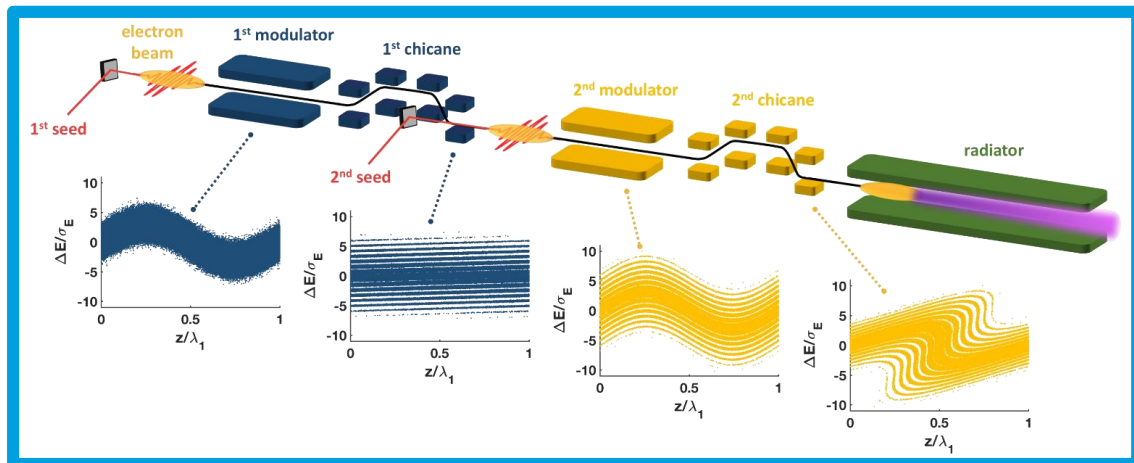
Starting from 2025 1 MHz coherent pulses in soft-X-ray



Combination of HGHG and EEHG:

Fully coherent pulses with variable wavelength (60 – 4 nm) tens of fs duration and 1 MHz repetition rate.

Apple III undulators:
Variable polarization



Successful seeding relies on **high quality** e-beam and seed lasers:

- Linac upgrade
- R&D for optimal lasers
- Seeding development

Seed 1: ~343 nm, 100 MW, 500 fs

Seed 2: 297-317 nm, 300 MW, 50 fs

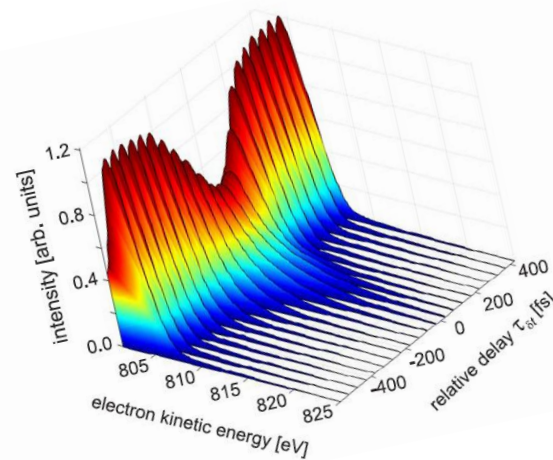
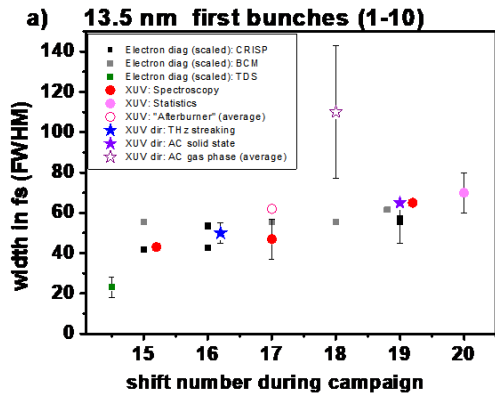
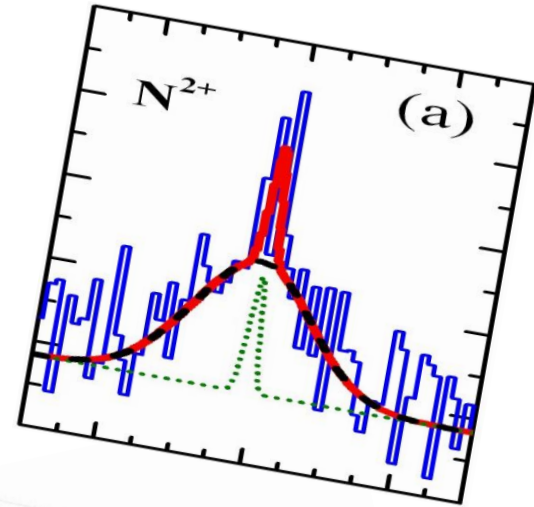
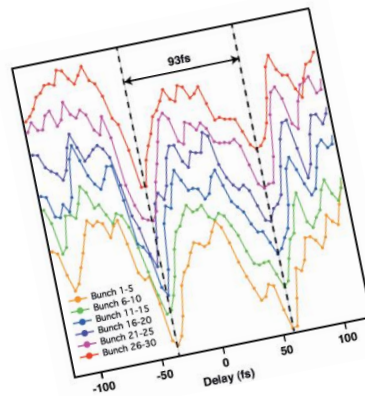
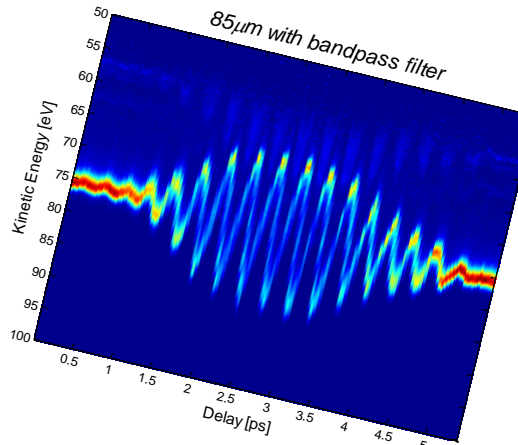
Thanks to S. Ackermann, T. Lang, M. Kazemi, M. Tischer

Thank you for your attention



Temporal distribution

Simultaneous Measurement of Electron and Photon Pulse Duration at FLASH



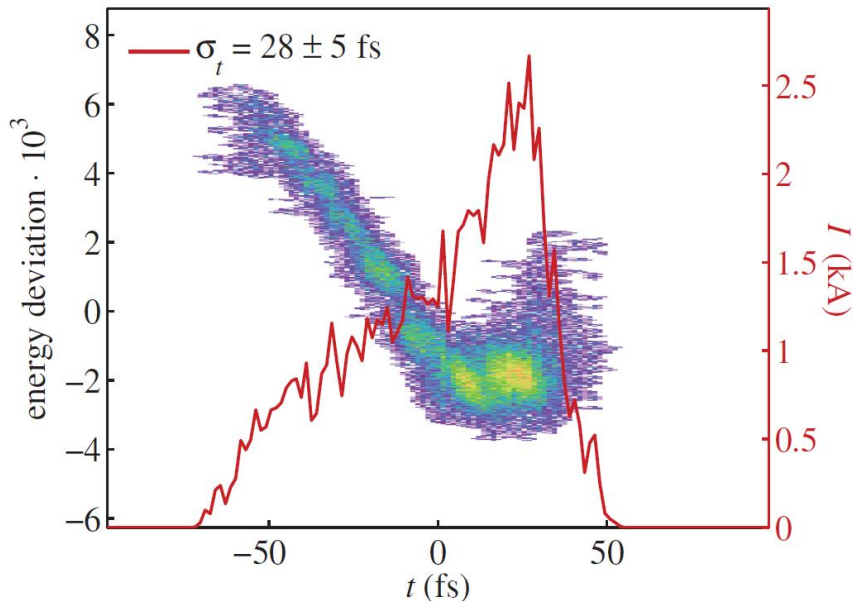
Goals for the short pulse studies

1. Can we setup the FEL to a **defined** pulse duration
2. Calibrate “**indirect**” methods against “**direct**” ones
3. Measure the scaling factor between **photon** pulse length and **electron** bunch length
4. Find out **advantages / disadvantages** of different methods

Outline – temporal distribution

- Electron beam diagnostics
 - Transverse Deflecting Structure (TDS)
 - (THz spectroscopy (CRISP))
 - (Bunch Compression Monitor (BCM))
- Indirect photon based methods
 - Spectral characteristics
 - (Pulse energy fluctuations – statistics)
 - (Mapping SASE to visible light: “afterburner”)
- Direct photon based methods
 - Autocorrelation
 - THz streaking
 - Optical-XUV cross-correlation

Electron Diagnostics: transverse deflecting cavity

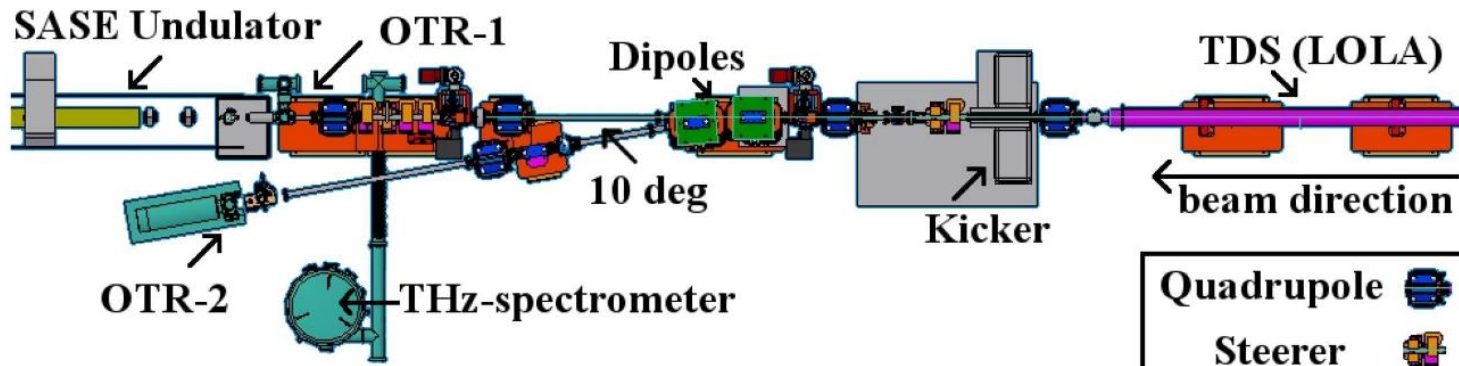


PRO:

- very good resolution (few fs)
- (meanwhile) online diagnostic
- Arbitrary pulse in bunch train can be measured

CON:

- only 1 bunch out of bunch train
-> destructive
- dispersive measurements (chirp)
-> not online



Courtesy: M. Yan, Ch. Gerth

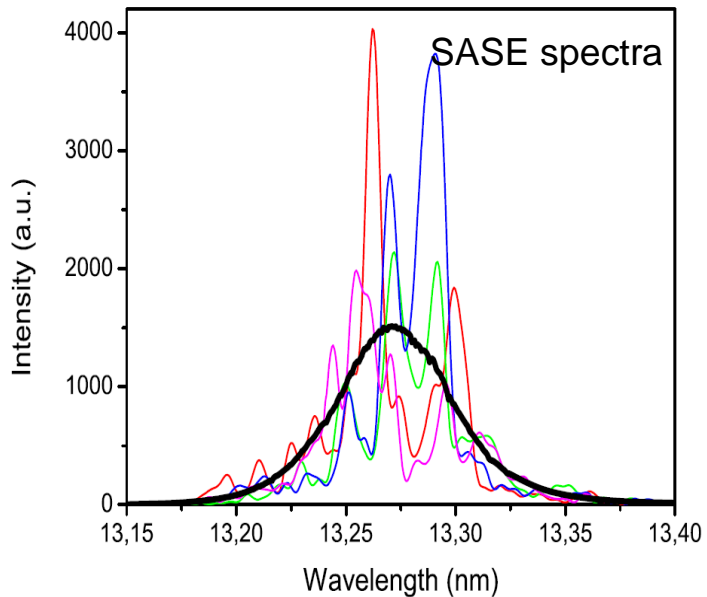
Photon pulse length diagnostics at PG2

Different methods/tools under development to measure photon pulse length & temporal distribution

- CRISP
- LOLA
- THz streaking
- Reflectivity method
- optical afterburner
-
-

Spectral analysis

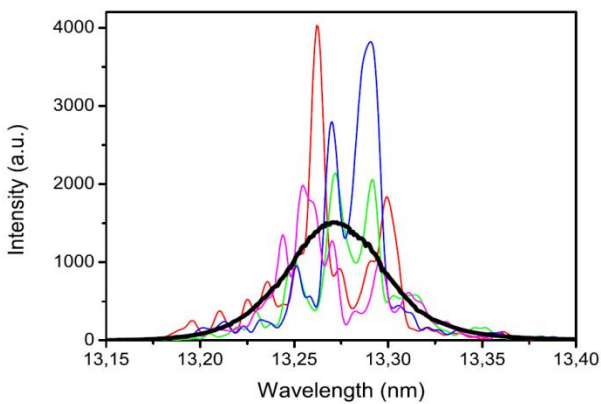
Employ Fourier relation between spectral distribution and temporal properties



- requires high resolution PG2 spectrometer
- Spectral correlation yields pulse duration

From spectra to photon pulse duration

Set of FEL spectra measured with PG2 beamline

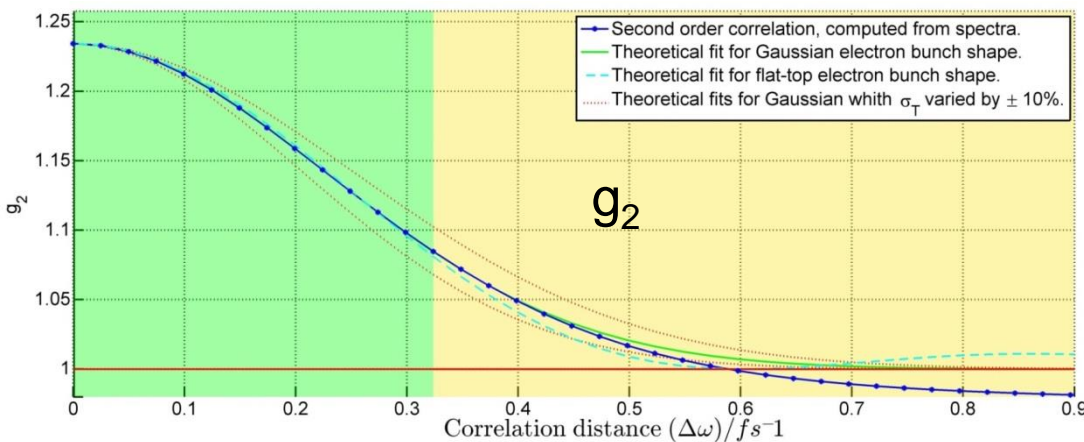


2nd order correlation function (from spectra):

$$g_2(\Delta\omega) \propto \frac{\left\langle S\left(\omega_0 - \frac{\Delta\omega}{2}\right) S\left(\omega_0 + \frac{\Delta\omega}{2}\right) \right\rangle}{\left\langle S\left(\omega_0 - \frac{\Delta\omega}{2}\right) \right\rangle \left\langle S\left(\omega_0 + \frac{\Delta\omega}{2}\right) \right\rangle}$$

Expected 2nd order correlation function for given σ_T and electron bunch shape:

$$g_2(\Delta\omega) = 1 + |\bar{F}(\Delta\omega, \sigma_T)|^2 \quad \text{Fit parameter}$$



Electron bunch shape

$$\bar{F}^g = e^{-\frac{\Delta\omega^2 \sigma_T^2}{2}} \quad \text{and} \quad \bar{F}^{ft} = \frac{\sin(\Delta\omega \frac{\sigma_T}{2})}{\Delta\omega \frac{\sigma_T}{2}}$$

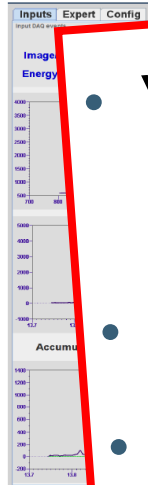
A least squares fit optimizes the rms pulse duration σ_T for maximum agreement within a set correlation window.

Real time analysis of FLASH spectra

Photon pulse length (PPL) server

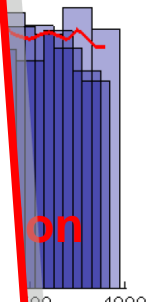
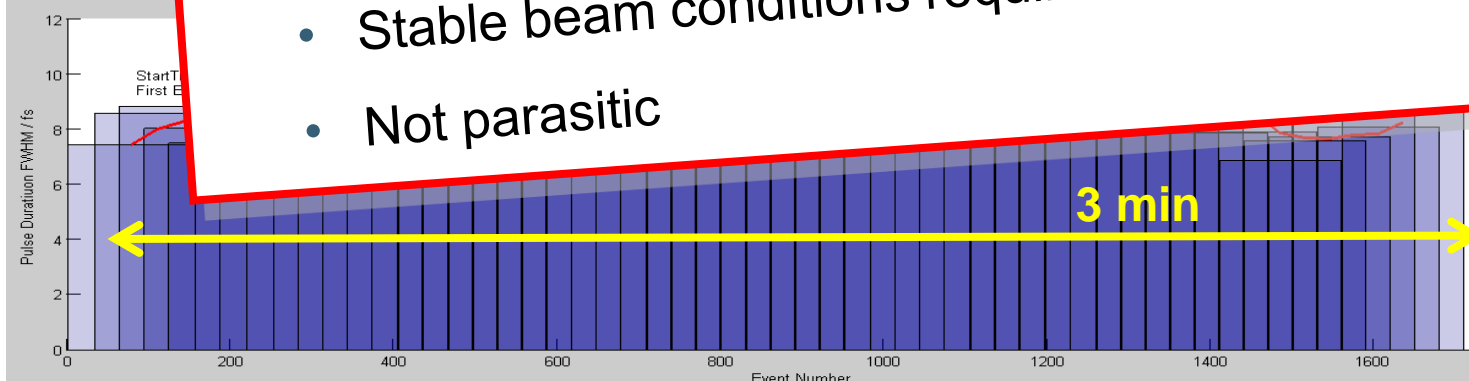
Multi

run



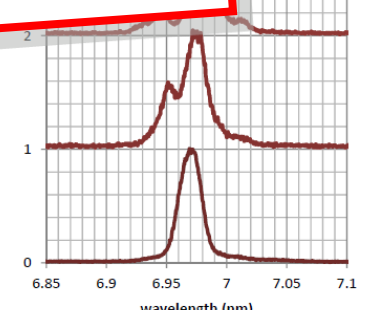
- Very useful tool for detailed photon pulse diagnostics
- Pulse length estimations during run time possible
- No additional setup required
- Limitations:
 - Sensitive to electron bunch shape & energy chirp
 - Stable beam conditions required
 - Not parasitic

FLASH
(J. Roen)



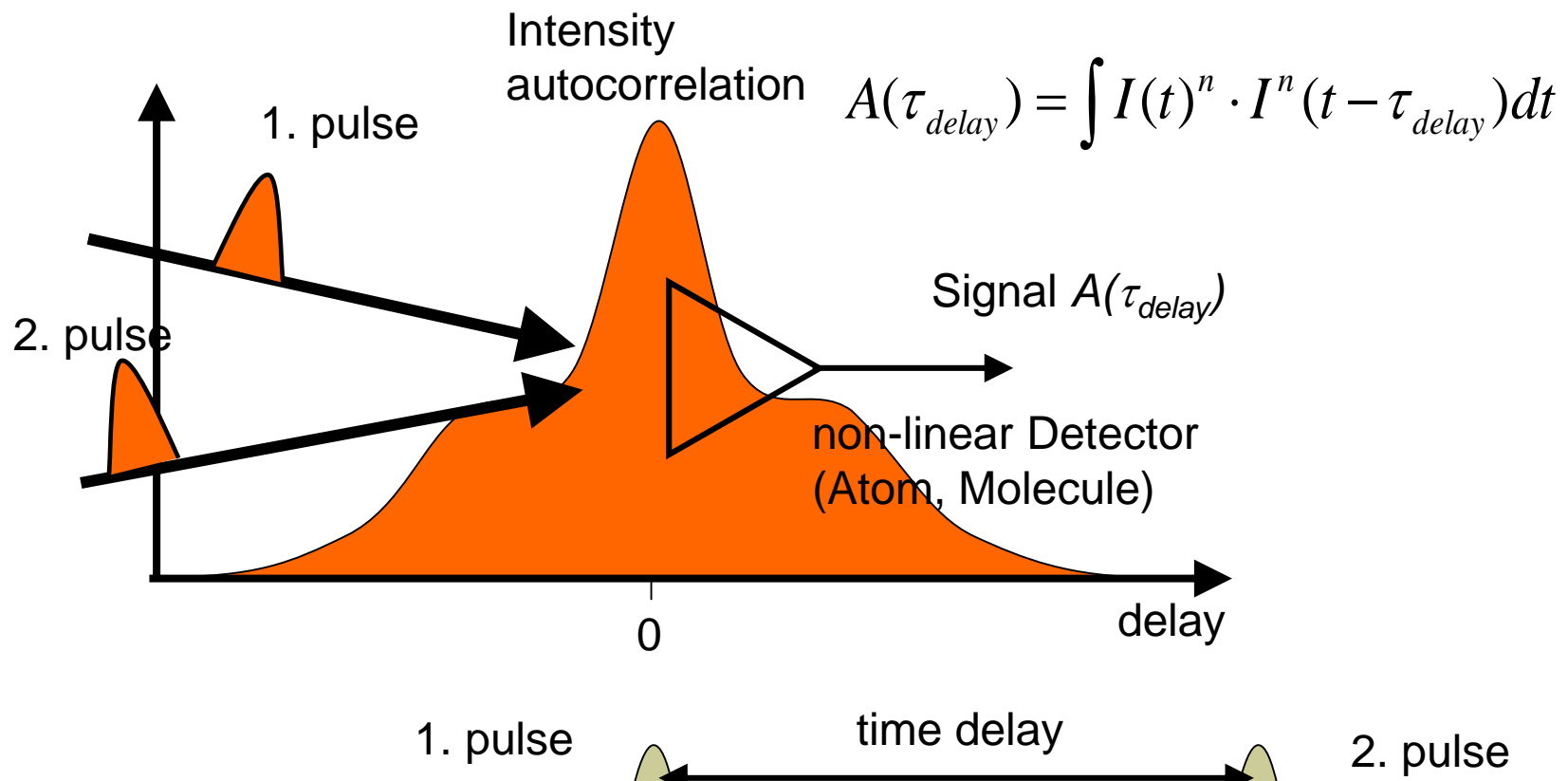
ement
spectra)

single
cta

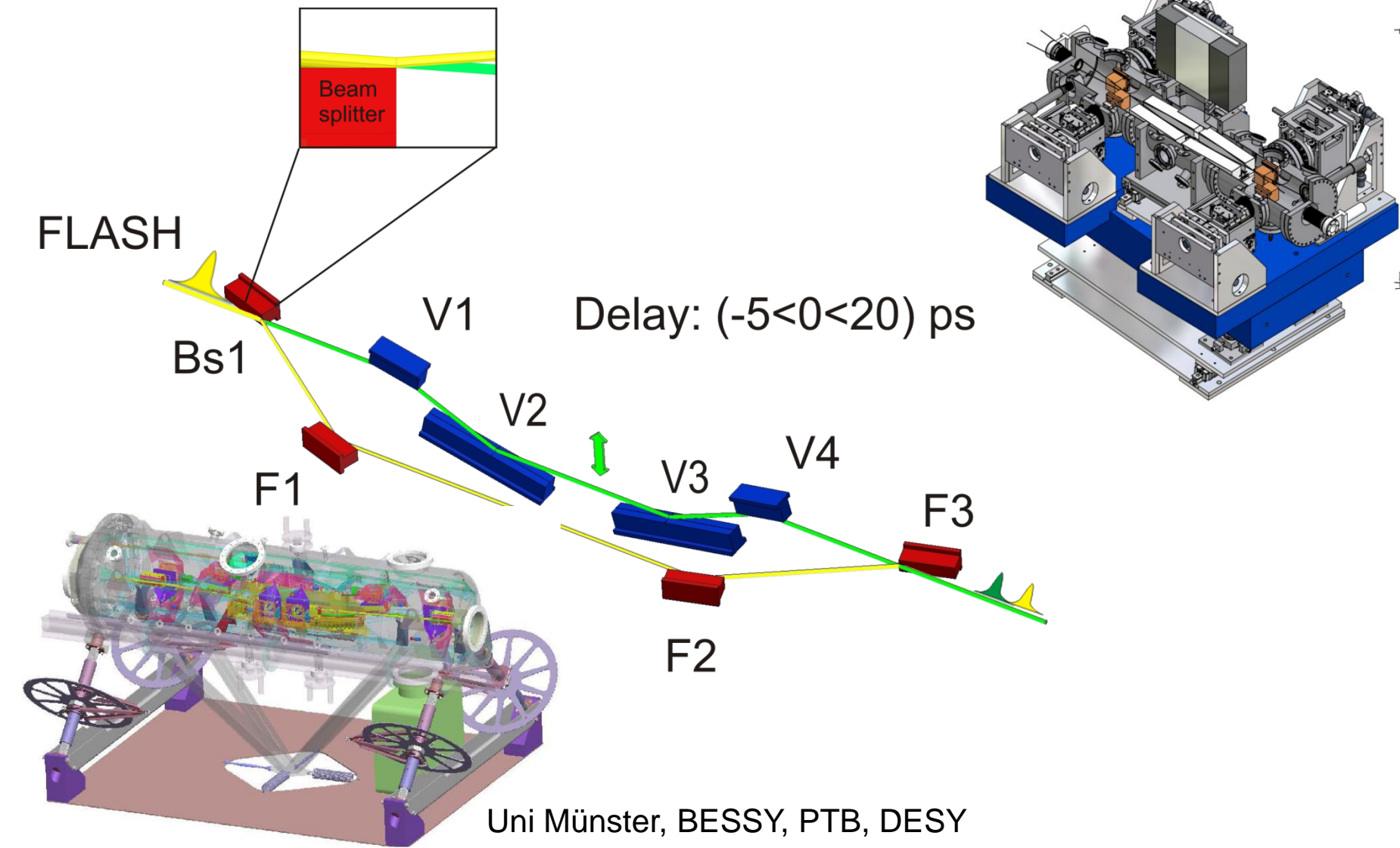


wavelength (nm)

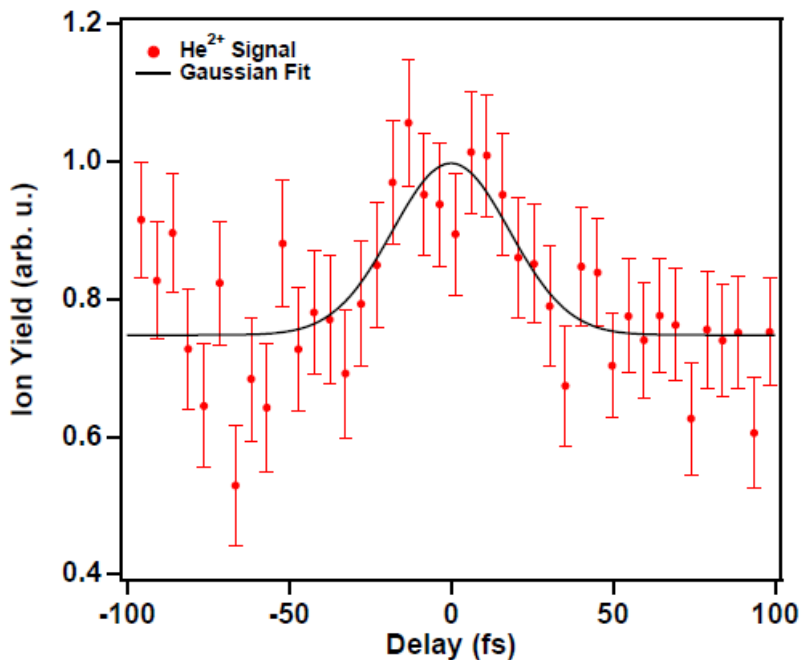
Direct PHOTON methods: auto correlation



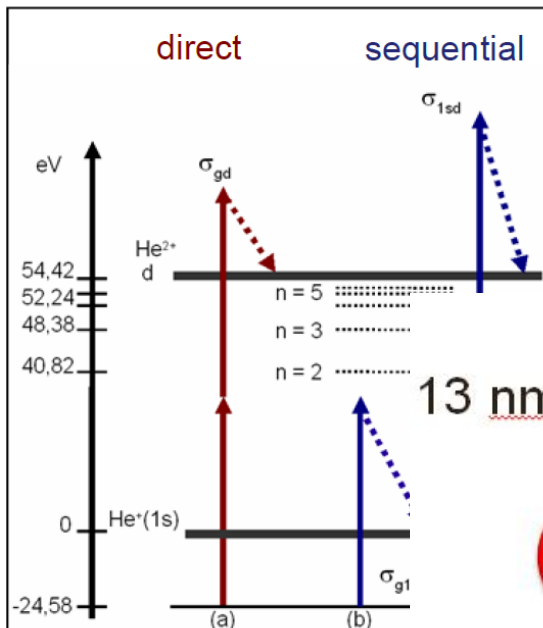
FEL split and delay



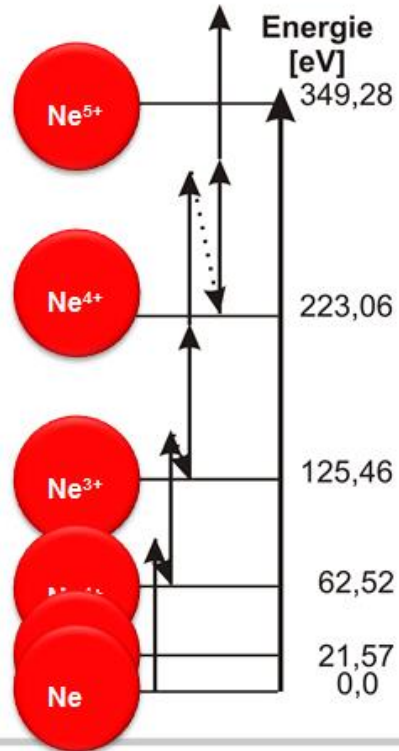
Direct PHOTON methods: auto correlation



Pathways to He^{2+} at 24 nm



13 nm (~92 eV)



Pro

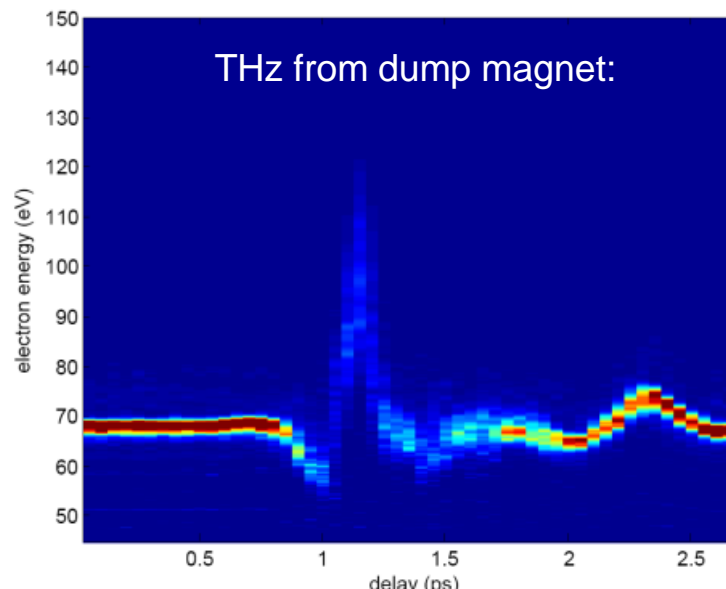
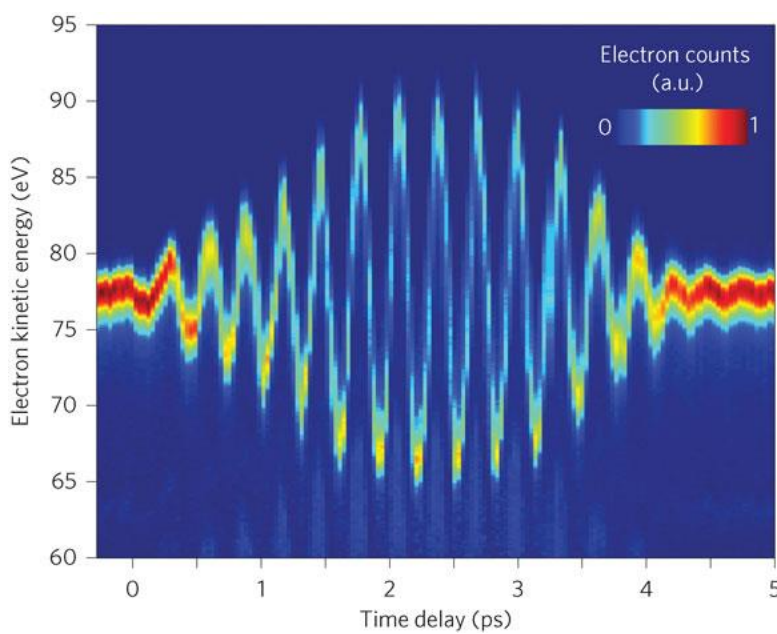
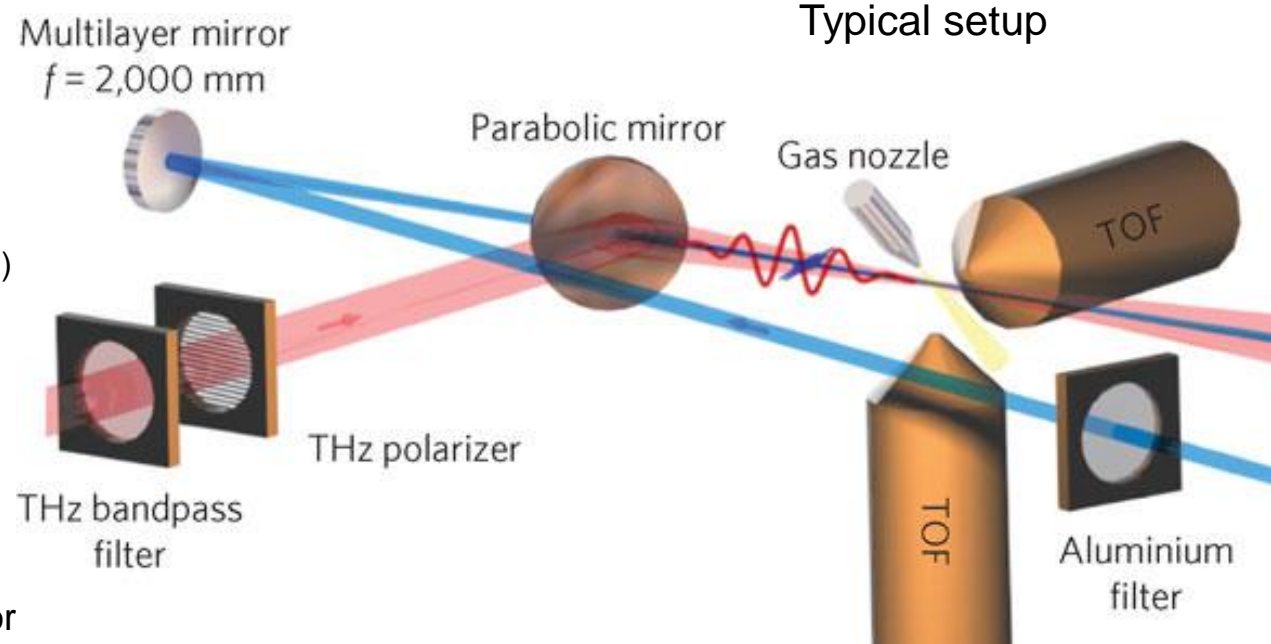
- “direct” measurement (for known reactions)

Con

- Experimentally challenging** (takes long time)
- (up to now) averaging technique
- well defined for < 25 nm**
- For XUV several path lead to same ionization state -> Simulations needed

Direct PHOTON methods: THz streaking

Nature Photonics **3**, 523 (2009)
Phys. Rev. Lett. **108**, 253003 (2012)



XUV photon diagnostics: pulse duration

The most difficult one

Extensive study to different techniques: Düsterer et al, PRSTAB **17**, 120702 (2014)

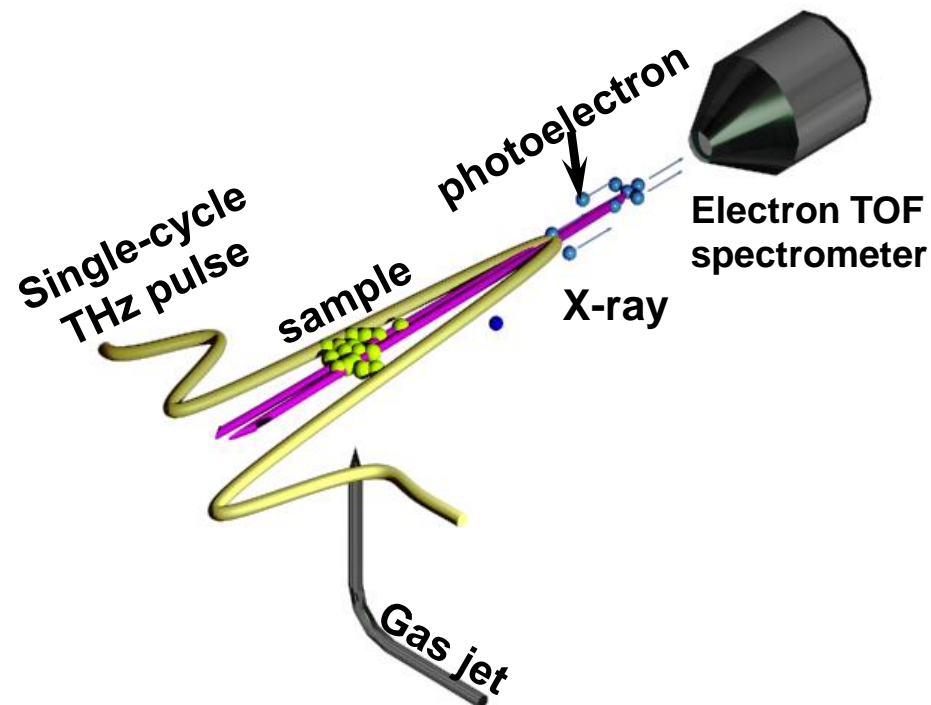
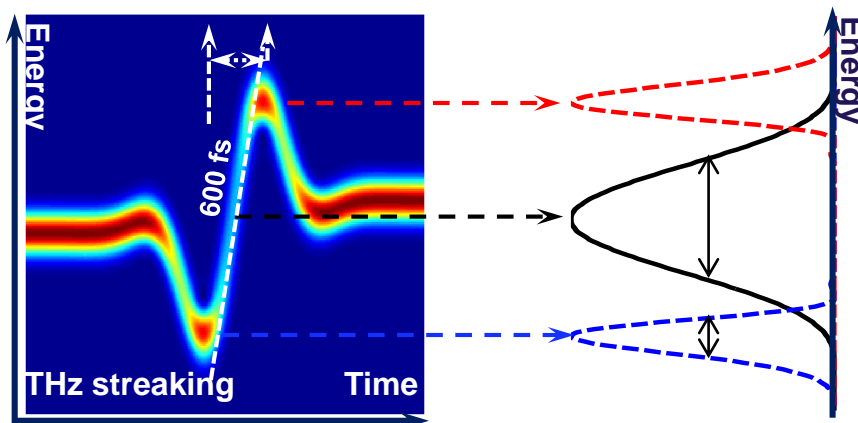
THz Streaking

measuring the pulse duration and arrival time
by means of a single cycle THz streaking field:

- online monitoring
- single bunch resolved measurement
- (almost) non-invasive
- High rep. rate possible

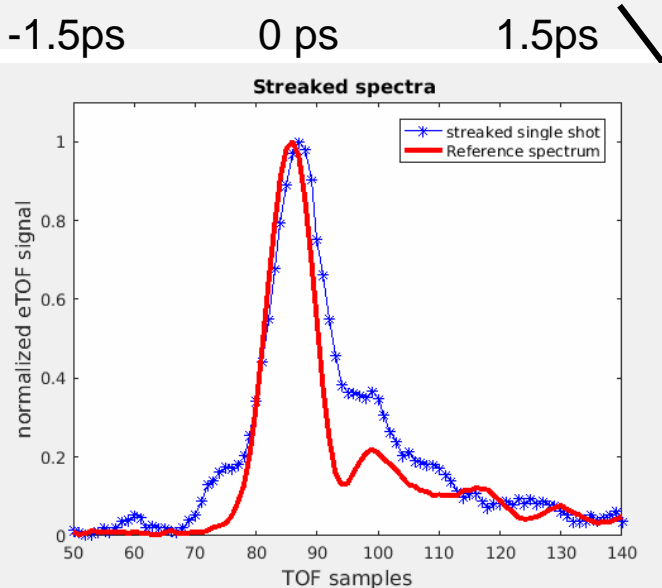
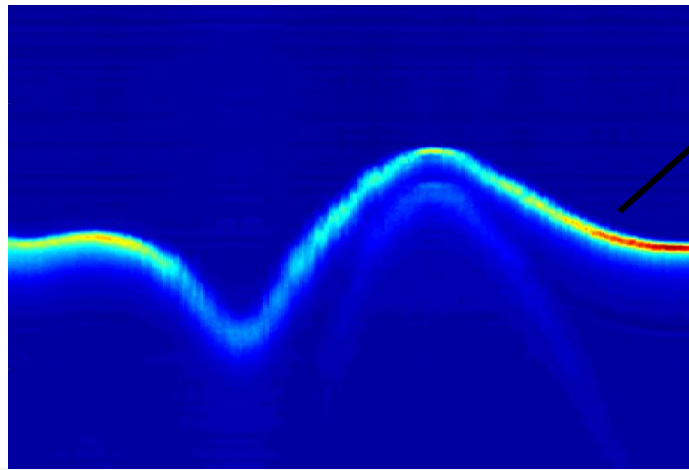
(usual) Parameter range

- 20 - 200 fs
- 4 - 40 nm
- 1 - 500 μ J

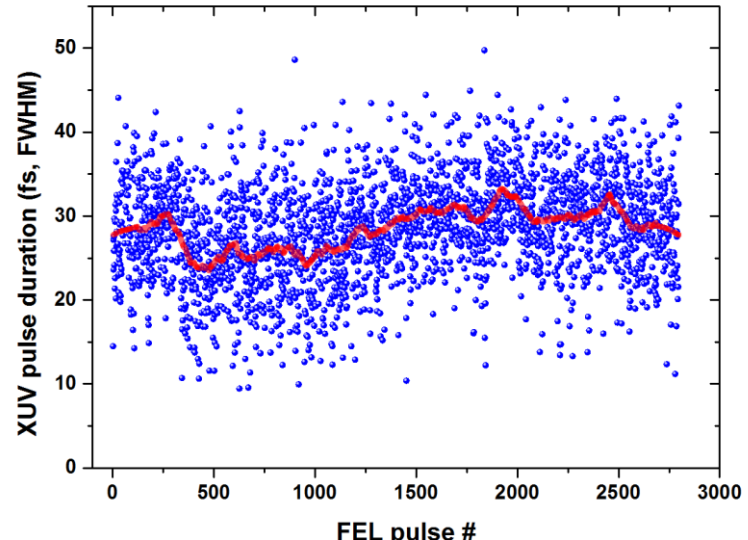


THz Streaking → observables

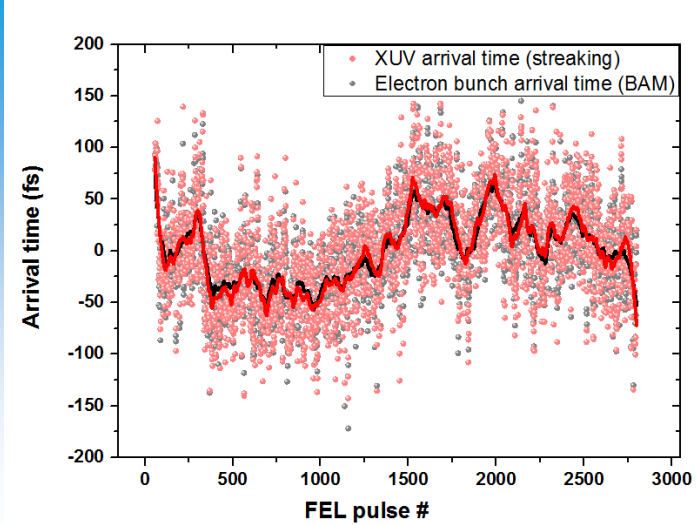
Streaking raw data
(delay scan)



Single shot XUV pulse duration

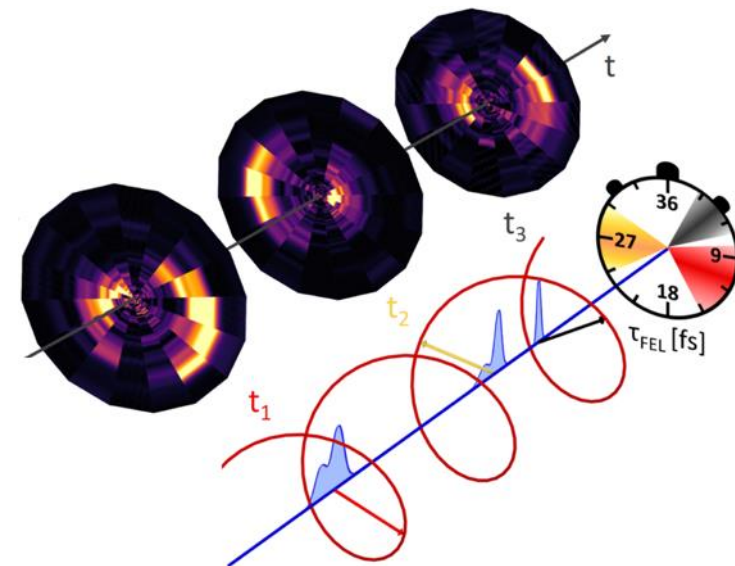
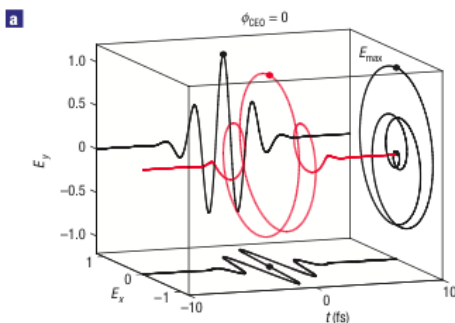


Arrival time



Towards attosecond pulses

Principle of angle-resolved streaking



Principle:

E. Constant, P. Corkum, *Phys. Rev. A.* **56** (1997)

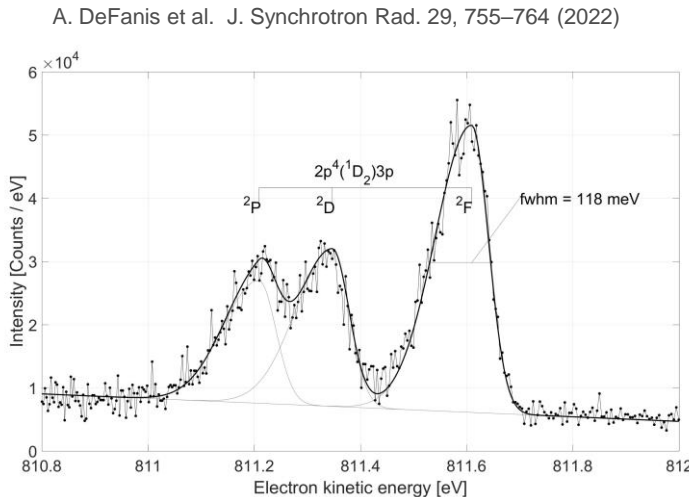
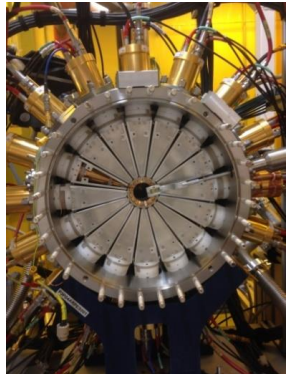
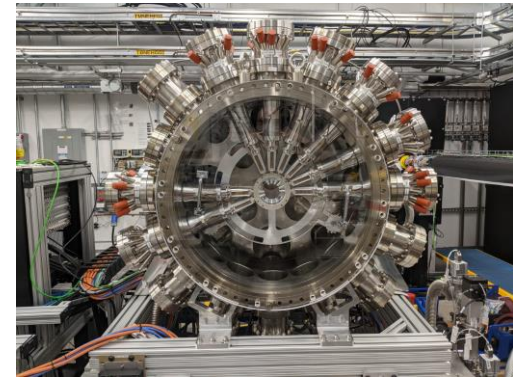
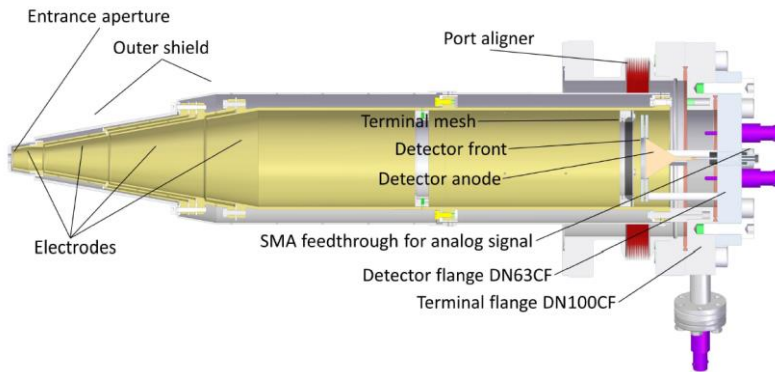
Experiment & figure (IR ionization):

P. Eckle, U. Keller, *Nat. Phys.* **4** (2008)

- Circularly polarized laser field introduces time-dependent shift in streaking angle
- Angle-resolved detection of the photoelectron energy acts like the hands of a stop watch

Instrumentation upgrades and advances

From diagnostic achievements to chirality science at the attosecond frontier in gas and liquid phase



J. Synchrotron Rad. 28, 1364 (2021)
P. Walter et al.,

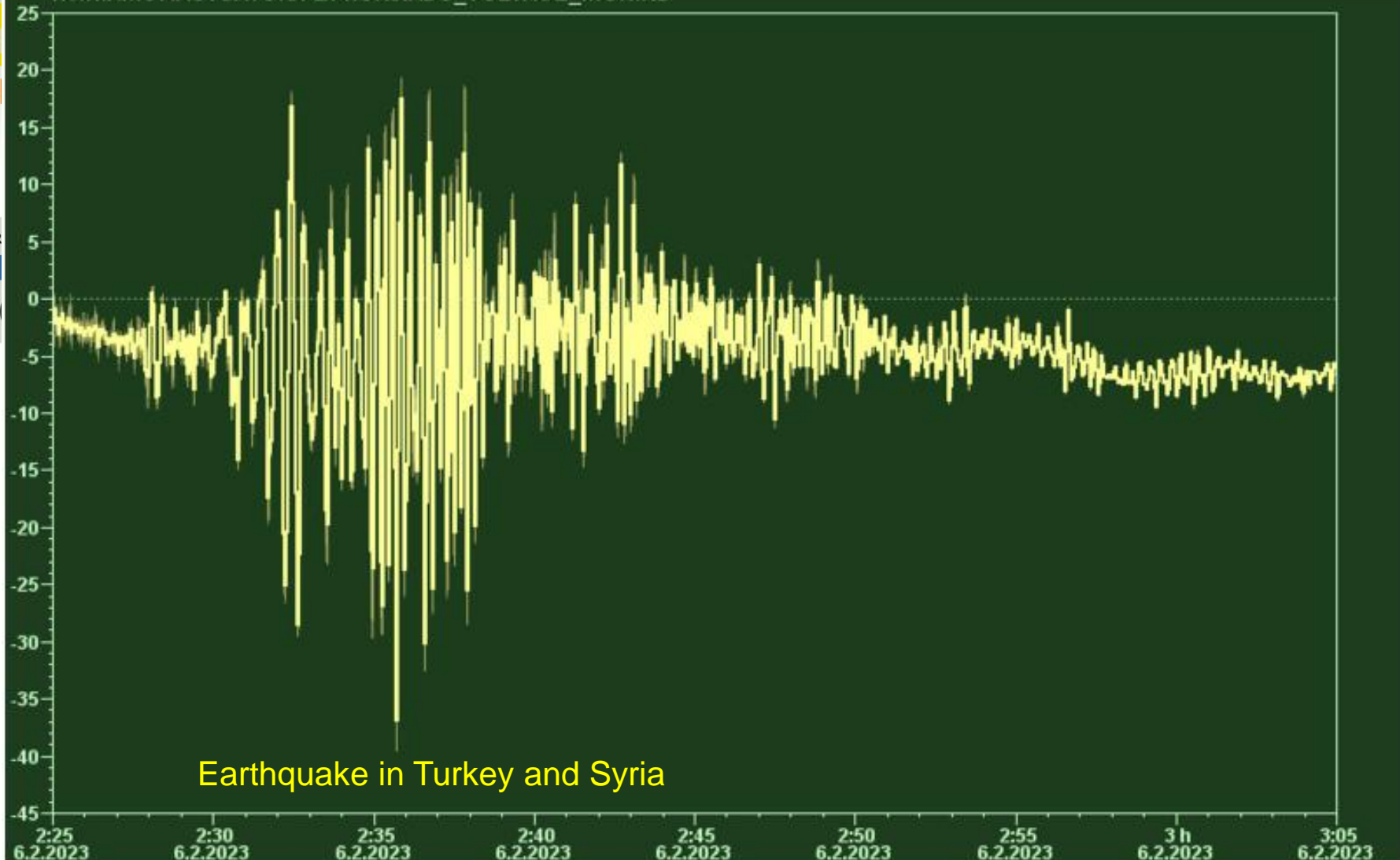
**SpeAR Project
for attō-streaking**
W. Helm et al.

Synchronization

Femtosecond Optical Synchronization Systems at FLASH and the European XFEL

Hist: XFEL SYNC/LINK/LOCK/XTIN.AMC7.ACTUATOR/PZT4.CH0.ADC_VOLTAGE_MON.RD

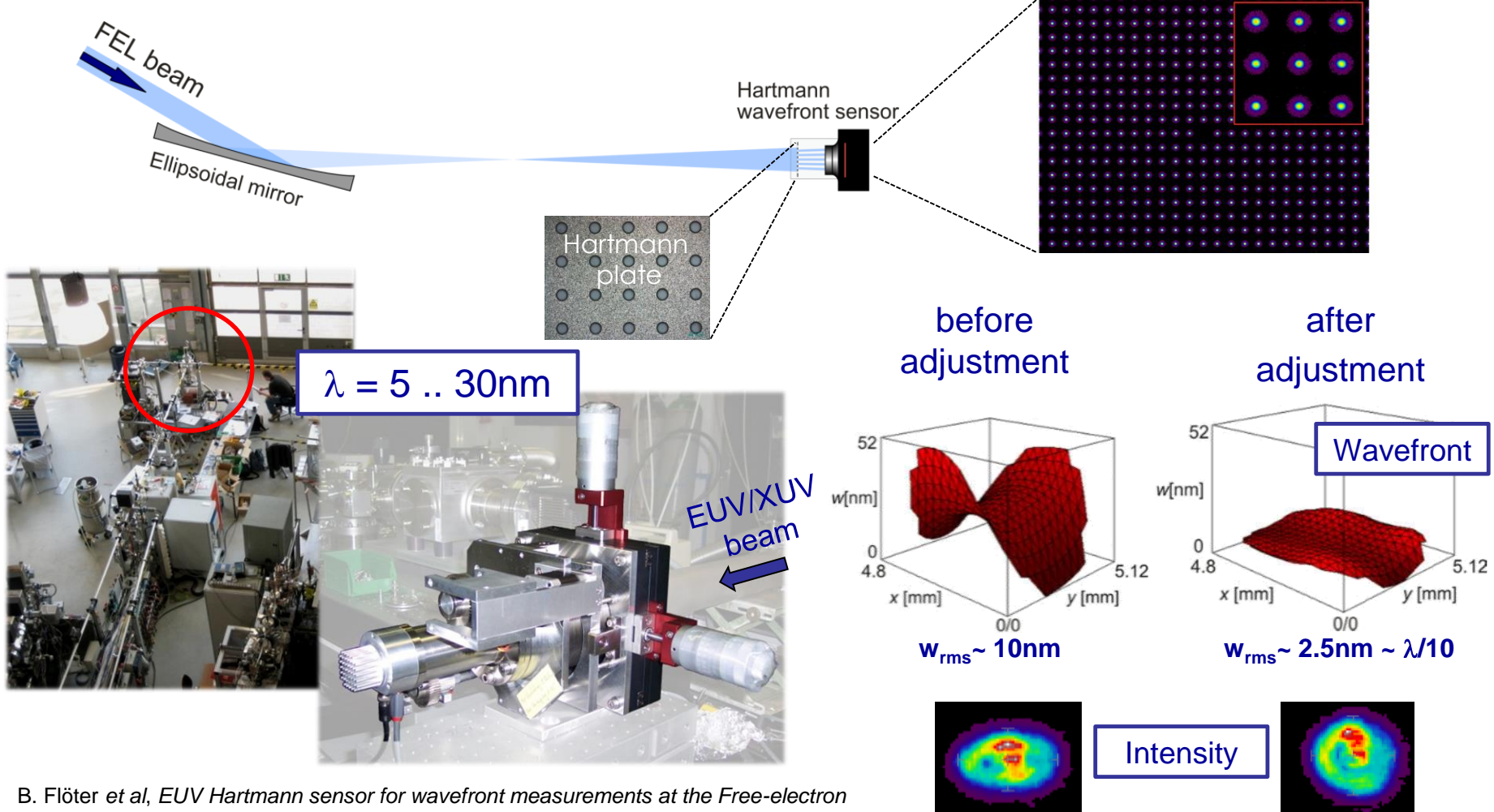
XTIN.AMC7.ACTUATOR/PZT4.CH0.ADC_VOLTAGE_MON.RD



Wigner distribution measurement of the spatial coherence properties of FLASH

Credits to: Tobias Mey (Laserlaboratorium Göttingen e.V.)

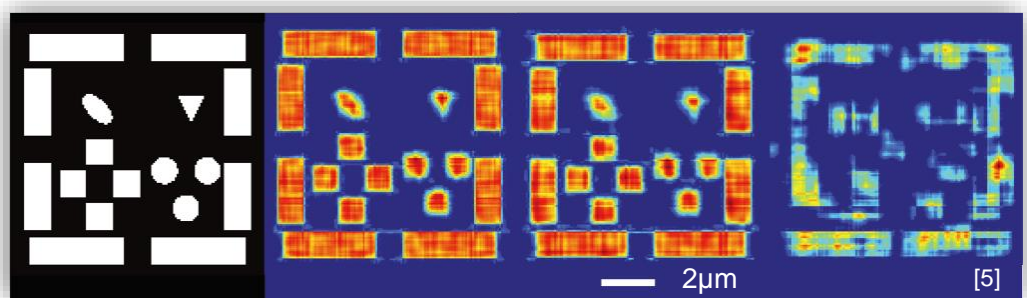
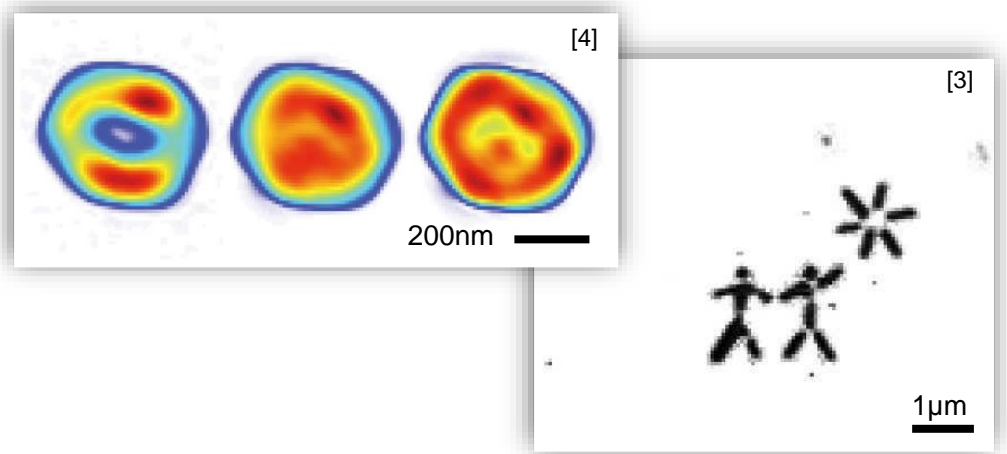
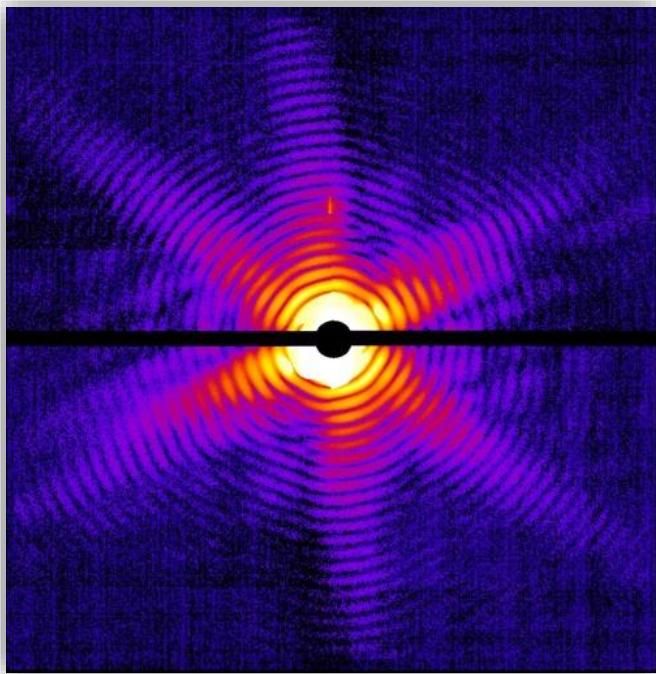
Experimental setup at BL2



[2] B. Flöter et al, EUV Hartmann sensor for wavefront measurements at the Free-electron LASer in Hamburg, New J. Phys. 12 (2010) 083015

Motivation

Coherent diffractive imaging



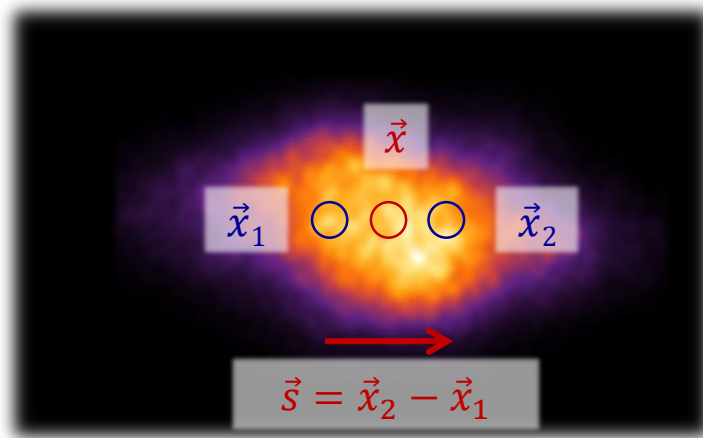
Decreasing coherence

[3] H. N. Chapman *et al.*, "Femtosecond diffractive imaging with a soft-X-ray free-electron laser," *Nature Phys.* **2**, 839-843 (2006)

[4] M. M. Seibert *et al.*, "Single mimivirus particles intercepted and imaged with an X-ray laser," *Nature* **470**, 78-82 (2011)

[5] B. Chen *et al.*, "Diffraction imaging: The limits of partial coherence," *Phys. Rev. B* **86**, 235401 (2012)

Coherence



Mutual coherence function

$$\begin{aligned}\Gamma(\vec{x}, \vec{s}) &= \langle E(\vec{x}_1, t) \cdot E^*(\vec{x}_2, t) \rangle \\ &= \langle E(\vec{x} - \vec{s}/2, t) \cdot E^*(\vec{x} + \vec{s}/2, t) \rangle\end{aligned}$$

Local degree of coherence

$$\gamma(\vec{x}, \vec{s}) = \frac{\Gamma(\vec{x}, \vec{s})}{\sqrt{I(\vec{x} - \vec{s}/2) \cdot I(\vec{x} + \vec{s}/2)}}$$

Global degree of coherence

$$K = \frac{\iint \Gamma(\vec{x}, \vec{s})^2 d\vec{x} d\vec{s}}{\left(\iint \Gamma(\vec{x}, 0) d\vec{x} \right)^2}$$

→ required for interference effects

[6] M. Born and B. Wolf, *Principles of Optics*, Cambridge University Press (1980)

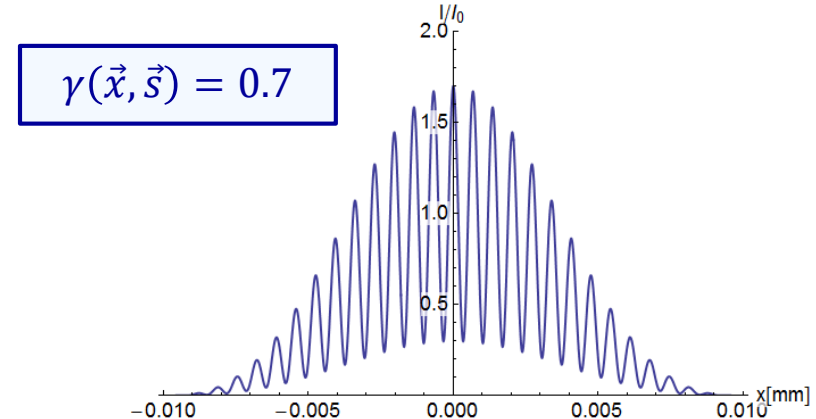
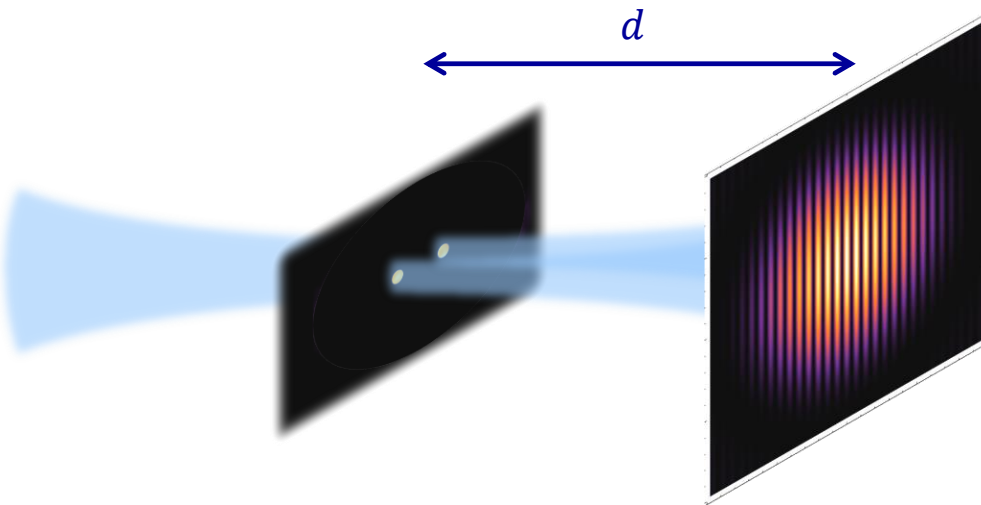
Coherence

Interference of elementary waves $\rightarrow \gamma(\vec{x}, \vec{s})$

$$\gamma(\vec{x}, \vec{s}) = 0.7$$

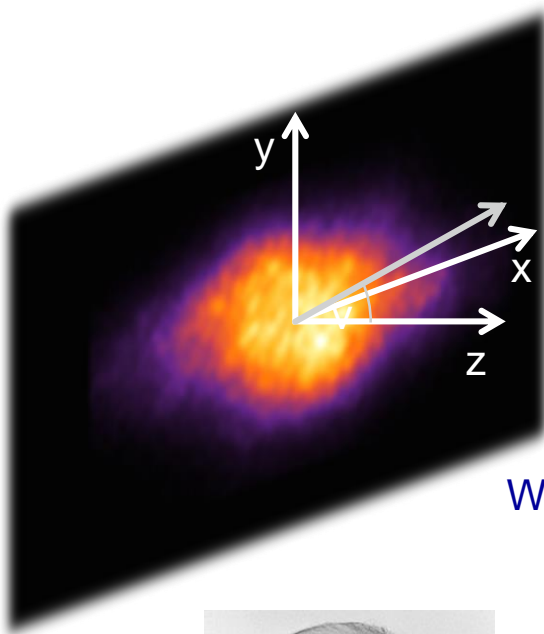
$$I(x, y) = I_0 \cdot \left(\frac{J_1\left(\frac{2\pi ar}{\lambda d}\right)}{\frac{2\pi ar}{\lambda d}} \right)^2 \cdot [1 + \gamma(\vec{x}, \vec{s}) \cdot \cos\left(\frac{2\pi s}{\lambda d}x\right)] \quad [6]$$

$$r = \sqrt{x^2 + y^2}$$



[6] M. Born and B. Wolf, *Principles of Optics*, Cambridge University Press (1980)

Wigner distribution function



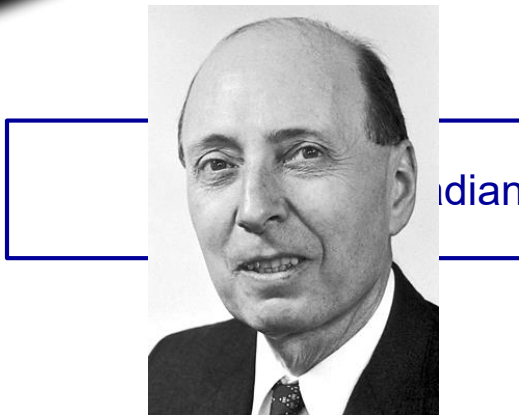
Spatial coordinate $\vec{x} = \begin{pmatrix} x \\ y \end{pmatrix}$

Mutual coherence function

$$h(\vec{x}, \vec{u}) = \left(\frac{k}{2\pi}\right)^2 \cdot \iint \Gamma(\vec{x}, \vec{s}) \cdot e^{ik\vec{u} \cdot \vec{s}} d^2 s$$

Wigner distribution

Radiation angle $\vec{u} = \begin{pmatrix} u \\ v \end{pmatrix}$



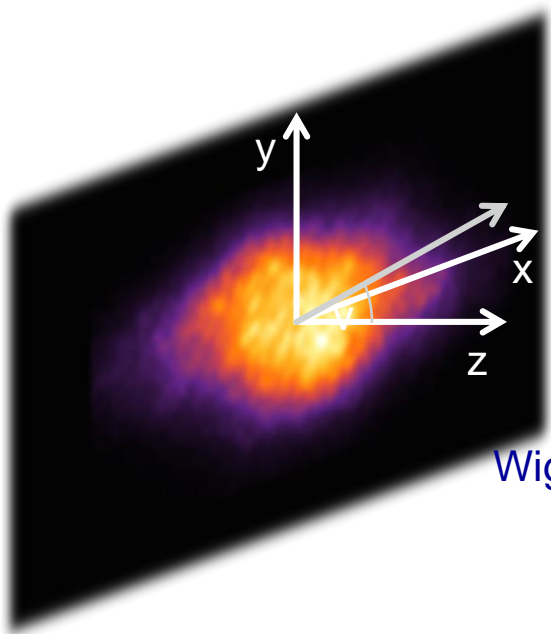
Eugene Paul Wigner
Nobel price 1963
(with J. H. D. Jensen and
M. Goeppert-Mayer)

Wilhelm-Weber-Straße 22,
Göttingen ►



[8] M. J. Bastiaans, "Application of the Wigner distribution function to partially coherent light," J. Opt. Soc. Am. A 3, 1227-1238 (1986)

Wigner distribution function



Spatial coordinate $\vec{x} = \begin{pmatrix} x \\ y \end{pmatrix}$

Mutual coherence function

$$h(\vec{x}, \vec{u}) = \left(\frac{k}{2\pi}\right)^2 \cdot \iint \Gamma(\vec{x}, \vec{s}) \cdot e^{ik\vec{u} \cdot \vec{s}} d^2 s$$

Wigner distribution

Radiation angle $\vec{u} = \begin{pmatrix} u \\ v \end{pmatrix}$

Irradiance

$$I(\vec{x}) = \iint h(\vec{x}, \vec{u}) du dv$$

→ Near field

Radiance

$$\hat{I}(\vec{u}) = (2\pi)^{-2} \iint h(\vec{x}, \vec{u}) dx dy$$

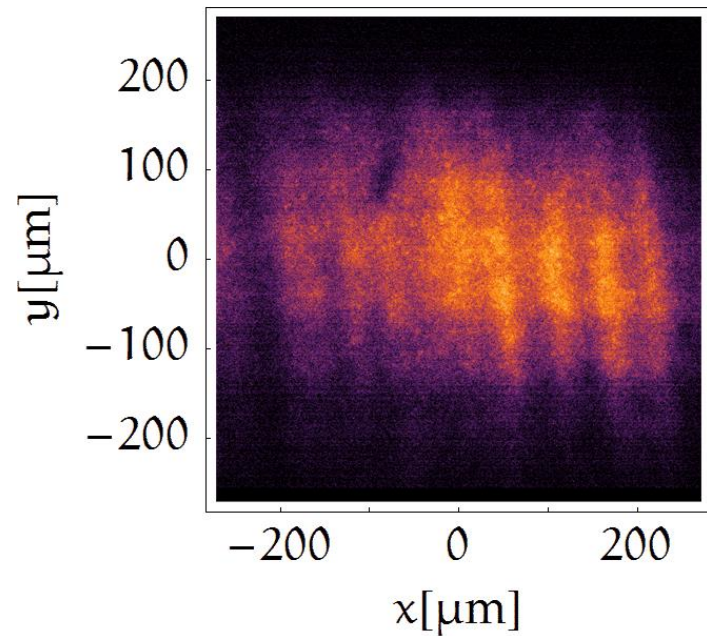
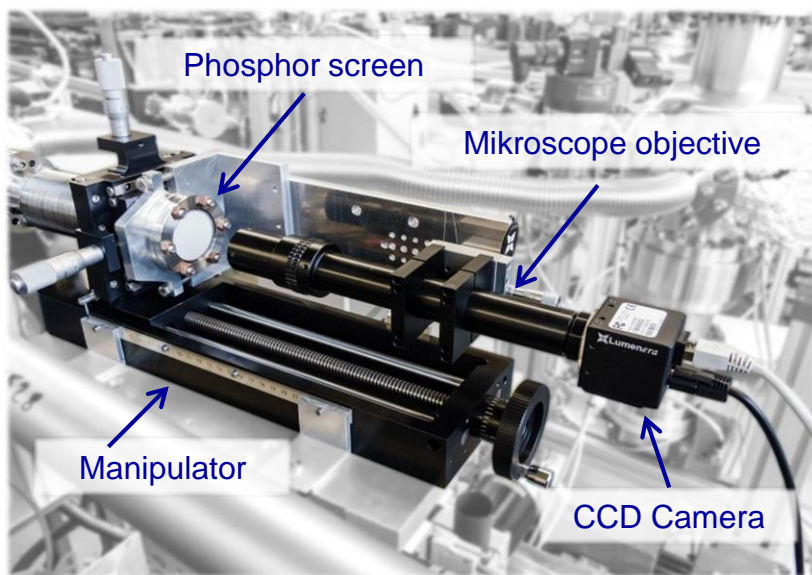
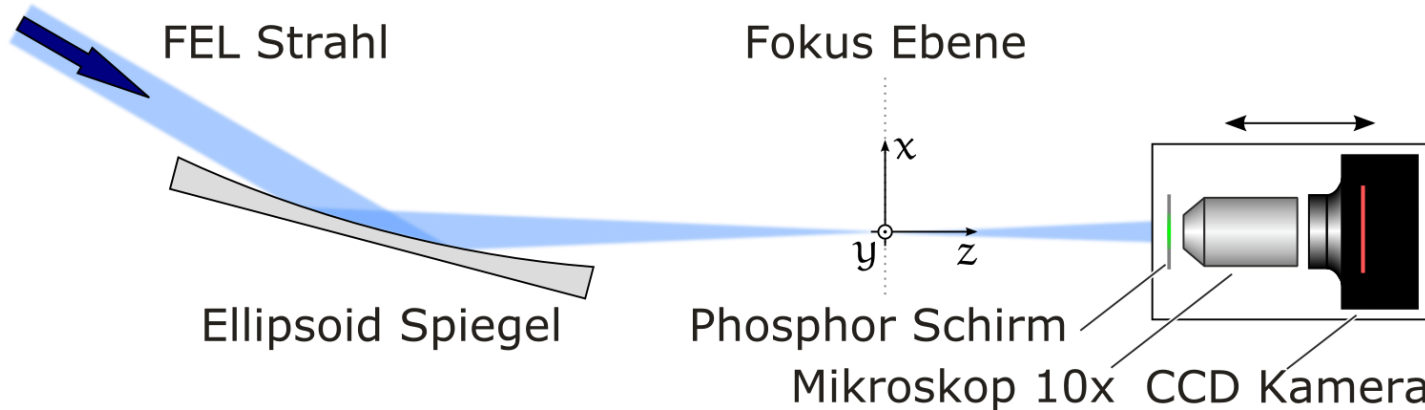
→ Far field

Global degree of coherence

$$K = \lambda^2 \frac{\iint h(\vec{x}, \vec{u})^2 dx^2 du^2}{\iint h(\vec{x}, \vec{u}) dx^2 du^2}$$

[8] M. J. Bastiaans, "Application of the Wigner distribution function to partially coherent light," J. Opt. Soc. Am. A 3, 1227-1238 (1986)

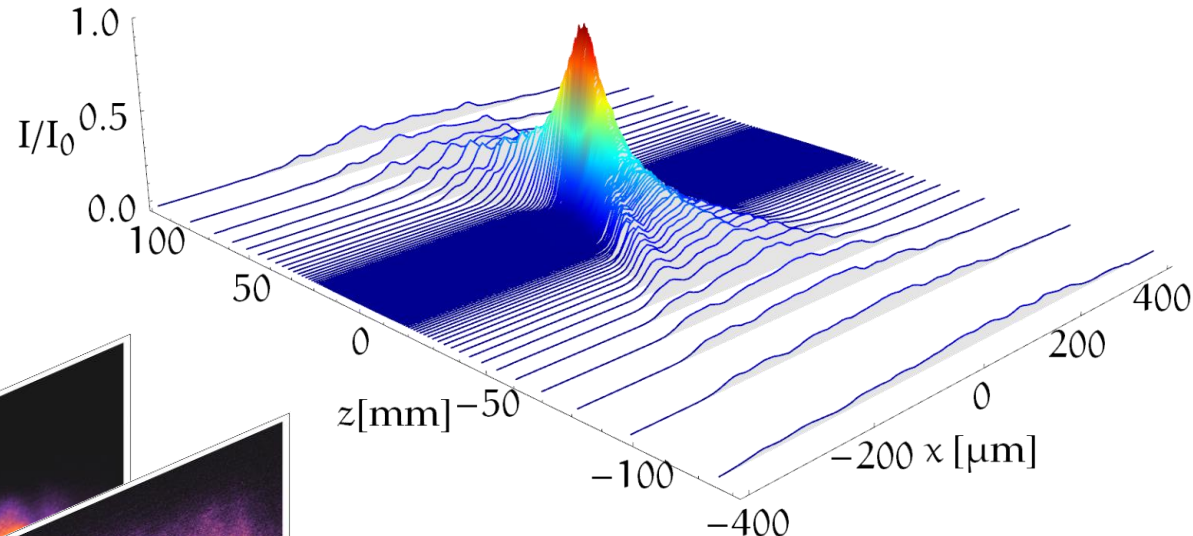
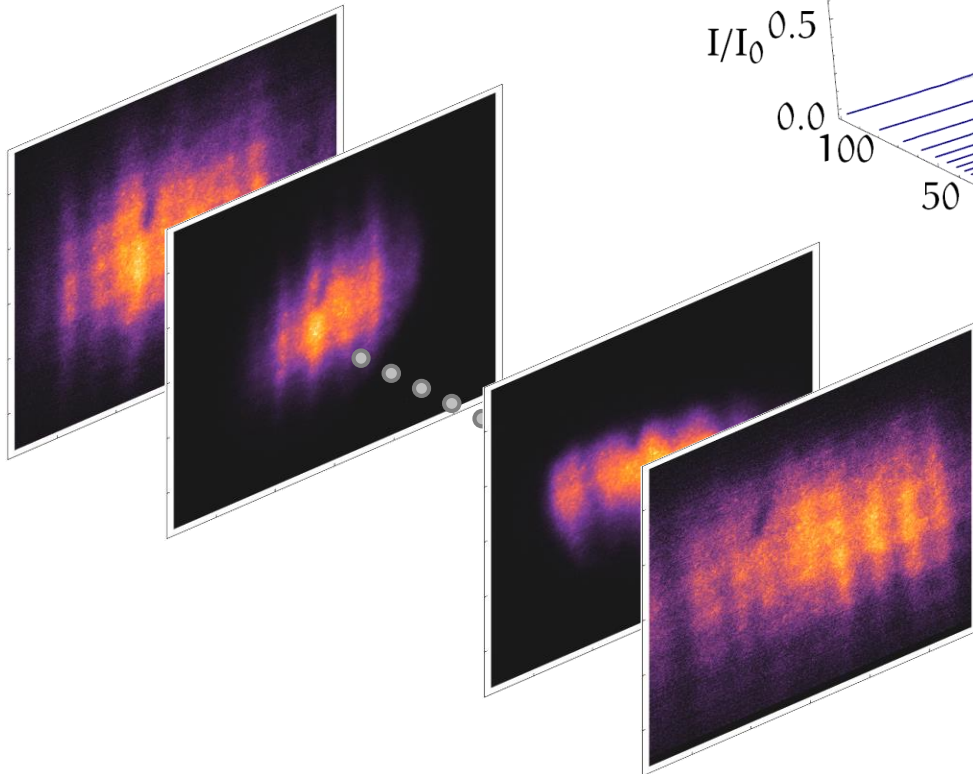
Caustic scan



Wigner distribution

Projection-slice theorem [9]

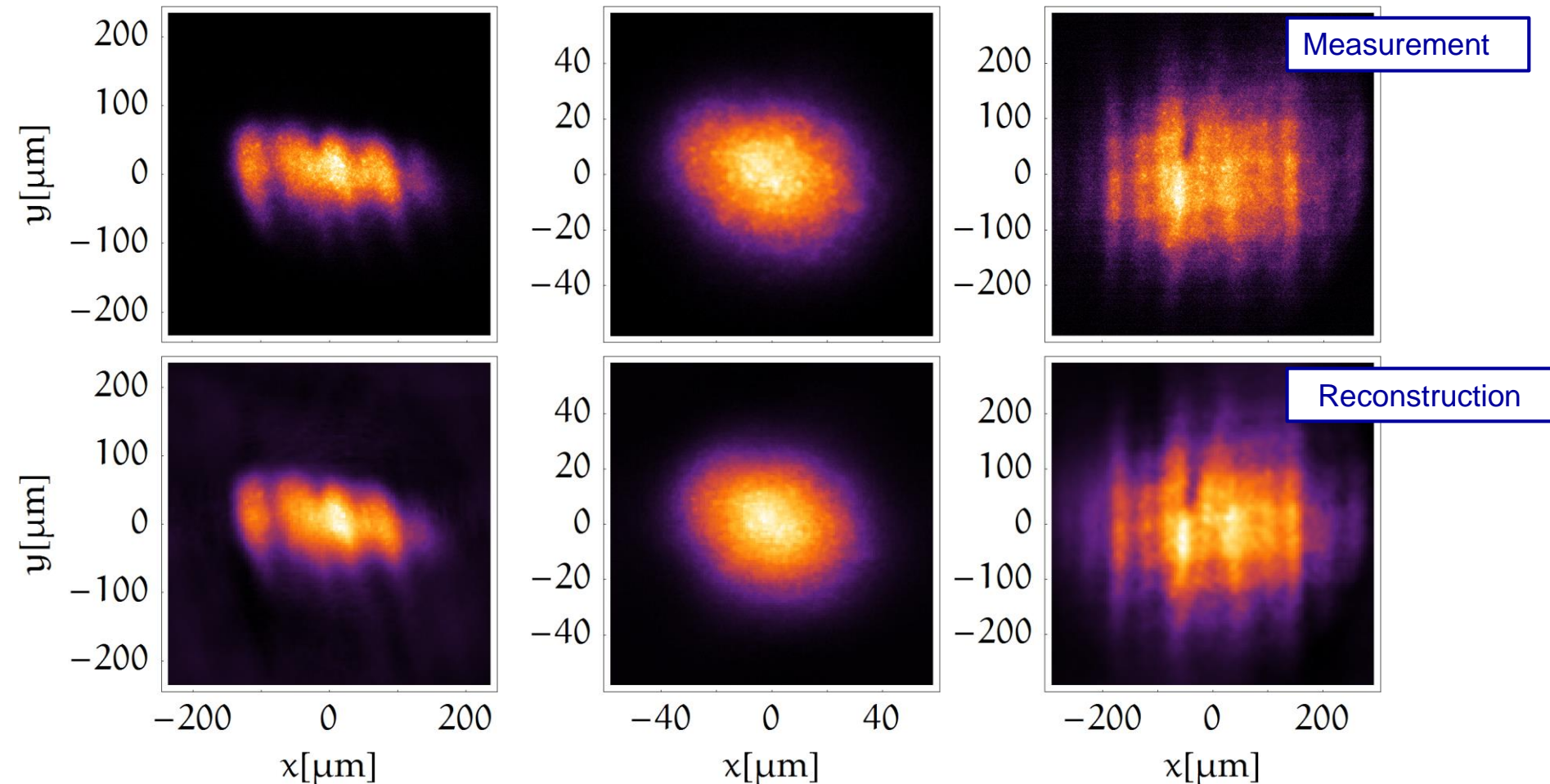
$$\tilde{h}(q_x, z \cdot q_x) = \tilde{I}_z(q_x)$$



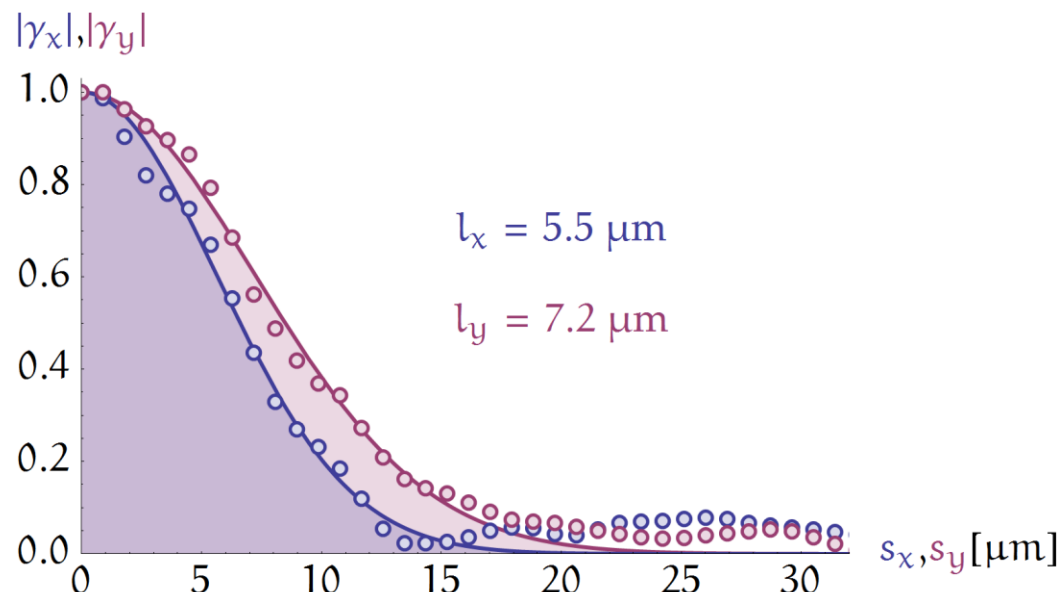
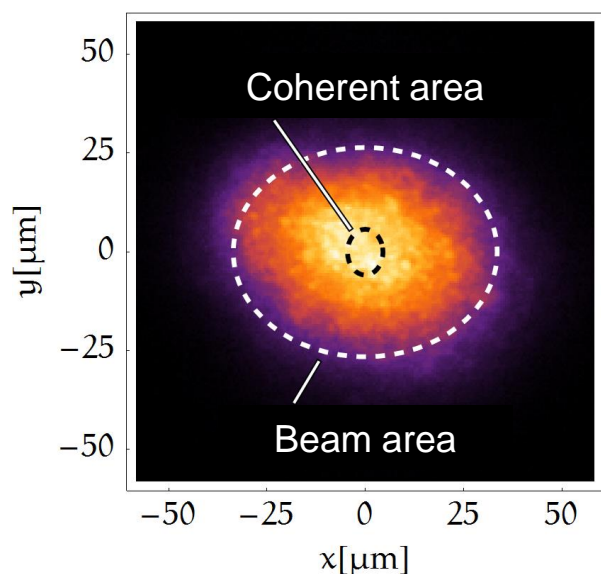
$$\int I(x, y) dy$$

[9] A. Torre, *Linear ray and wave optics in phase space*, Elsevier B.V. Netherlands (2005)

Wigner distribution



Coherence properties



	Wavelength λ [nm]	Beam diameter d_x / d_y [μm]	Coherence length l_x / l_y [μm]	Global degree of coherence K
Wigner [10]	24.7	67 / 53	5.5 / 7.2	0.032
Double pinhole [7]	8.0	17 / 17	6.2 / 8.7	0.42

[7] A. Singer *et al.*, "Spatial and temporal coherence properties of single free-electron laser pulses," Opt. Expr. **20**, 17480-17495 (2012)

[10] T. Mey *et al.*, "Wigner distribution measurements of the spatial coherence properties of the free-electron laser FLASH," Opt. Expr. **22**, 16571-16584 (2014)

Thank you for your attention



Plasma Timing Tool

M. Harmand, R. Coffee, M.R. Bionta, M. Chollet, D. French, D. Zhu, D.M. Fritz, H.T. Lemke, N. Medvedev, B. Ziaja, S. Toleikis and M. Cammarata,
“Achieving few-femtosecond time-sorting at hard X-ray free-electron lasers”,
Nature Photon. 7, 215 (2013)

R. Riedel, A. Al-Shemmary, M. Gensch, T. Golz, M. Harmand, N. Medvedev, M.J. Prandolini, K. Sokolowski-Tinten, S. Toleikis, U. Wegner, B. Ziaja, N. Stojanovic and F. Tavella,
“Single-shot pulse duration monitor for extreme ultraviolet and X-ray free-electron lasers”,
Nature Comm. 4, 1731 (2013)

Experimental setup of spatial encoding tool

- **Ultrafast plasma switch (a)**

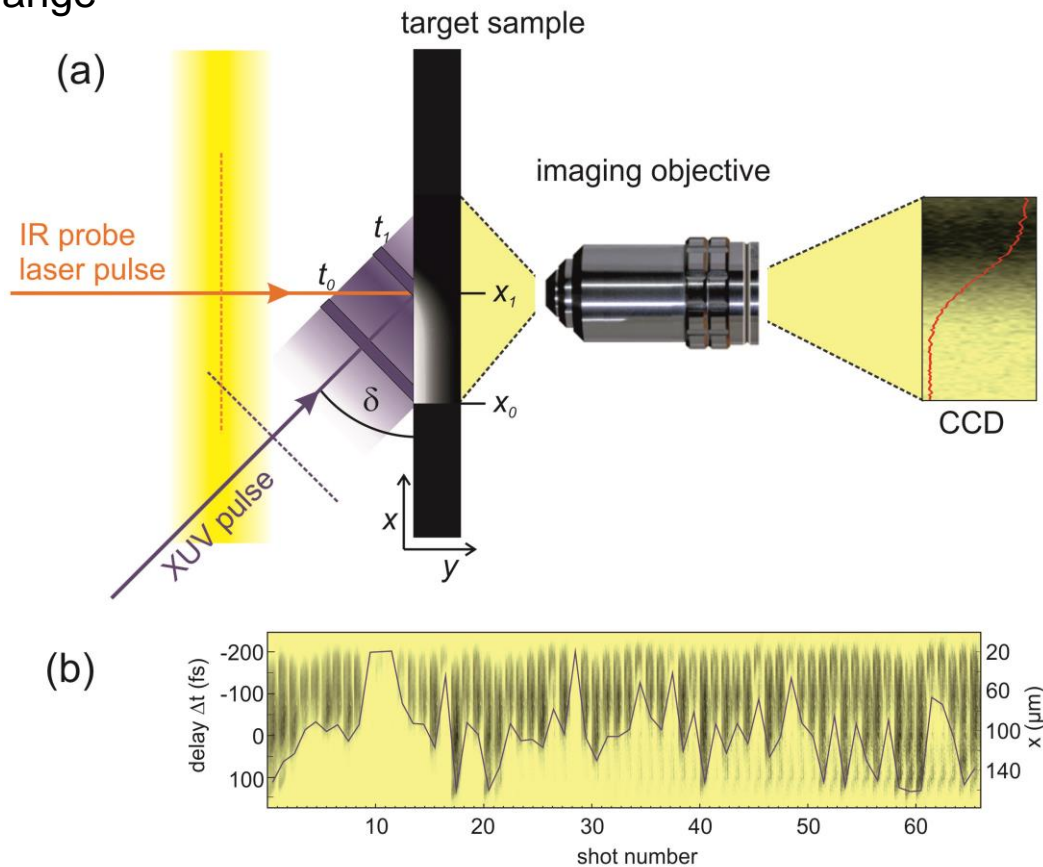
- FEL triggers reflectivity/transmission change
- oblique angle of incidence δ
- different parts of FEL wavefront reach sample at different positions
- time axis spatially resolved:

$$\Delta t = \Delta_x \cdot \cos(\delta) / c$$

(Δ_x : imaged pixel size, c : vacuum speed of light)

→ extract arrival time (b)

→ extract pulse duration



Experimental set-up at XPP (LCLS)

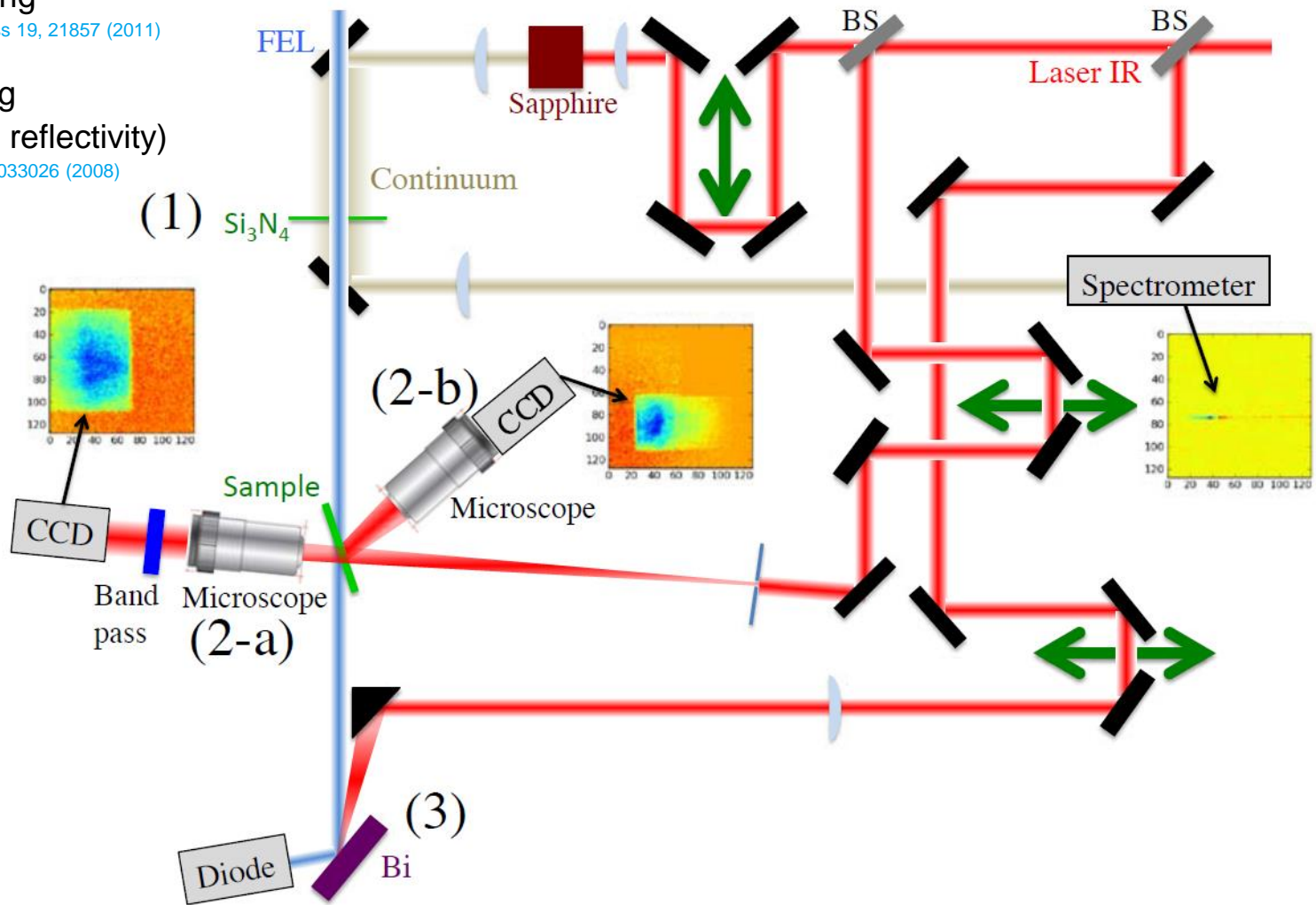
- (1) Spectral encoding

M.R. Bionta et al., Optical Express 19, 21857 (2011)

- (2) Spatial encoding

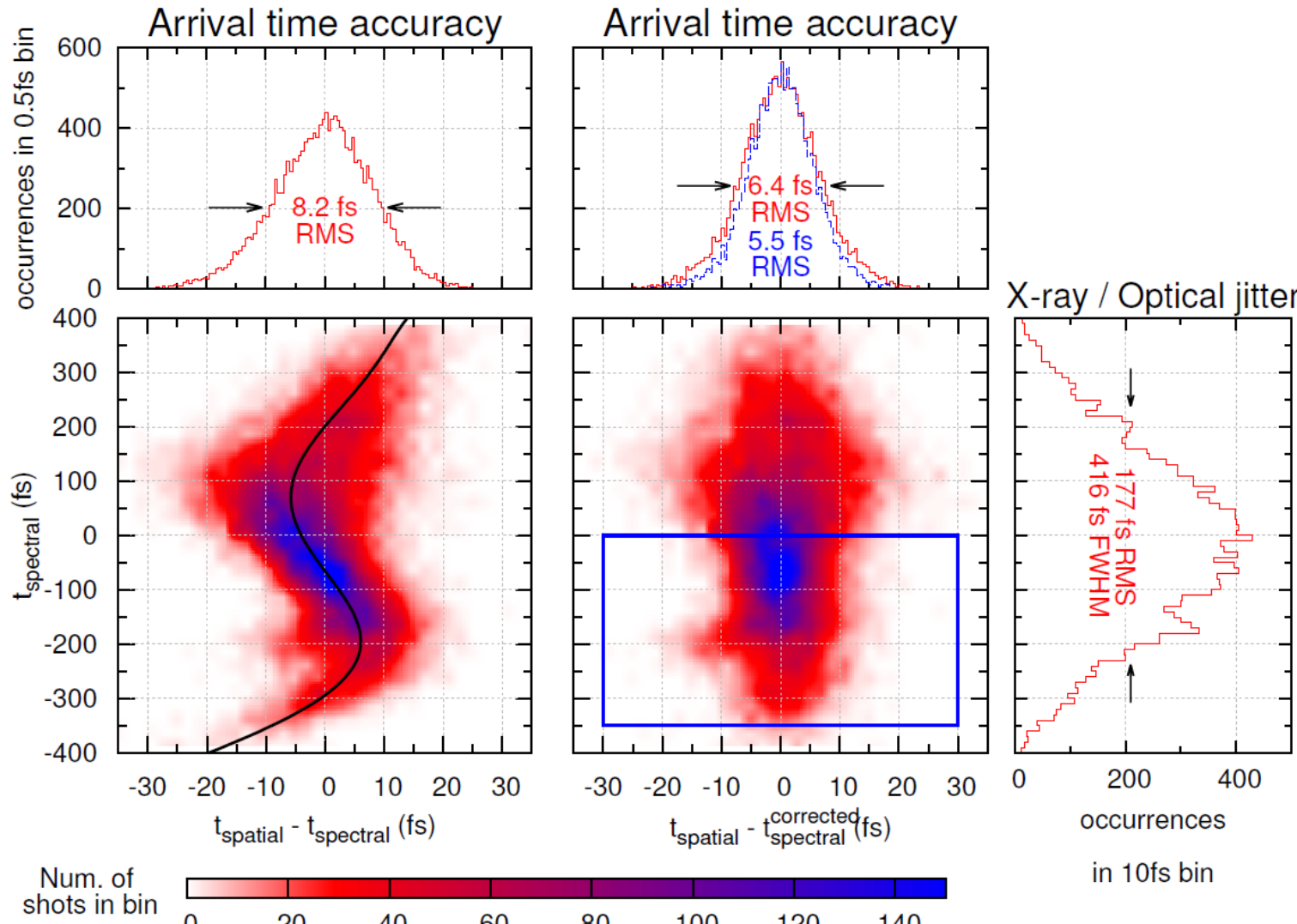
(a: transmission, b: reflectivity)

T. Maltezopoulos et al., NJP 10, 033026 (2008)

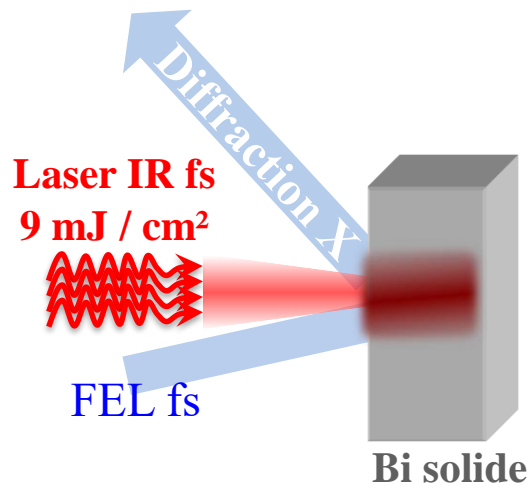


Diagnostic correlation of LCLS experiment at XPP

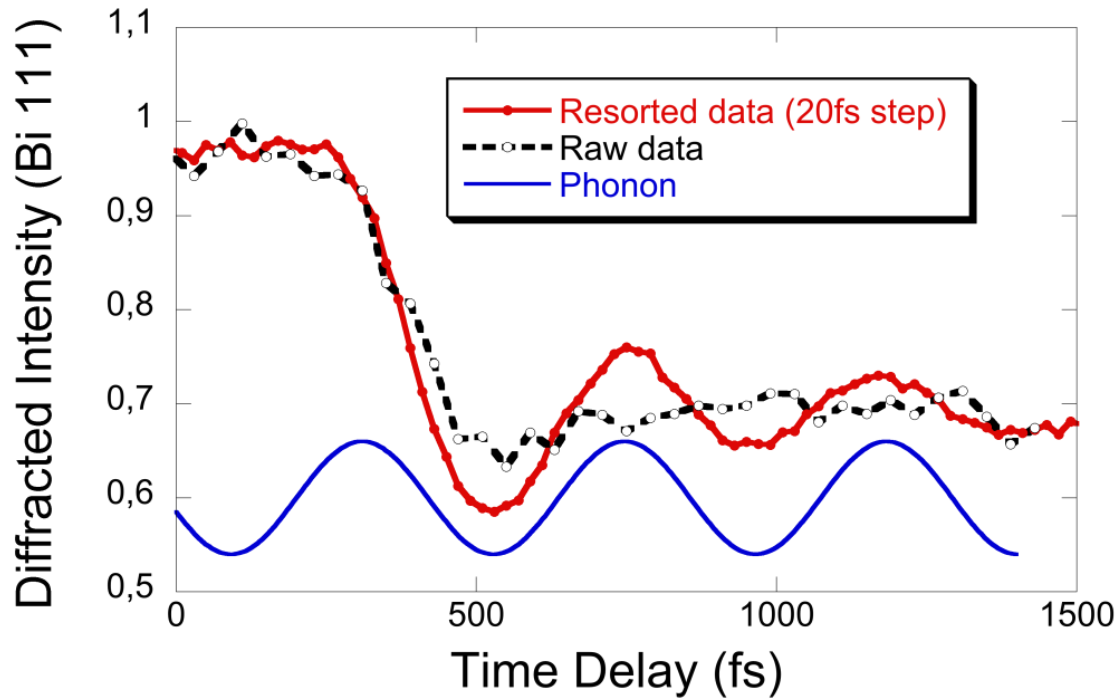
Spectral vs. Spatial (transmission)



Experimental test on Bi



fs atomic displacements generated in Bi samples, in response to ultrafast photoexcitation by an optical laser



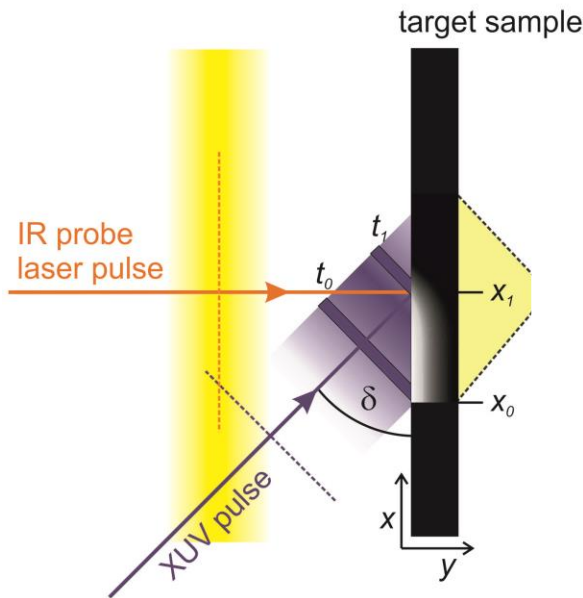
- by resorting data according to their arrival time
ultrafast processes can be resolved

D.M Fritz et al., *Science* 315, 633 (2007)

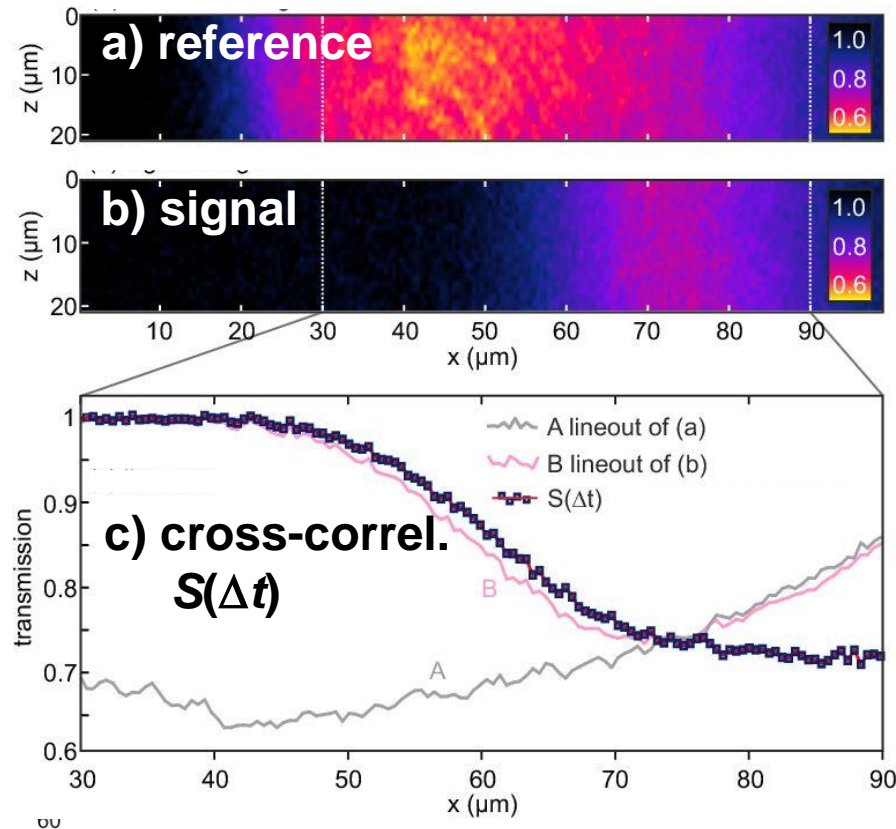
K. Sokolowski-Tinten et al., *Nature Phys.* 422, 287 (2003)

Signal processing for optical–FEL cross correlation

- measured transmission change



- a) probe pulse arrives after XUV pulse
- b) probe pulse arrives simultaneously
- c) cross-correlation
(corrected for FEL beam profile)



Data analysis

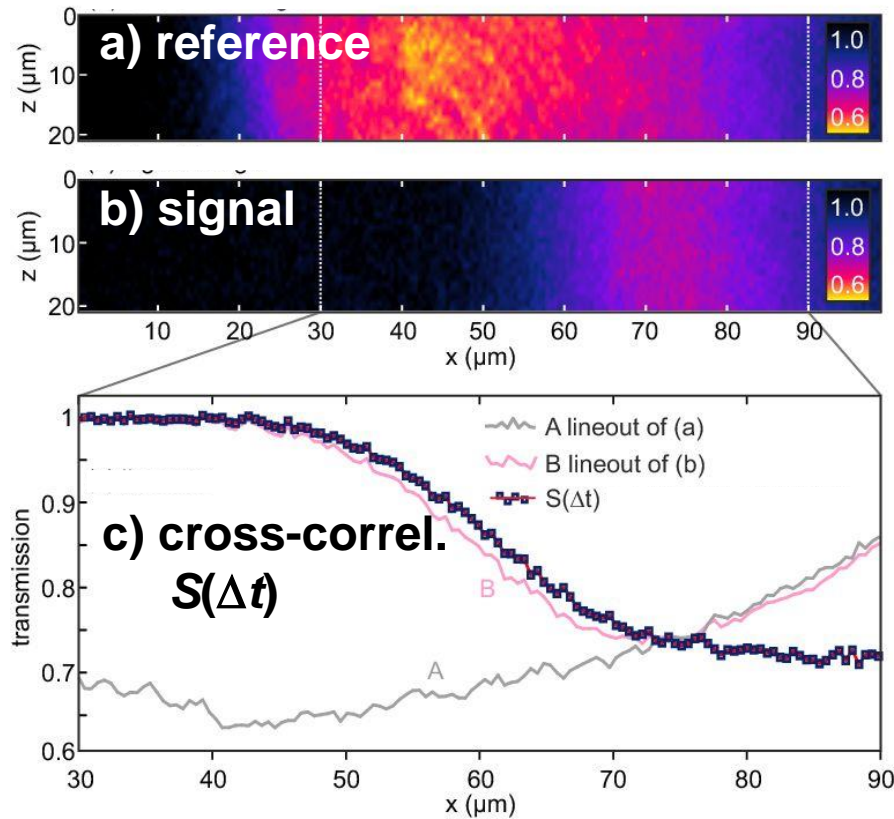
- Cross-correlation function

$$S(\Delta t) = \int_{-\infty}^{+\infty} I_{\text{Laser}}(t) G(t - \Delta t) dt$$

measured measured study
Gaussian (64±7) fs at 800 nm

- arrival time directly obtained from $S(\Delta t)$
- $G(t)$ ultrafast transmission change
- contains information about FEL intensity

$$G(t) = G[I_{\text{FEL}}(t)]$$



Data analysis and results

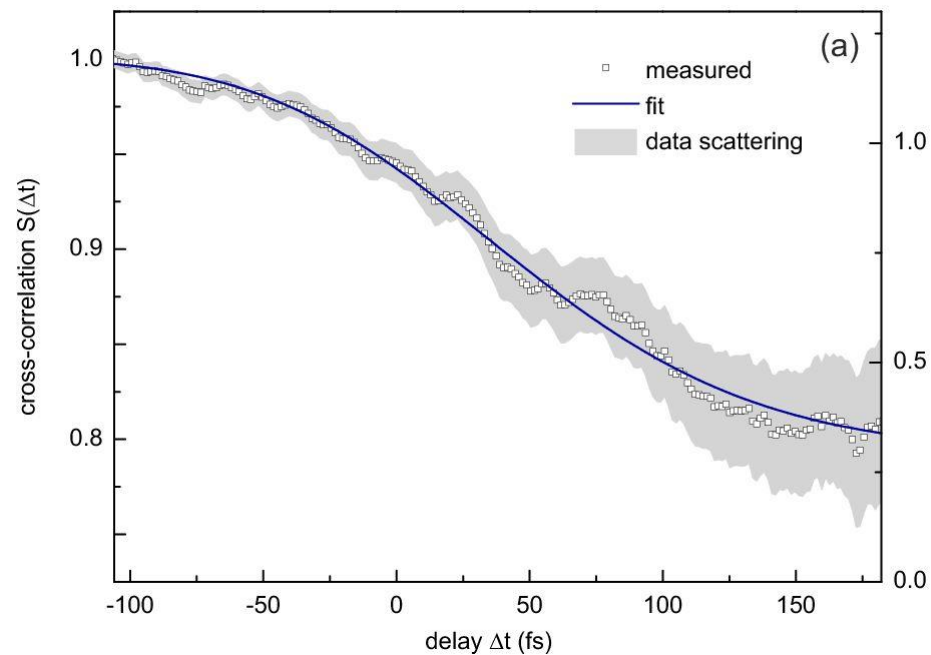
- **FLASH pulse durations at different wavelengths (fused silica sample)**

FEL wavelength: 41.5 nm

FEL pulse energy: $(84 \pm 4) \mu\text{J}$

Bunch charge: 0.50 nC

Pulse duration: $(184 \pm 14) \text{ fs}$

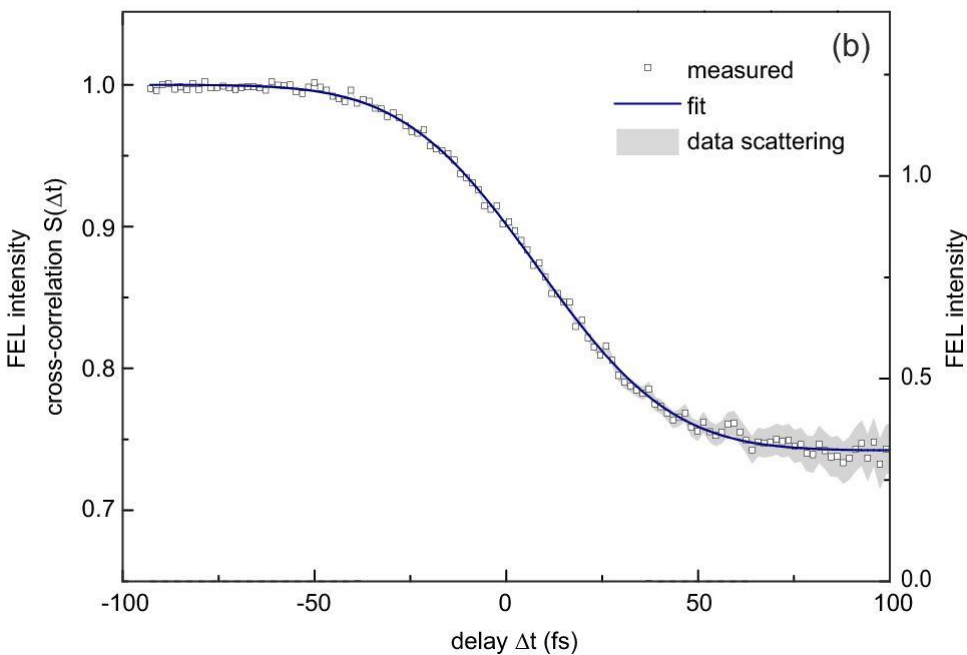


FEL wavelength: 5.5 nm

FEL pulse energy: $(29 \pm 10) \mu\text{J}$

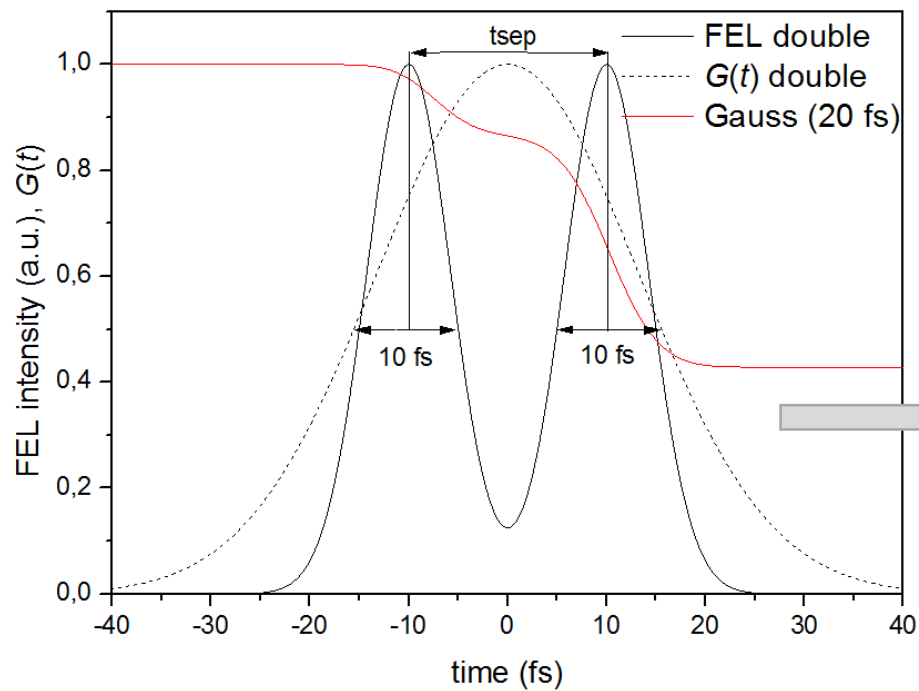
Bunch charge: 0.25 nC

Pulse duration: $(21 \pm 19) \text{ fs}$

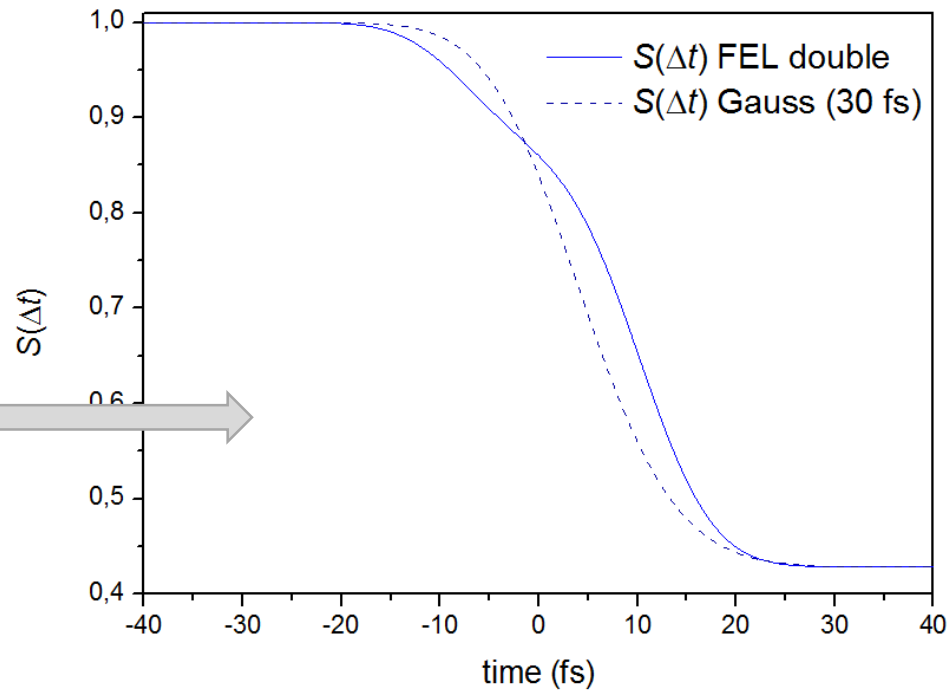


FEL double pulses

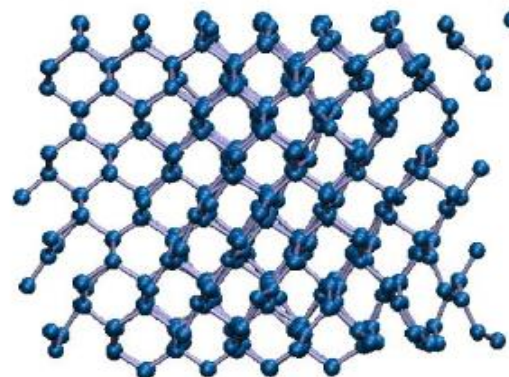
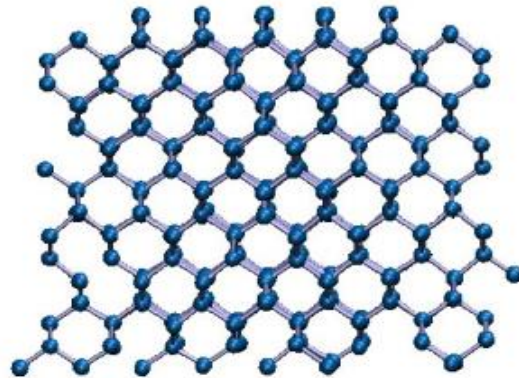
- Example: FEL double pulses (2x 10 fs)
(separated by 20 fs)



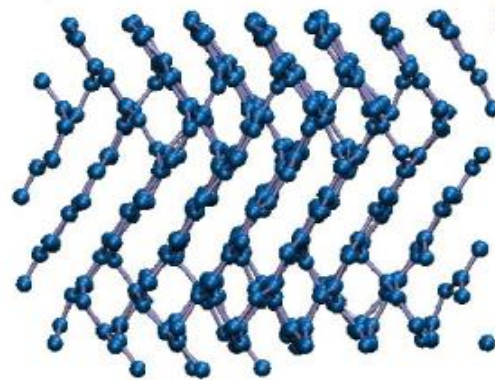
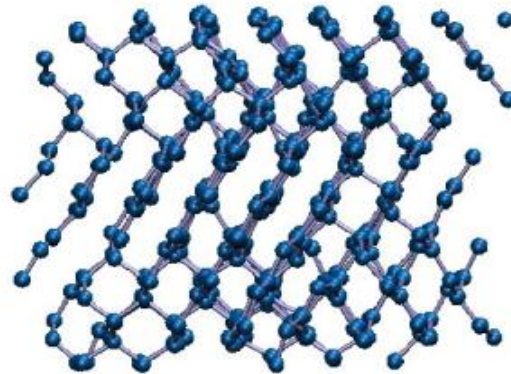
$S(\Delta t)$ with 10 fs probe laser



Ultra-fast solid to solid phase transition in diamond.



Sven Toleikis



Nonthermal graphitization of diamond induced by a femtosecond x-ray laser pulse

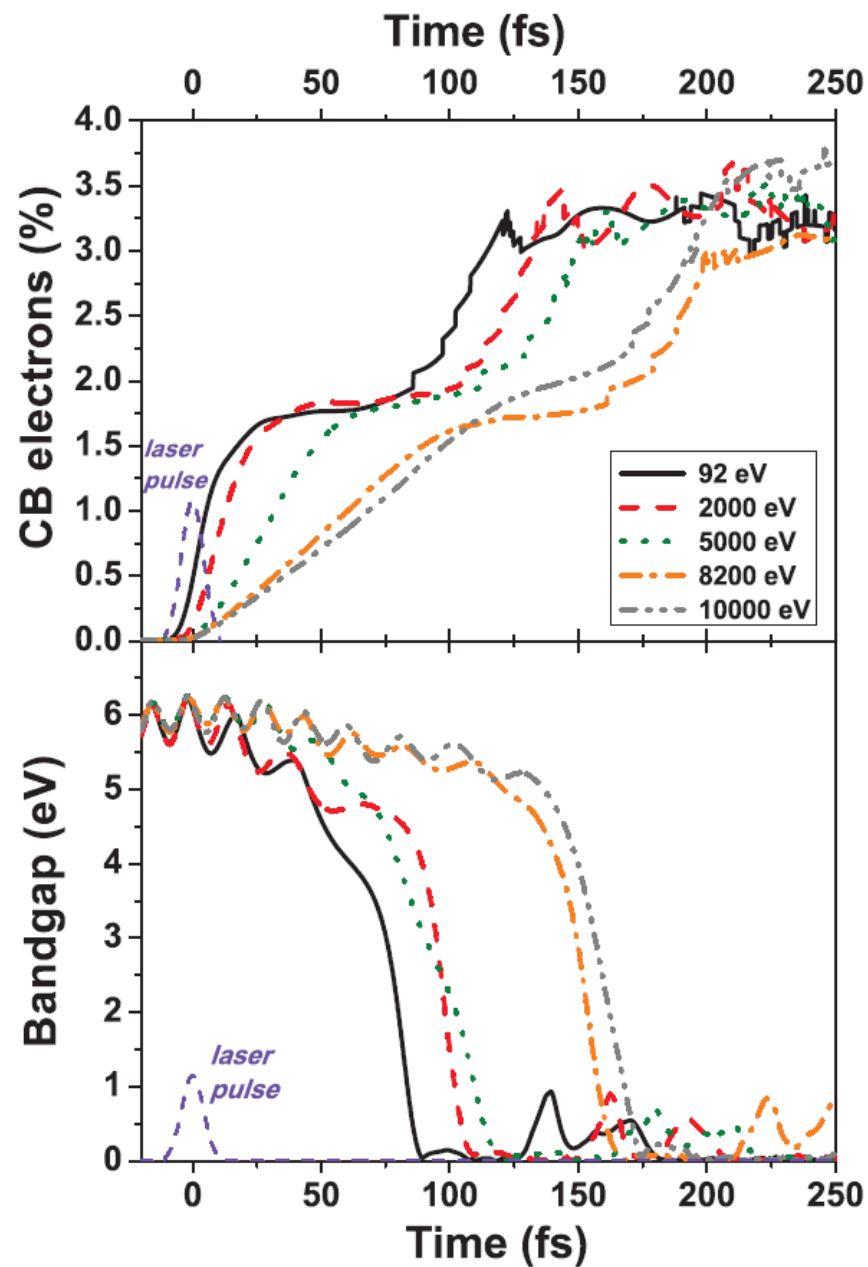
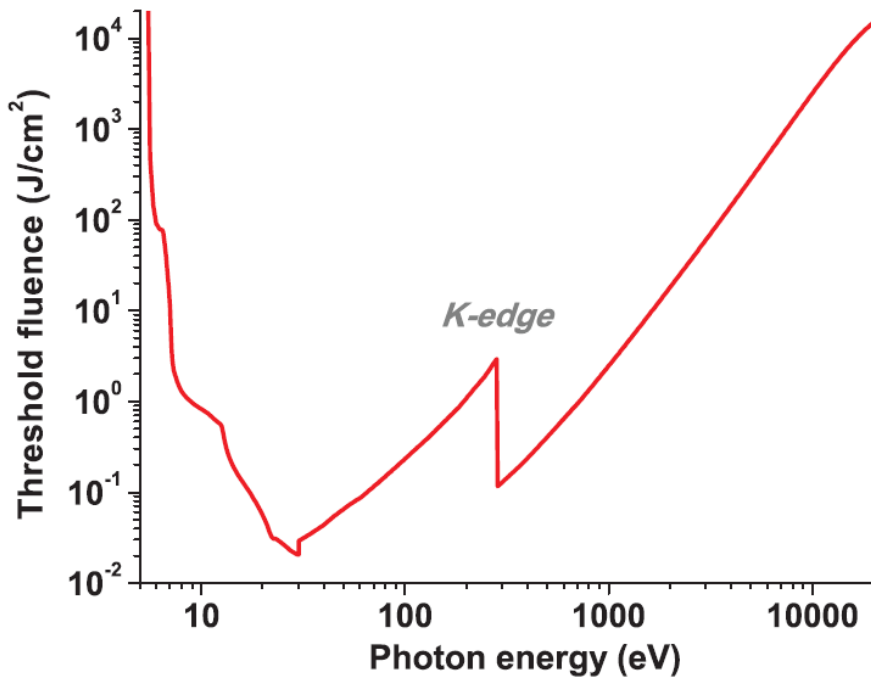
- N. Medvedev, H.O. Jeschke, and B. Ziaja; Phys. Rev. B **88**, 224304 (2013)
- Mechanism:
 - short x-ray pulses -> photoionization
 - > photoelectrons
 - > K-shell / L-shell holes -> Auger decays -> impact ionization -> secondary e⁻
 - > further cascading
- Hybrid model described in:
N. Medvedev, H. O. Jeschke, and B. Ziaja, New J. Phys. **15**, 015016 (2013)

Combines different theoretical approaches:

- MC method to describe photoabsorption and Auger decays + transient nonequilibrium kinetics of high energy electrons and their secondary cascading
 - > transient electron distribution:
low-energy Fermi-like distribution (e⁻ temperature equation) + high-energy electrons
- The potential energy surface, the collective forces acting on each atom, and the transient electronic band structure are calculated by diagonalizing a tight-binding (TB) Hamiltonian
- Atom dynamics is followed by classical molecular dynamics (MD)

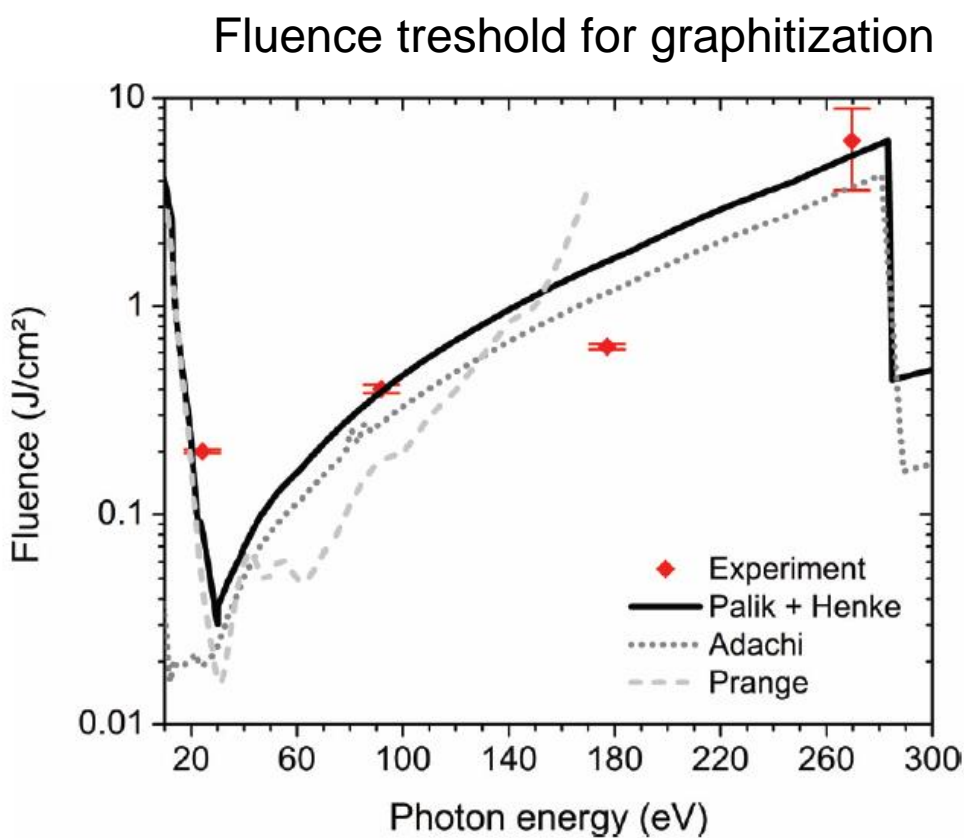
Results / Prediction for diamond

- Damage threshold fluence for a broad photon energy range is always **~0.7 eV / atom**
- The x-rays induces an ultrafast non-thermal phase transition:
nonthermal graphitization of diamond

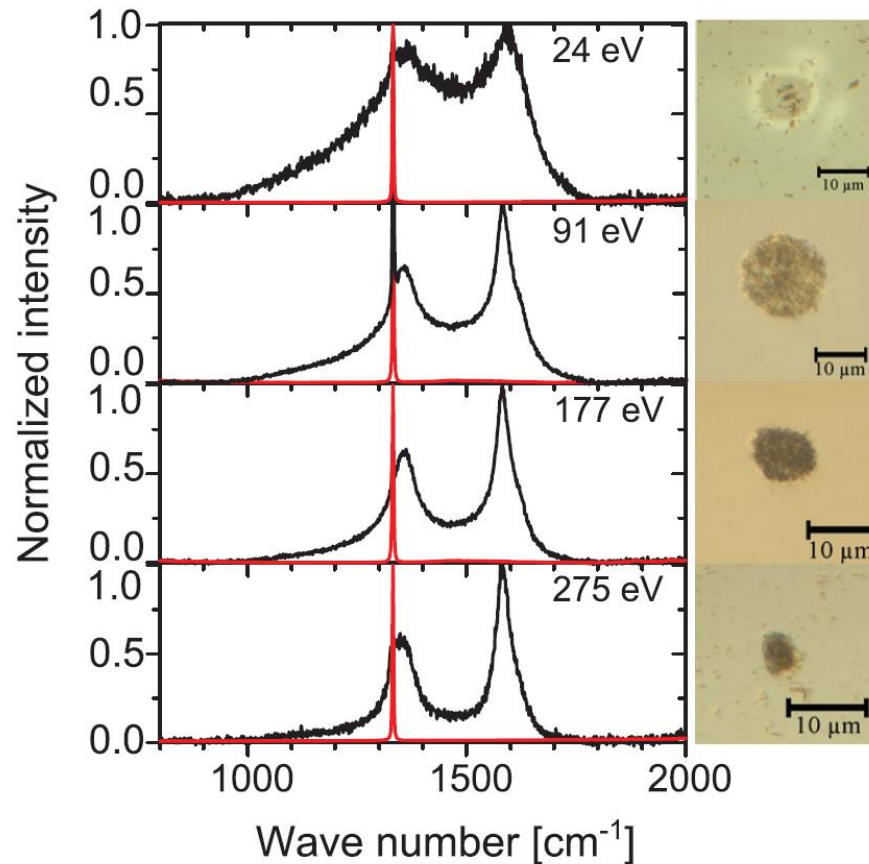


Damage experiment @ FLASH

- J. Gaudin, N. Medvedev, J. Chalupsky, T. Burian, S. Dastjani-Farahani, V. Hajkova, M. Harmand, H.O. Jeschke, L. Juha, M. Jurek, D. Klinger, J. Krzywinski, R.A. Loch, S. Moeller, M. Nagasono, C. Ozkan, K. Saksl, H. Sinn, R. Sobierajski, P. Sovak, S. Toleikis, K. Tiedtke, M. Toufarova, T. Tschentscher, V. Vorlicek, L. Vysin, H. Wabnitz, and B. Ziaja;
Phys Rev. B **88**, 060101(R) (2013)



Post-mortem micro-Raman spectra
of the diamond samples

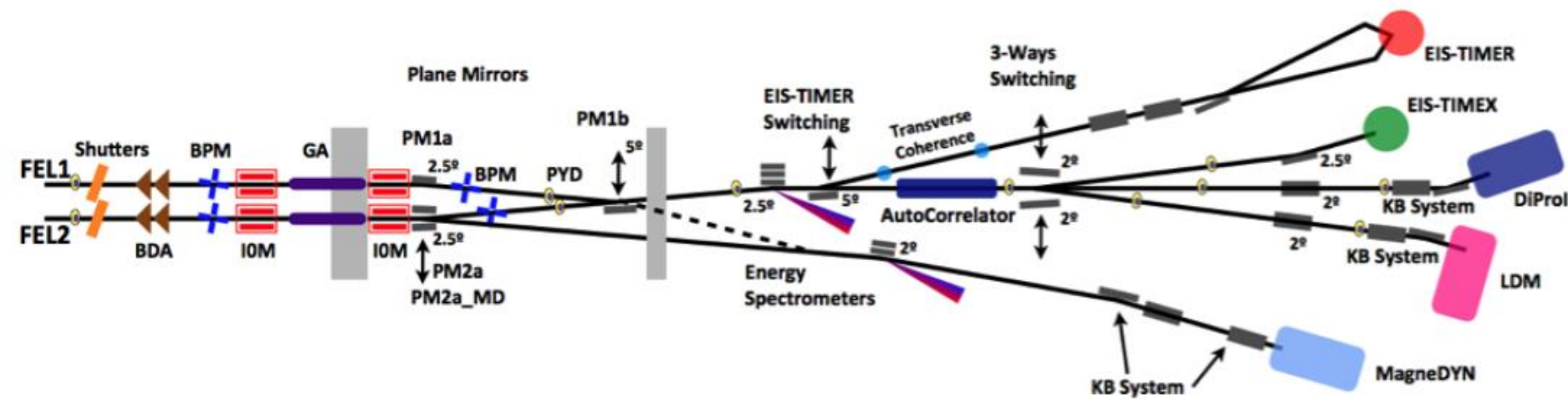


Experiment @ FERMI (a seeded XUV FEL)

F. Tavella, H. Höppner, V. Tkachenko, N. Medvedev, F. Capotondi,
T. Golz, Y. Kai, M. Manfredda, E. Pedersoli, M.J. Prandolini,
N. Stojanovic, T. Tanikawa, U. Teubner, S. Toleikis, and B. Ziaja,

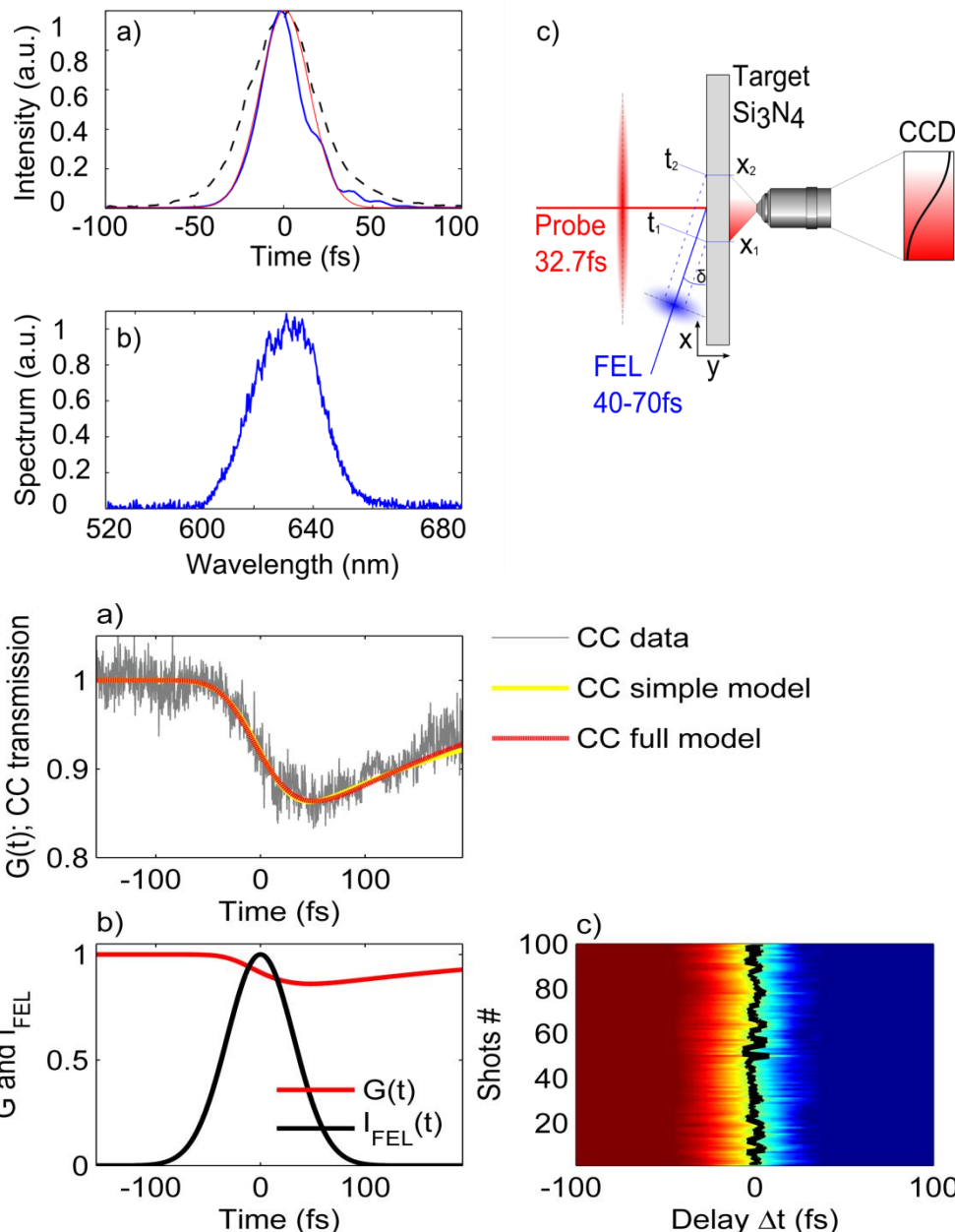
Soft x-rays induced femtosecond solid-to-solid phase transition

High Energy Density Physics 24, 22 (2017)



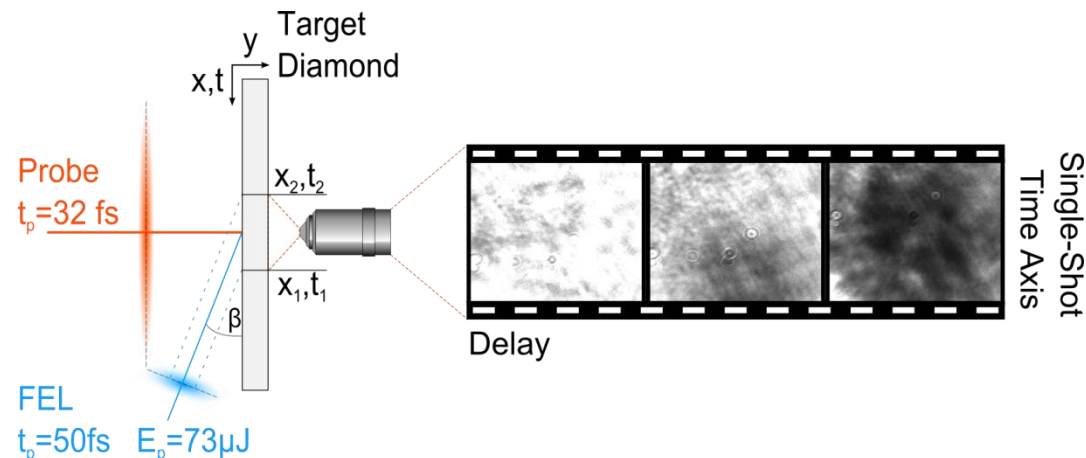
Timing tool @ FERMI

- Experimental setup @ FERMI (c)
- Using own NOPA driven by the seed laser: 32.7 fs (a), 630 nm (b), 300 nJ on target
- Spatial time resolution (of the imaging system and the angle δ): ~ 4 fs
- XUV beam spot size on target: $150 \times 30 \mu\text{m}^2$
- Non-damaging mode

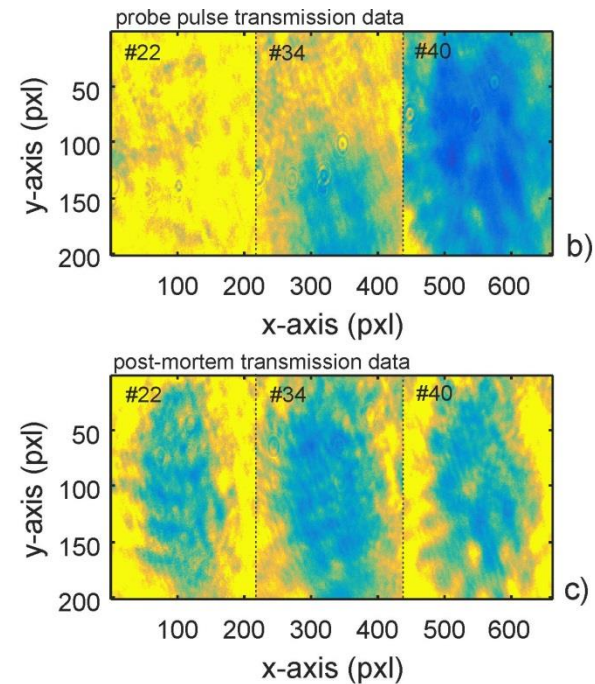
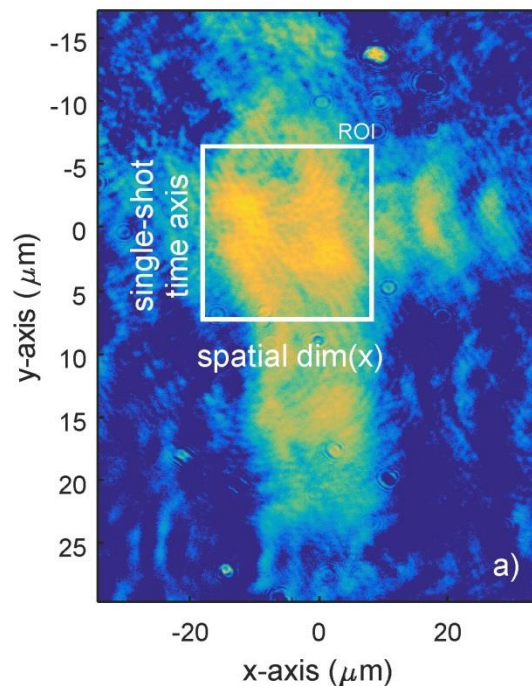


Ultra-fast solid to solid phase transition in diamond

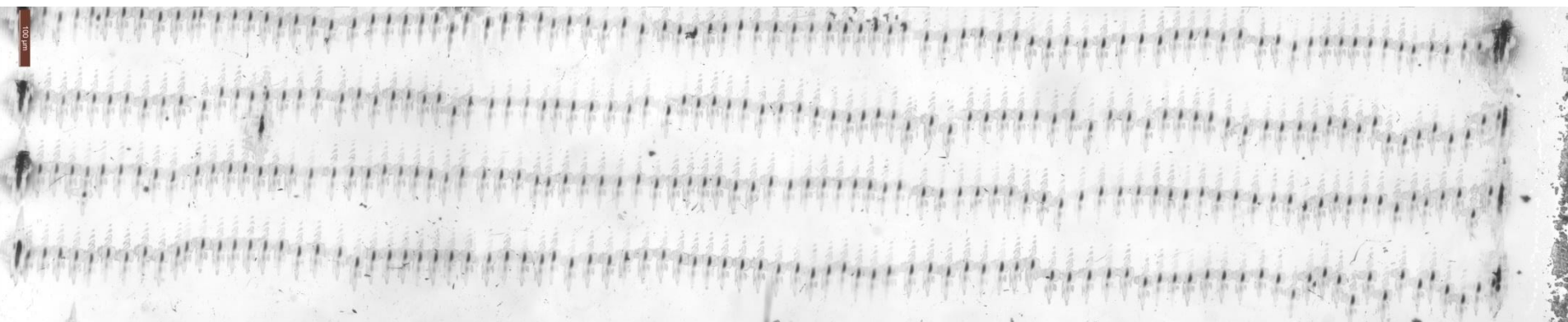
- Setup @ DiProl beamline
- Target: 300 μm thick poly-crystalline CVD diamond
- XUV beam spot size on target: 17x7.5 μm^2
- FEL wavelength: 26.17 nm
- FEL pulse length: 52.5(3.4) fs



- Single shot raw data example
- Scanning time delay in 10 fs steps
- Shot #22:
probe pulse hits target prior to FEL pulse
- Shot #34:
probe pulse hits the target at the same time as the FEL pulse
- Shot #40:
probe pulse hits the target after the FEL pulse

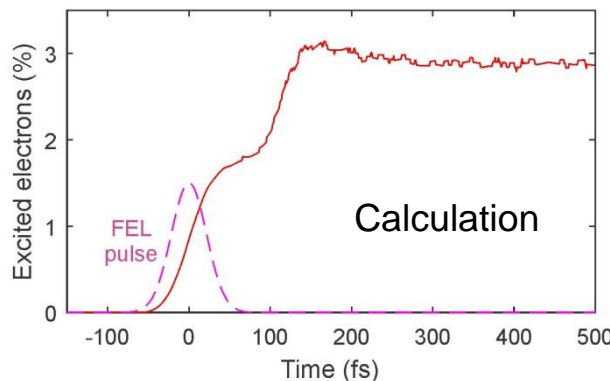


Scanning the target and shooting the diamond target with 10 Hz

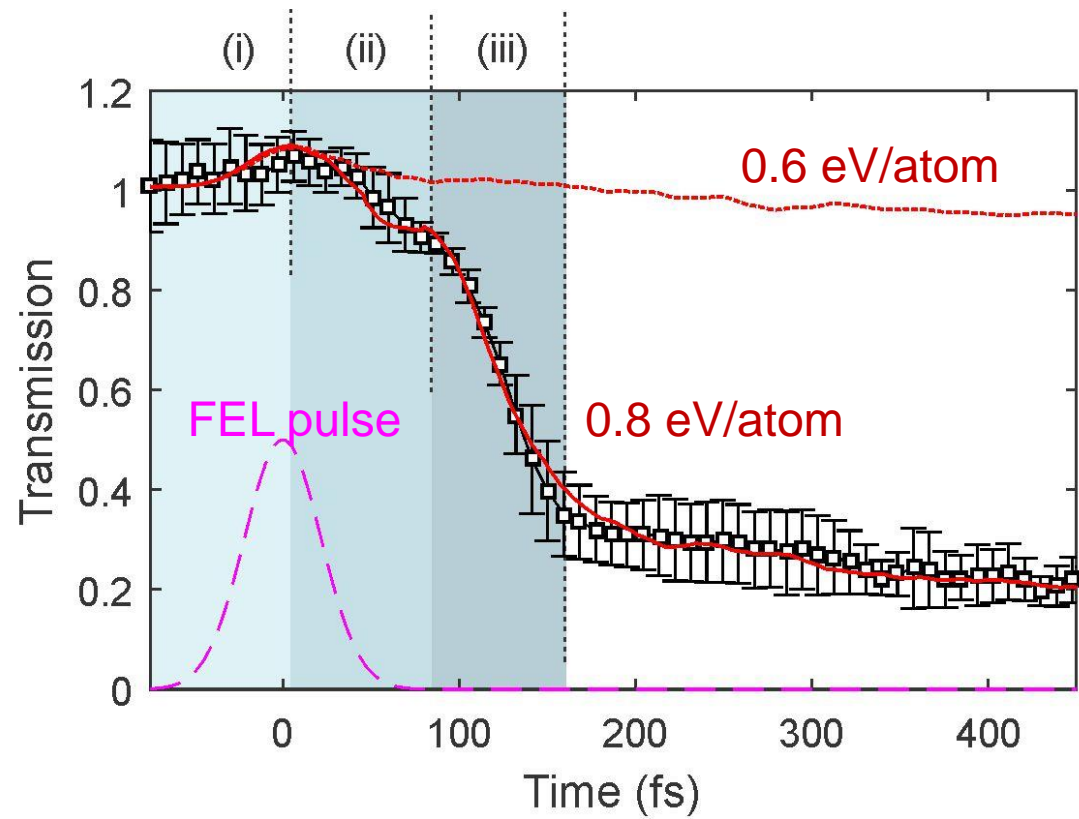
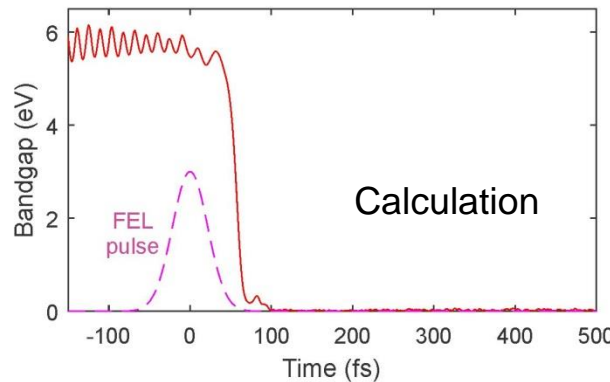


Ultra-fast solid to solid phase transition in diamond

- Transient optical transmission at ~630 nm from a diamond sample irradiated with XUV
 - Non-thermal graphitization in three steps:
 - (i) initial electronic excitation to the conduction band

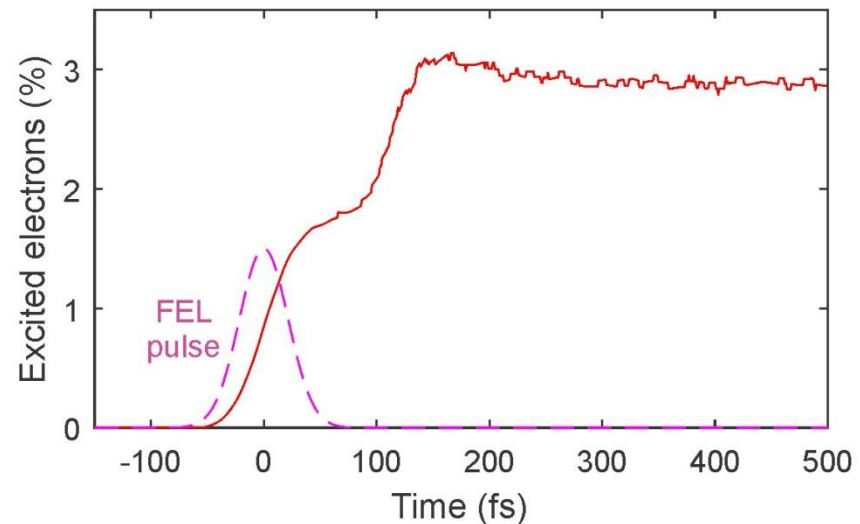
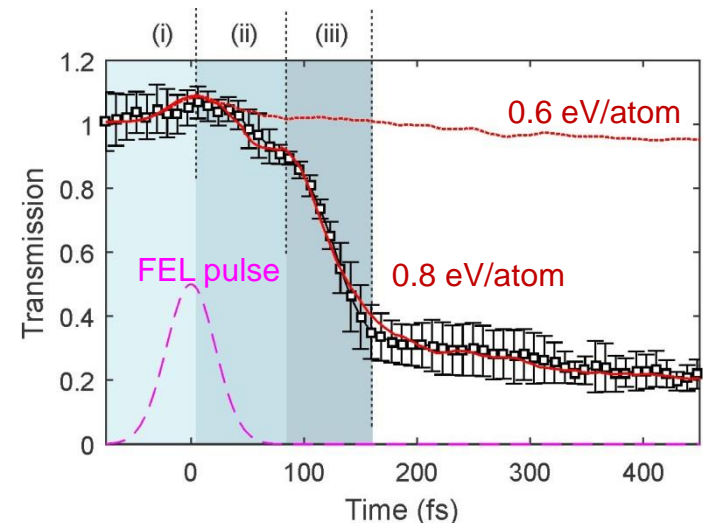
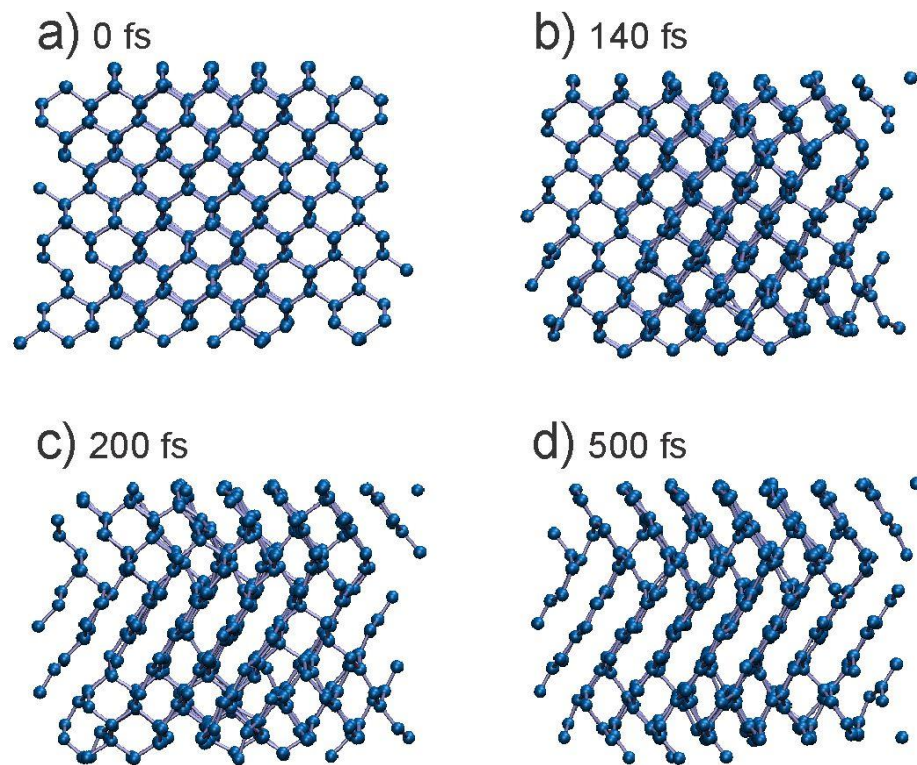


- (ii) electronic excitation triggers band gap collapse



Ultra-fast solid to solid phase transition in diamond

- (iii)
 - Significant decrease of transmission
 - Atomic relocation (from ~140 fs on)
 - Changing the material properties from insulating diamond to semi-metallic graphite
 - Further increase of electron density in CB
- Final atomic relocation in overdense graphite with broken plane orientations

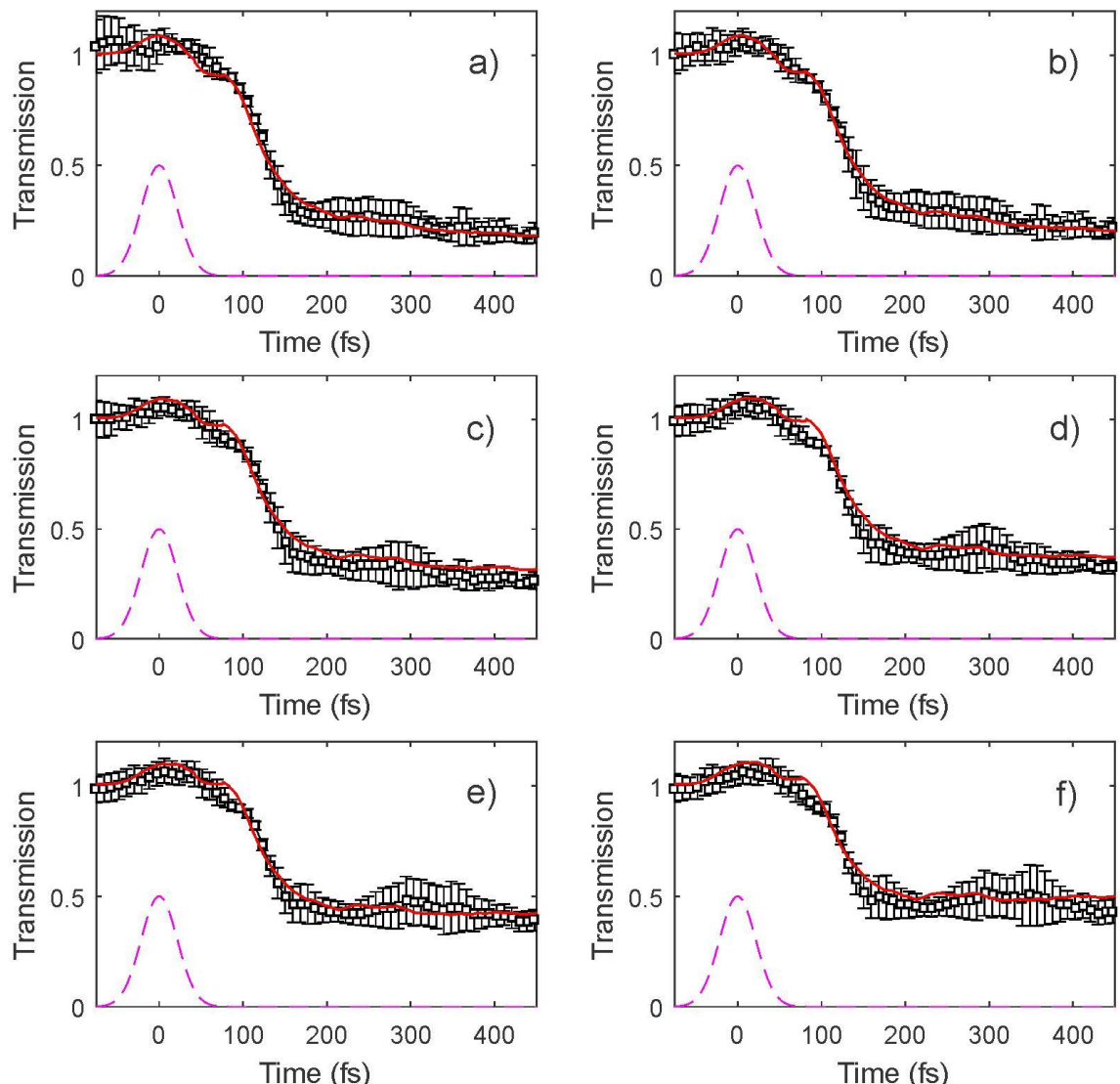
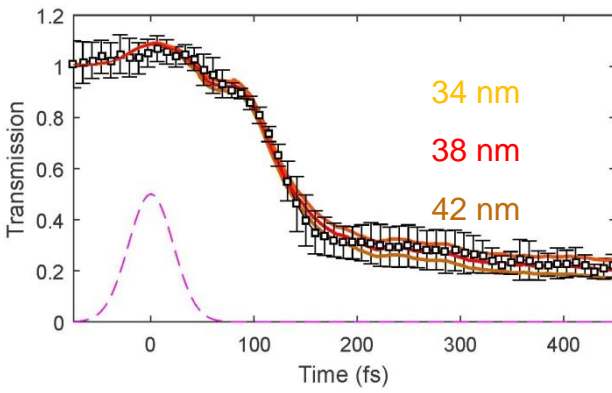


Ultra-fast solid to solid phase transition in diamond

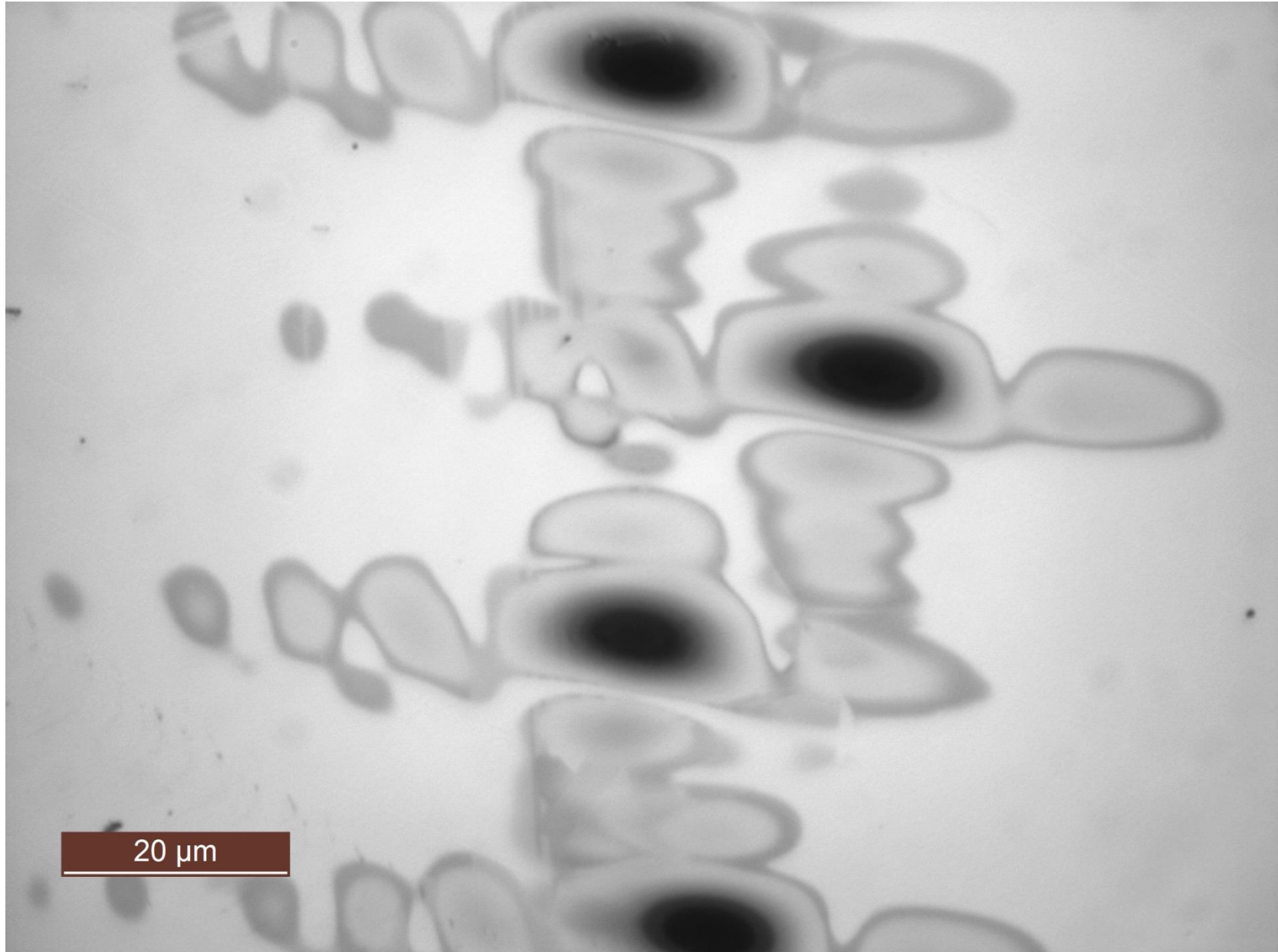
- Temporal behavior is independent from the fluence (if above 0.7 eV/atom)

➤ Transient graphite layer thickness at t=400 fs:

- a) 40 nm
- b) 38 nm
- c) 29 nm
- d) 25 nm
- e) 22 nm
- f) 17 nm

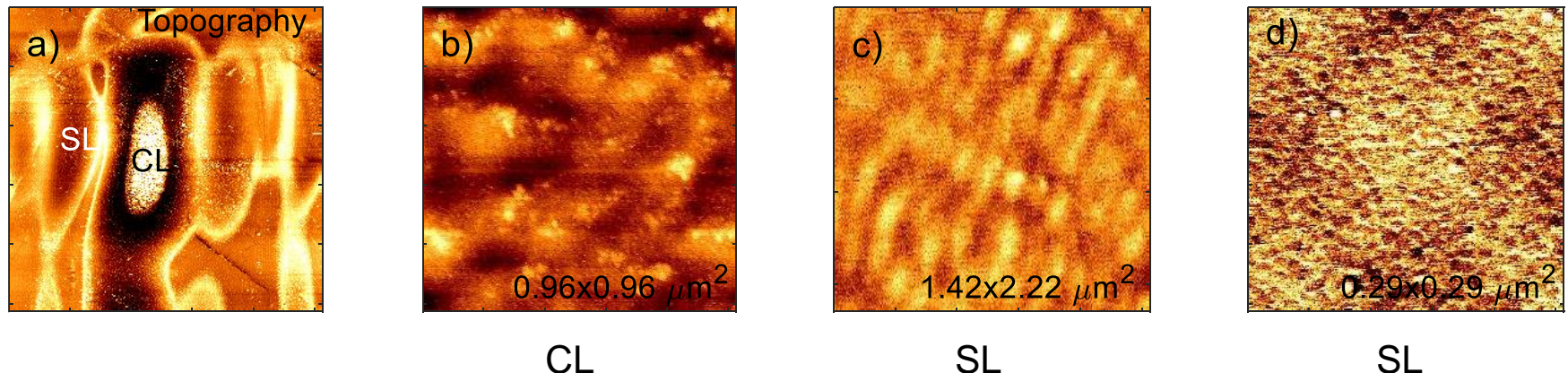
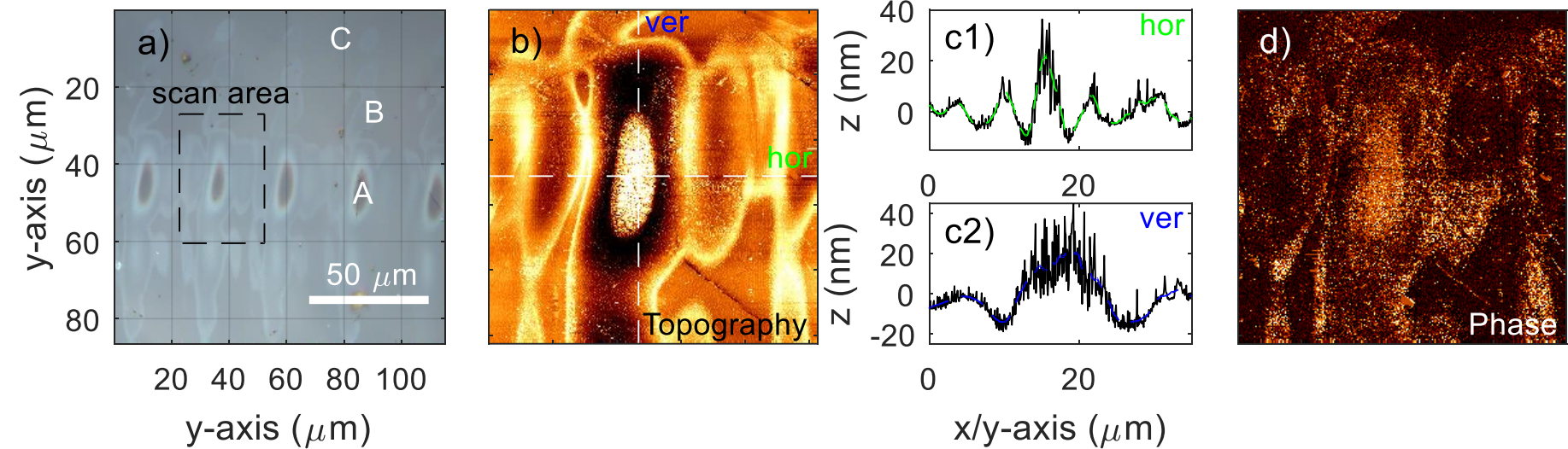


Post-mortem analysis



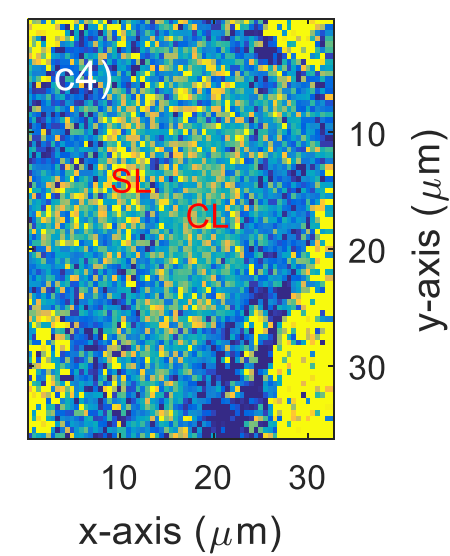
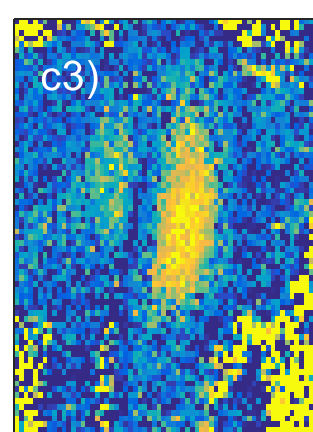
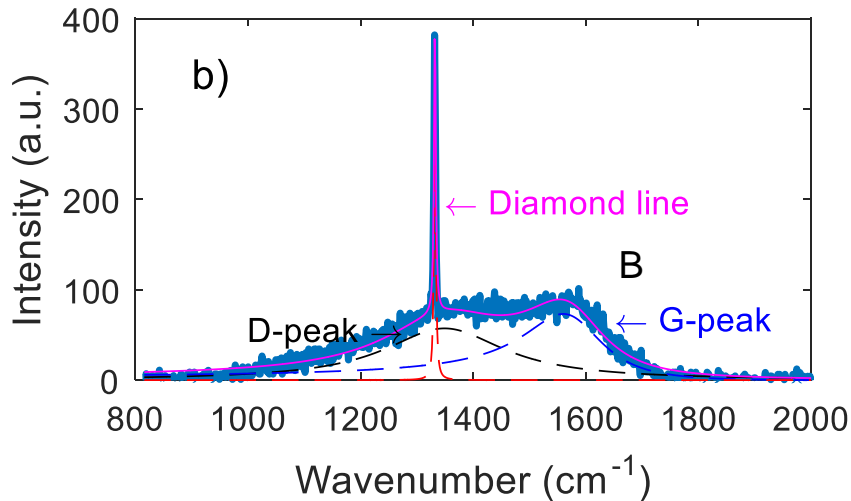
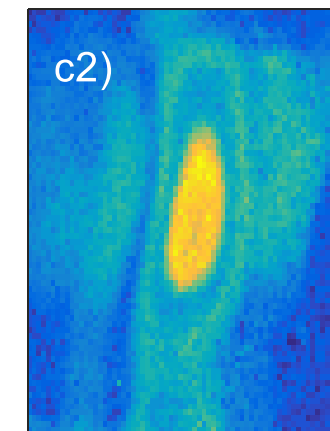
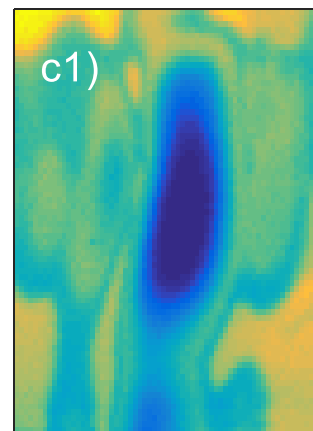
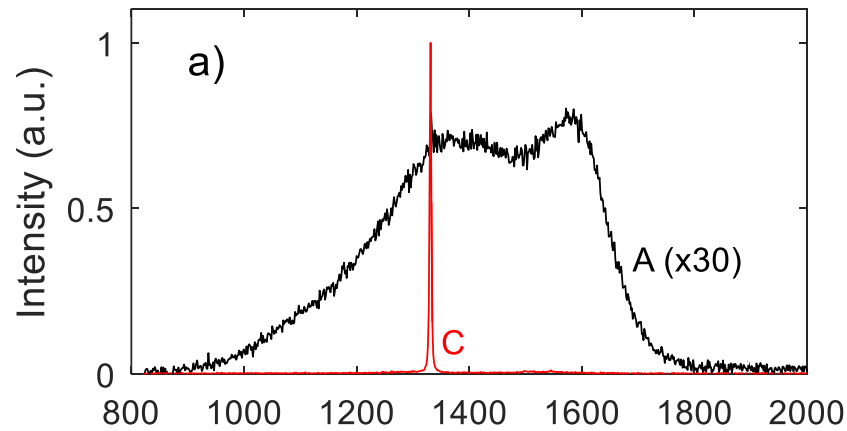
Post-mortem analysis I

> Scanning probe microscopy (a), non-contact AFM Scan (b), line-outs (c), phase scan (d)



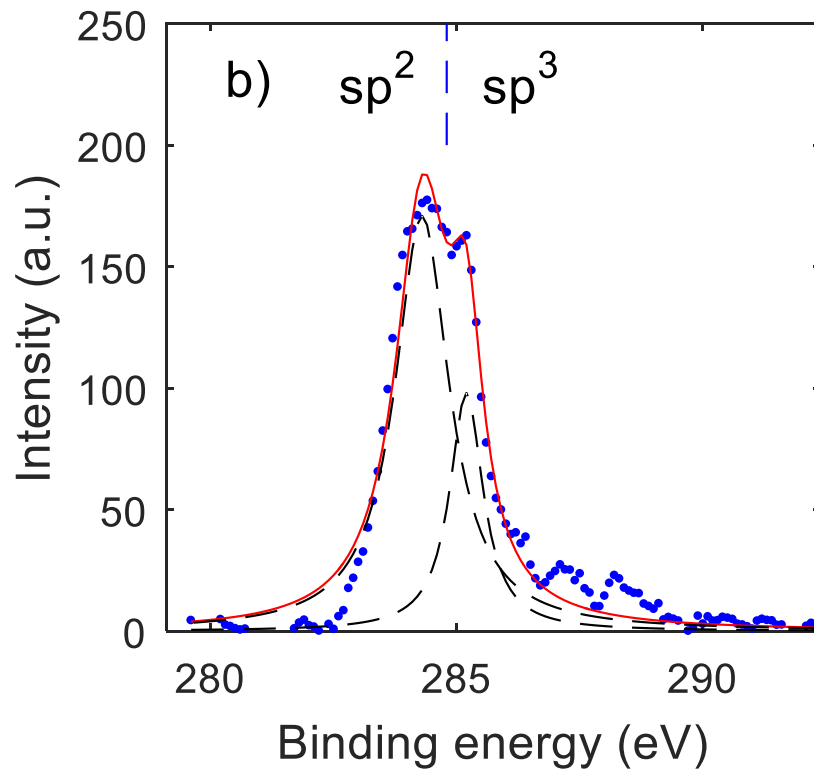
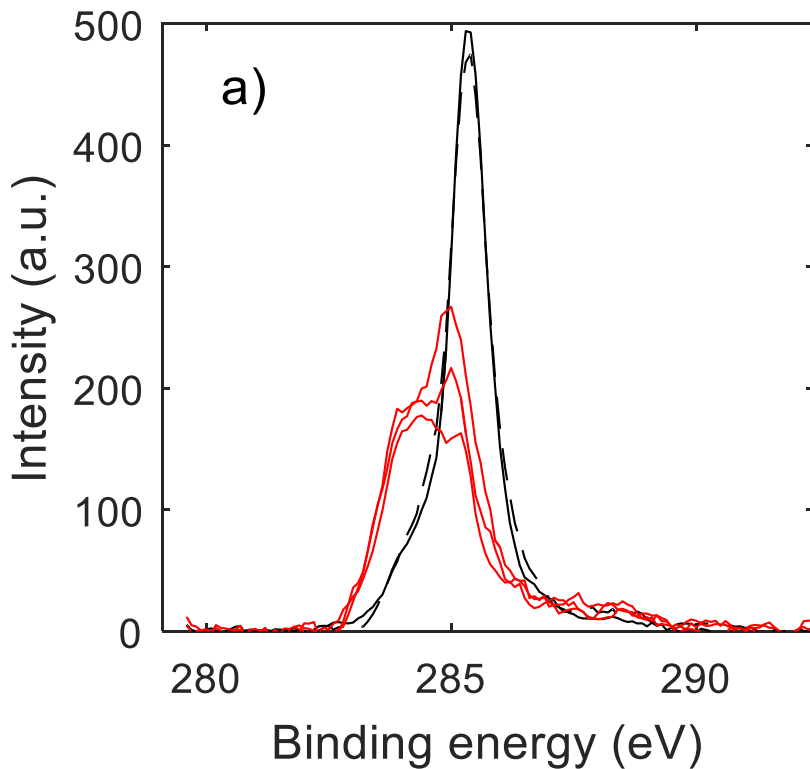
Post-mortem analysis II

- Confocal Raman Micro-Spectroscopy (spot size: $\sim 1 \mu\text{m}$)
C: diamond line @ 1332 cm^{-1}
A: graphitized layer: D peak ($\sim 1350 \text{ cm}^{-1}$), and G peak ($\sim 1580 \text{ cm}^{-1}$)



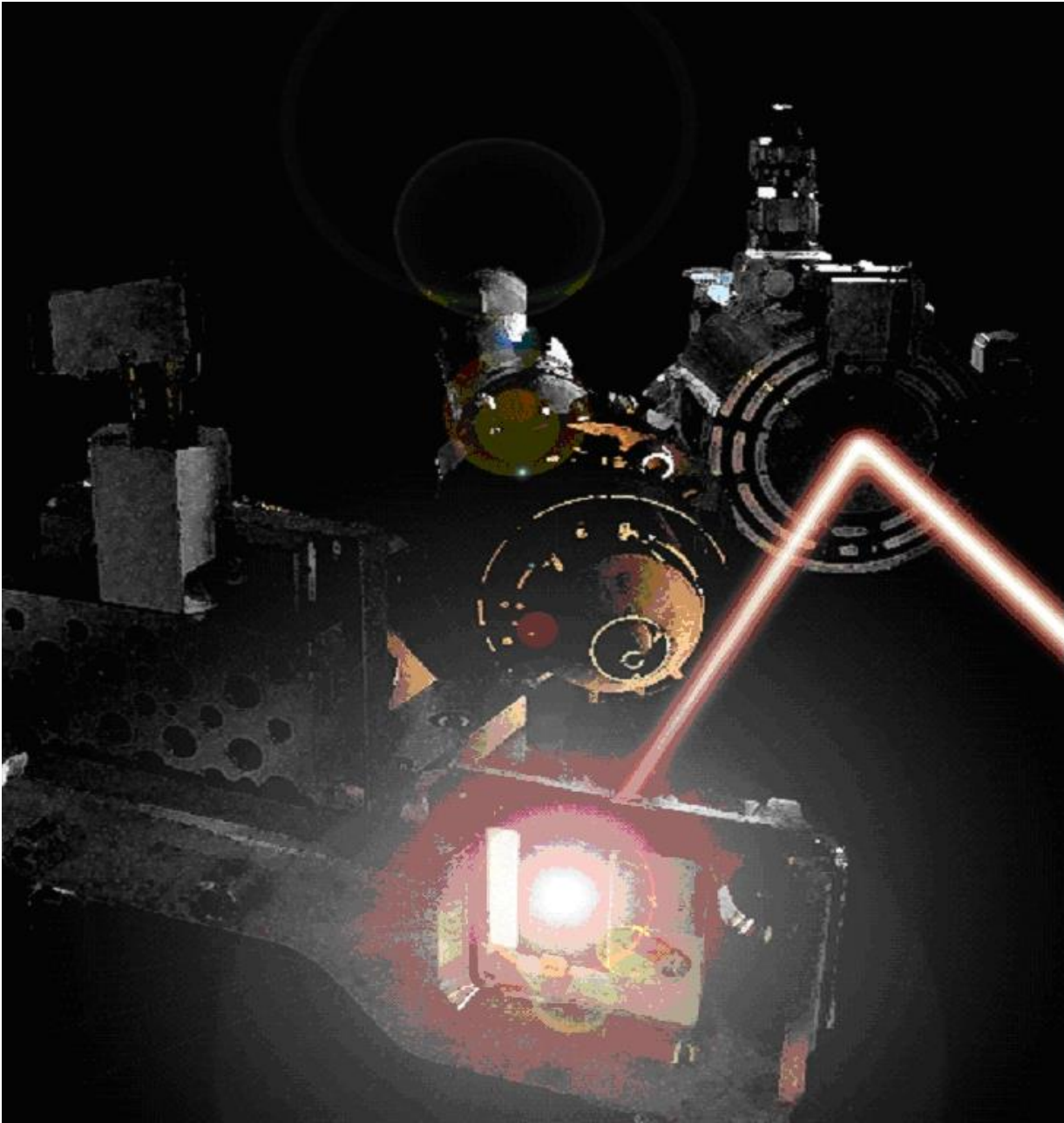
Post-mortem analysis III

- X-ray Photoelectron Spectroscopy (XPS) with an Al (K- α) source (1486 eV): spot size: ~9 μm , measurement depth: 1-5 nm
- a) black lines: non-irradiated diamond sample, 2 different positions, diamond peak @ 285.5 eV
a) red lines: irradiated sample, 3 different positions of graphitization
- b) determine sp^2/sp^3 ratio (sp^2 carbon ~284 eV and sp^3 carbon ~284.9 eV)
-> sp^3 hybrid carbon content in irradiated sample positions varies between 27-42 %



“Transparent” aluminium

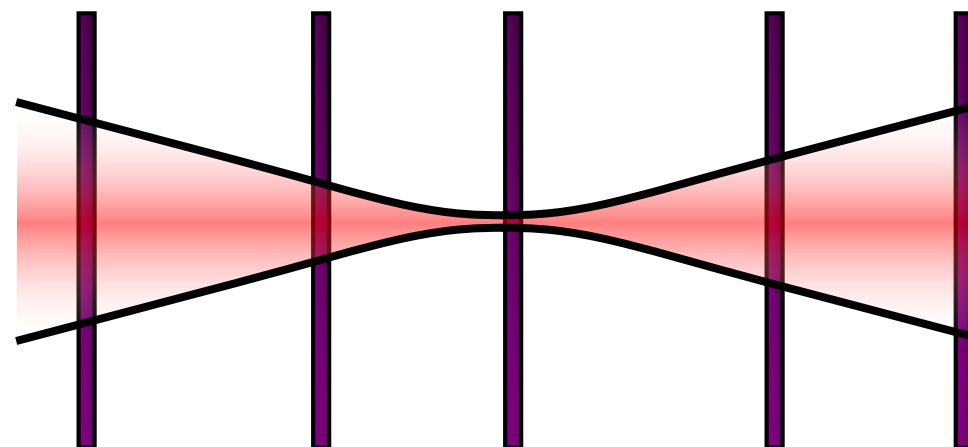
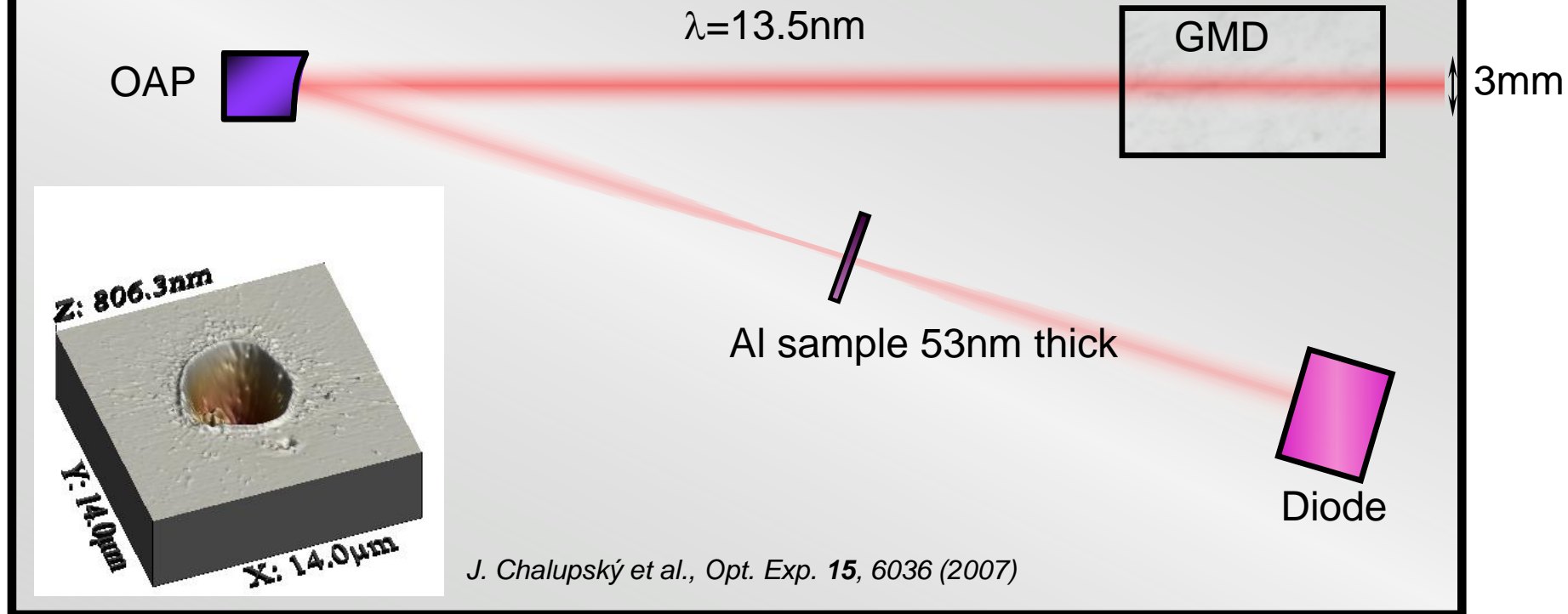
Microfocusing @ FLASH



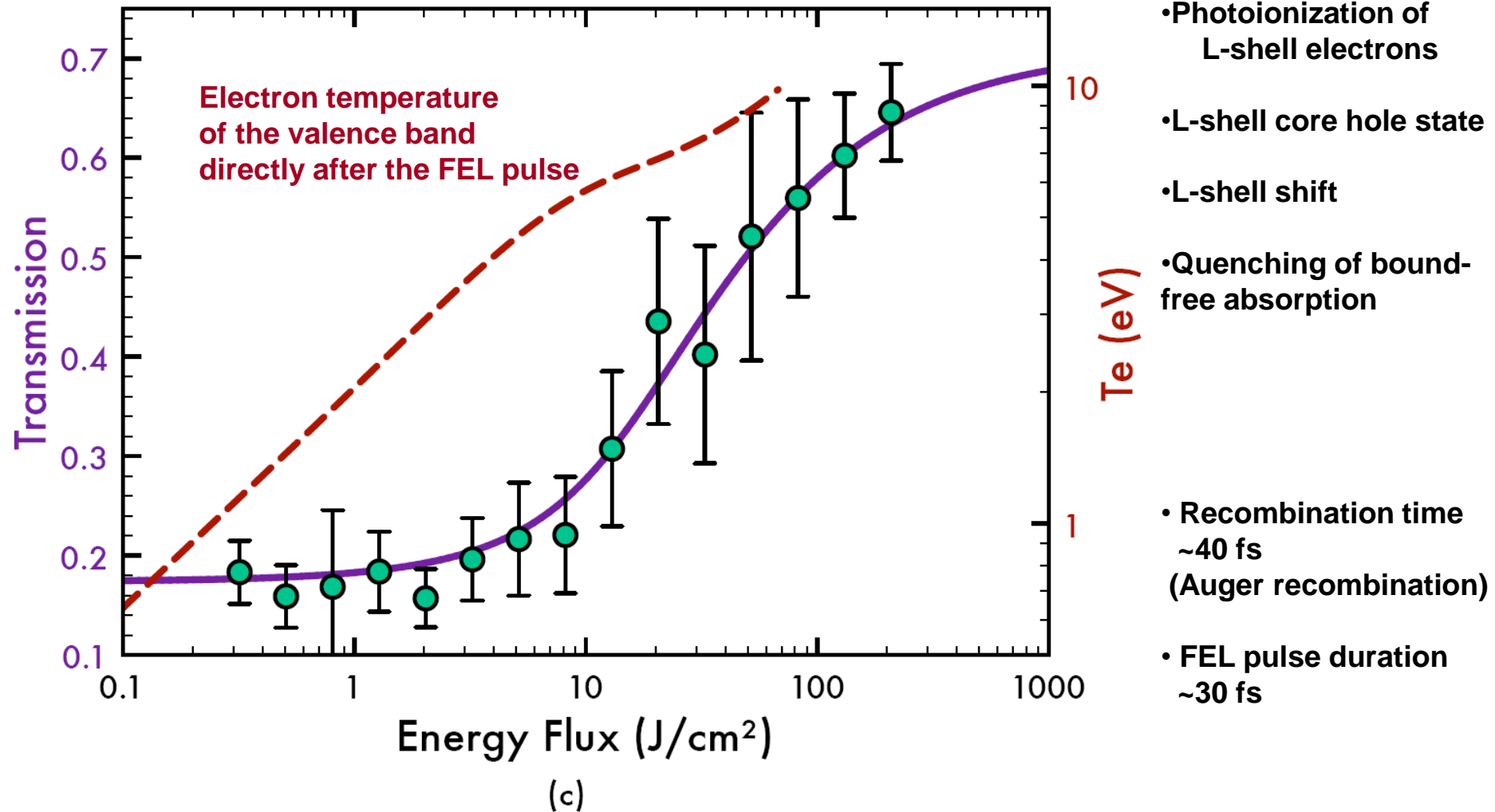
Transparent Aluminium - Experimental Setup

S. Bajt et al., Proc. of SPIE Vol. 7361, 73610J1-10 (2009)

A. Nelson et al., Opt Exp. 17, 18271 (2009)

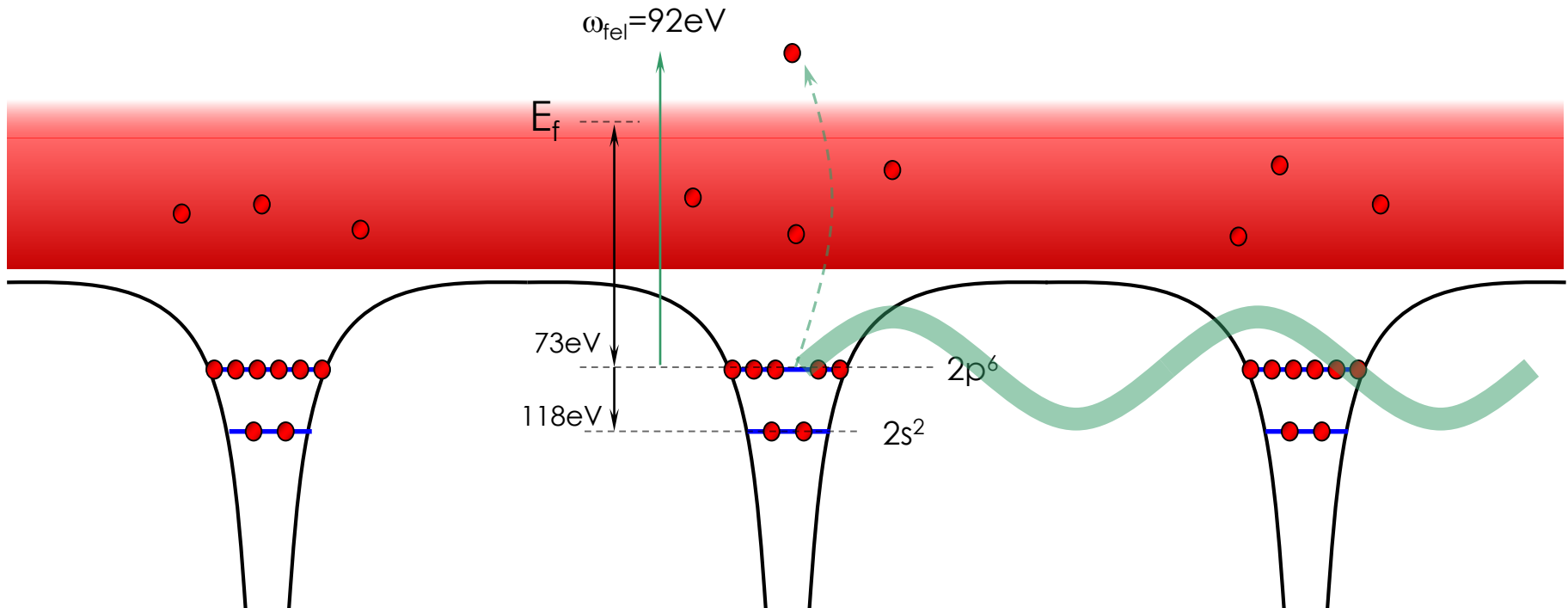


Transmission of 92 eV photons thru 53 nm Al foil including 10 nm oxide layers

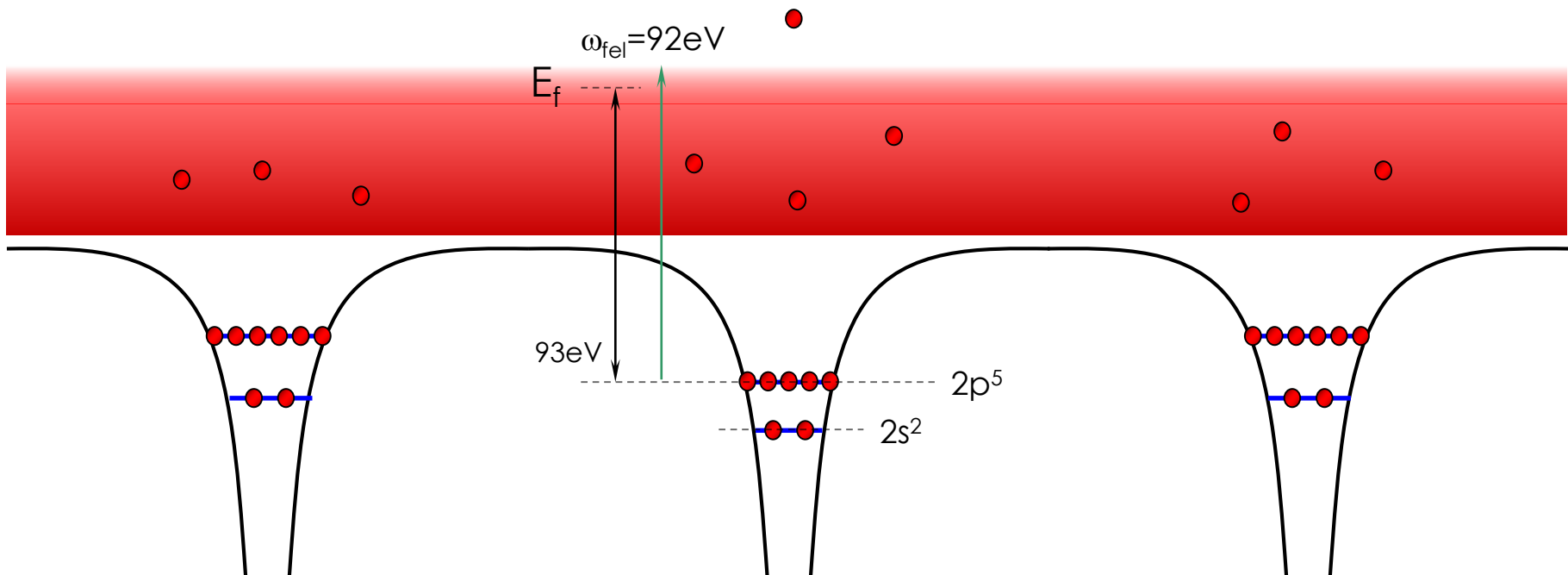


B. Nagler et al., Nature Physics 5, 693 (2009)

Al after a single photoionization



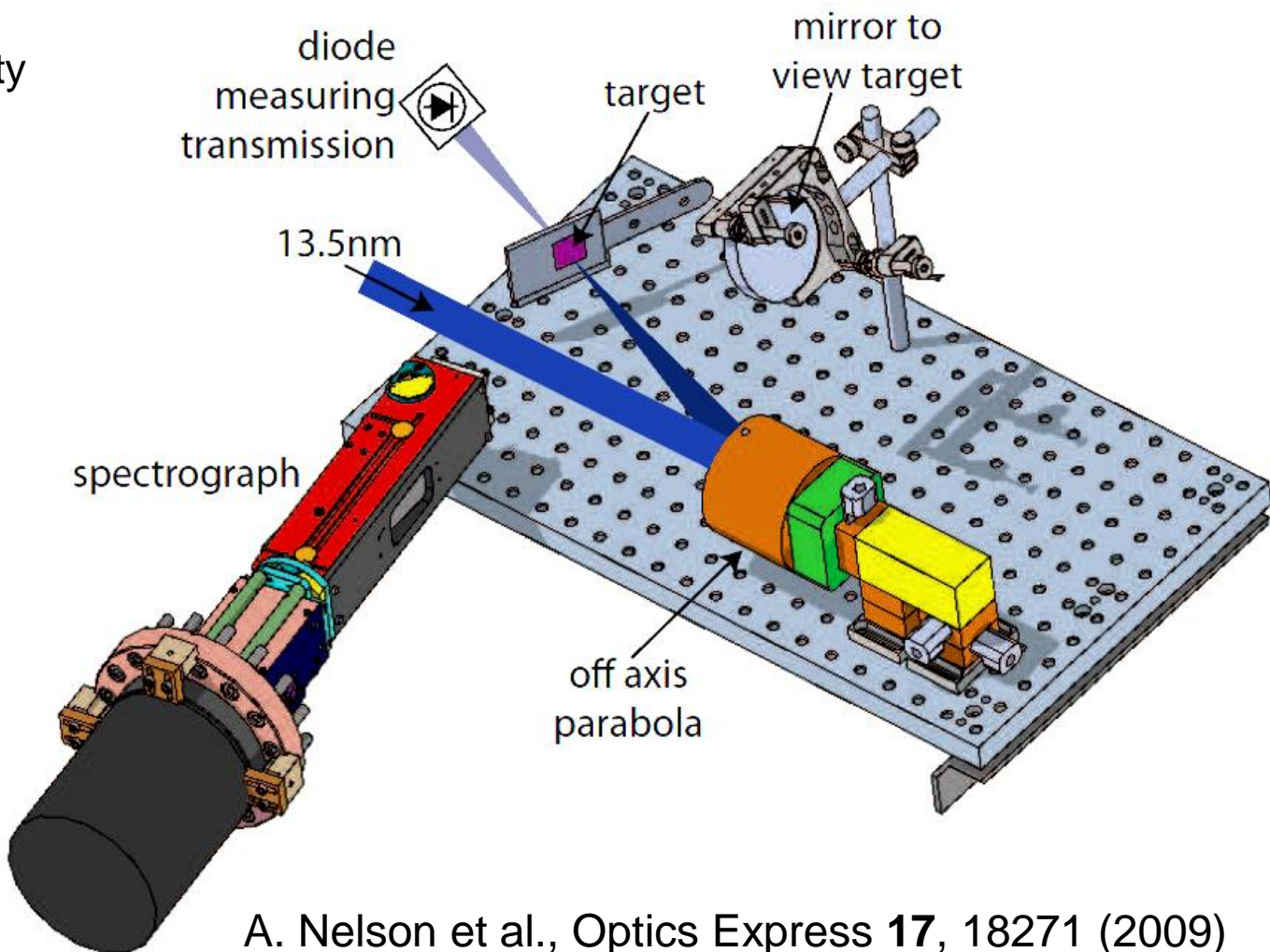
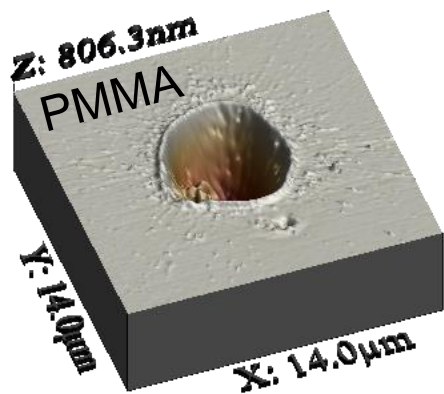
Al L-edge shift after photoionization



- Removal of 1st 2p electron causes shift of $n = 2$ shell due to loss of the outer screening.
- Further photons cannot ionize the L-shell
- E_f will increase as there are now four electrons in the conduction band ($\sim 2.4 \text{ eV}$)

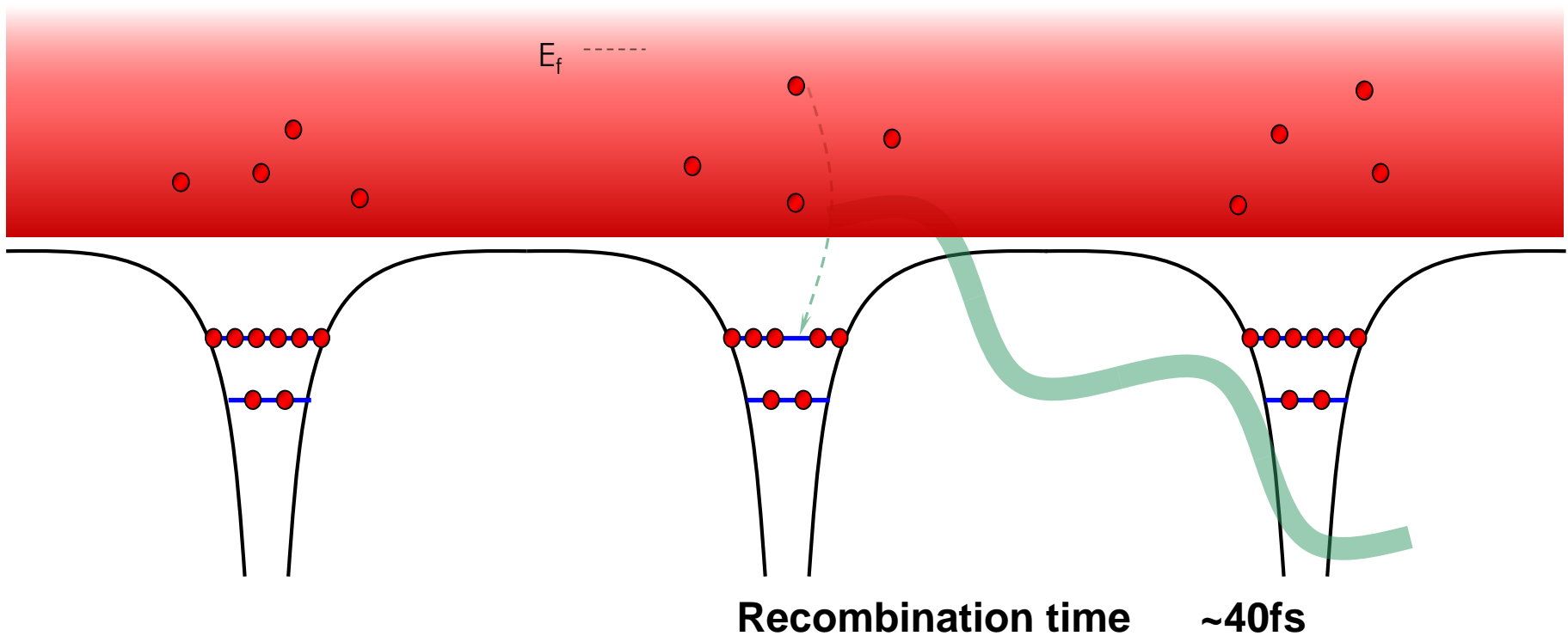
Microfocusing FLASH

- High Energy Density
 - 10^{17} W/cm^2
 - Focus $\sim 0.7 \mu\text{m}$



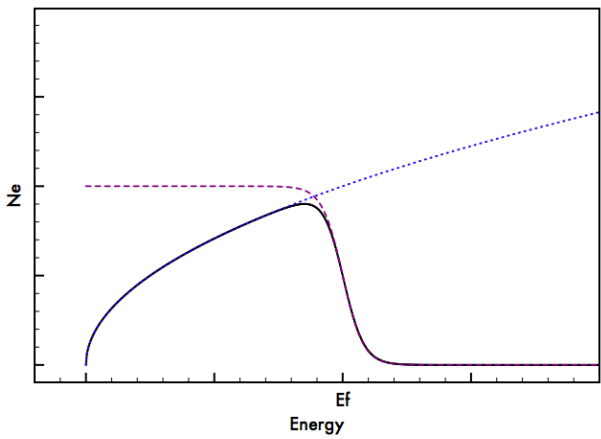
A. Nelson et al., Optics Express 17, 18271 (2009)

Recombination Time



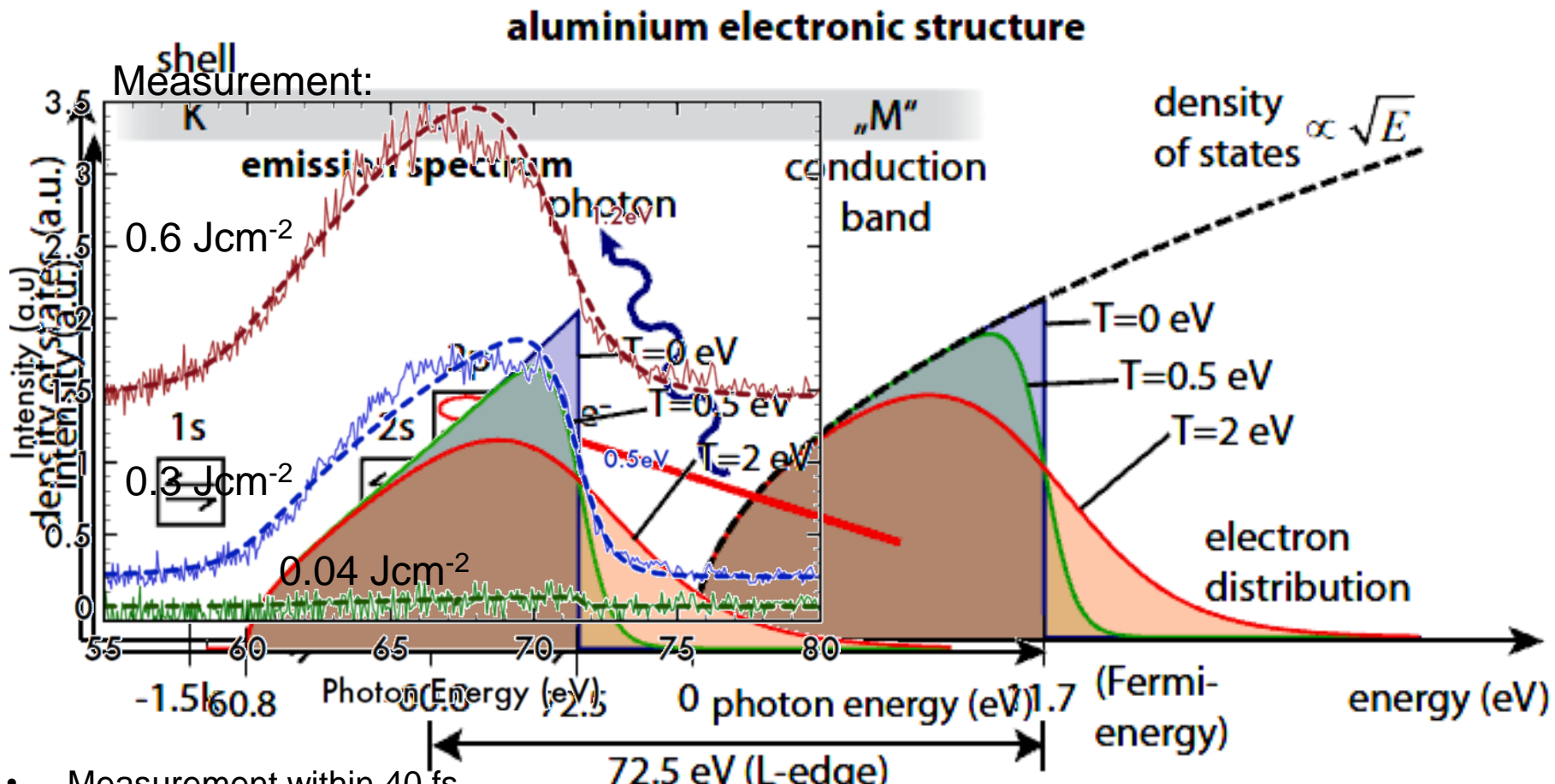
Recombination time ~40fs

Should see fluorescence before lattice moves.



Fluorescence proportional to $\omega^3 g(E)f(E, T)$
(better model under development)

Fluorescence Maps Valence Band



- Measurement within 40 fs
- Time limited by Auger decay

S. Vinko et al., PRL 104, 225001 (2010)

Thank you for your attention

